

On the control and automation of a novel membrane electro-bioreactor (MEBR)

Alexandre Bélanger

A Thesis

in

The Department

of

Building, Civil and Environmental Engineering

Presented in Partial Fulfillments of the Requirements

For the Degree of Master of Applied Science (Civil Engineering) at

Concordia University

Montreal, Quebec, Canada

March 2017

©Alexandre Bélanger, 2017

CONCORDIA UNIVERSITY

School of Graduate Studies

This is to certify that the thesis prepared

By: **Alexandre Bélanger**

Entitled: **On the control and automation of a novel membrane electro-bioreactor (MEBR)**

And submitted in partial fulfillment of the requirements for the degree of

Master of Applied Science (Civil Engineering)

Complies with the regulations of the University and meets the accepted standards with respect to originality and quality.

Signed by the final examining committee:

Dr. Zhenhua Zhu Chair

Dr. Lyes Kadem External Examiner

Dr. Fuzhan Nasiri Examiner

Dr. Zhenhua Zhu Examiner

Dr. Maria Elektorowicz Supervisor

Approved by:

Dr. Mohammed Zaheeruddin
Chair of Building, Civil and Environmental Engineering

2017

Dean Amir Asif
Dean of Engineering and Computer Science

Abstract

On the control and automation of a novel membrane electro-bioreactor (MEBR)

Alexandre Bélanger

The membrane electro-bioreactor (MEBR) has demonstrated to be effective in the treatment of wastewater, where superior quality of the effluent was achieved. The MEBR is a compact hybrid unit that uses several processes, such as activated sludge, membrane filtration, and electrokinetic phenomena. The objective of this study was to improve the treatment of wastewater by monitoring and controlling MEBR processes on-line, which was accomplished by implementing an automation system. As the complexity of the processes increase in the treatment wastewater, it is difficult to their guarantee performance; the automation system maintained the wastewater treatment to satisfactory performance.

Automation of the system was accomplished through control algorithms using on-line instrumentation of critical parameters such as: dissolved oxygen, aeration, and water levels. The MEBR system demonstrated removal of carbon and nutrients (phosphorus, and nitrogen) for water recovery. Automated aeration ensured biological treatment without excessive aeration, fluctuating low dissolved oxygen concentrations allowed for simultaneous aerobic and anoxic conditions without inhibiting biological treatment. Automated electrokinetic improved nutrient removal with reduced energy consumption, also biological treatment was not inhibited. Electrokinetic demonstrated even lower than previously observed energy consumption. A user interface was implemented to allow on-site monitoring of the processes as well as allow adjustment of process parameters. Having a completely automated MEBR allowed this novel wastewater treatment system to be implemented in a remote location, as a decentralized system, in order to simulate an effective wastewater treatment system which may be applied to improve the quality of life for the secluded population of northern Canada and Quebec.

Acknowledgement

I would like express my sincere gratitude and appreciation to my supervisor Dr. Maria Elektorowicz, professor in the department of Building, Civil and Environmental Engineering at Concordia University, for her help, knowledge and support during this project. I would also like to thank Dr. Sharif Ibeid for his help and knowledge.

I appreciate the financial support that the Natural Sciences and Engineering Research Council of Canada (Idea to Innovation Program) has awarded to Dr. Maria Elektorowicz. I also express my sincere thanks to Mr. Christian Sauvageau, Mrs. Marie-Claude Hurteau, and the employees of the wastewater treatment plant in L'Assomption for their kind collaboration.

Dedication:

This thesis is dedicated to my family and wife Cybèle Prince. Their constant encouragement and support during my study has been tremendously helpful in achieving my objectives. I would also like to dedicate this thesis to my brother and sister.

Table of Contents

LIST OF FIGURES.....	X
LIST OF TABLES.....	XII
ABBREVIATIONS.....	XIII
CHAPTER 1: INTRODUCTION.....	14
1.1. WASTEWATER TREATMENT	14
1.2. WASTEWATER CHARACTERISTICS.....	15
1.3. MOTIVATION.....	17
1.4. OBJECTIVE	18
CHAPTER 2: WASTEWATER TREATMENT	20
2.1. CONVENTIONAL REMOVAL OF CARBON, PHOSPHOROUS AND NITROGEN VS ELECTRO-BIOLOGICAL	20
<i>Carbon Removal - Activated Sludge Process.....</i>	<i>20</i>
<i>Phosphorus Removal.....</i>	<i>21</i>
<i>Classical Nitrogen Removal – Nitrification & Denitrification</i>	<i>22</i>
<i>Novel Nitrogen Removal - Anammox.....</i>	<i>23</i>
2.2. ELECTROKINETIC	24
2.3. AERATION & DISSOLVED OXYGEN	27
2.4. OPERATIONAL PARAMETERS FOR ACTIVATED SLUDGE PROCESS.....	28
<i>Hydraulic Retention Time</i>	<i>28</i>
<i>Solid Retention Time</i>	<i>29</i>
2.5. MBR	30
<i>Membrane Filtration.....</i>	<i>30</i>
<i>Membrane: Material, Modules & Configuration.....</i>	<i>31</i>
<i>Membrane Operational Parameters</i>	<i>32</i>
<i>Fouling.....</i>	<i>33</i>
CHAPTER 3: PROCESS CONTROL.....	36
3.1. INTRODUCTION TO PROCESS CONTROL	36
3.2. PROCESS MODELING	37
3.3. SYSTEM IDENTIFICATION	38
3.4. CONTROL STRATEGY – PID CONTROL	40
3.5. IMPLEMENTATION	41
CHAPTER 4: AUTOMATION OF THE MEBR	45
4.1. AUTOMATION OVERVIEW.....	45
4.2. MEBR SYSTEM OVERVIEW.....	45
4.3. INSTRUMENTATION	48

<i>Water Level Sensors</i>	48
<i>Dissolved Oxygen & Temperature</i>	49
<i>Aeration & Air Flow Control</i>	51
<i>EK Power Supply and Current Measurement</i>	52
4.4. PROTOTYPING & ARDUINO.....	54
<i>Prototyping</i>	54
<i>Arduino</i>	54
<i>Prototype 1 – Pump Control System</i>	55
<i>Prototype 2 – EK Control System</i>	56
<i>Arduino Software Implementation</i>	57
4.5. INDUSTRIAL AUTOMATION.....	57
<i>Programmable Controller</i>	58
<i>Remote Connectivity & Network</i>	59
<i>Control Panel</i>	60
CHAPTER 5: PUMP CONTROL SYSTEM	63
5.1. OVERVIEW	63
5.2. PUMP CONTROLLER ALGORITHM	63
5.3. SOFTWARE IMPLEMENTATION	65
5.4. RESULTS & ANALYSIS.....	66
<i>MEBR & Feed – Water Levels</i>	66
<i>Safety</i>	67
CHAPTER 6: AERATION CONTROL SYSTEM	69
6.1. OVERVIEW	69
6.2. AERATION CONTROLLER ALGORITHM	69
6.3. SOFTWARE IMPLEMENTATION	70
6.4. RESULTS & ANALYSIS.....	71
<i>Dissolved Oxygen & Aeration</i>	71
<i>Temperature</i>	72
CHAPTER 7: EK CONTROL SYSTEM	73
7.1. OVERVIEW	73
7.2. MODELLING & SYSTEM IDENTIFICATION	73
<i>Modelling EK Process</i>	73
<i>Data Acquisition – P2000 & MATLAB TCP/IP Communication</i>	76
<i>System Identification for EK Process</i>	76
7.3. CONTROLLER DESIGN	78
<i>P2000 – PID Controller Implementation</i>	78

<i>Design of PI controller</i>	79
<i>Selection of Sampling Rate & PI Fine-Tuning</i>	80
7.4. CARBON DOSING	82
7.5. SOFTWARE IMPLEMENTATION	82
7.6. RESULTS & ANALYSIS.....	83
<i>PI Controller</i>	83
<i>Fluctuating Conditions</i>	83
CHAPTER 8: DISCUSSION.....	86
8.1. WASTEWATER TREATMENT	86
<i>Influent & Operating Conditions</i>	86
<i>Carbon Removal</i>	86
<i>Phosphorus Removal</i>	87
<i>Nitrogen Removal</i>	88
8.2. FLEXIBILITY OF THE MEBR	88
<i>Pumps</i>	88
<i>Aeration & DO Control</i>	89
<i>Temperature Control</i>	89
<i>Membrane Filtration</i>	89
<i>EK & CD Control</i>	89
<i>MEBR</i>	90
8.3. SIMPLIFIED PI DESIGN GUIDELINES FOR EK.....	90
8.4. POWER & ENERGY CONSUMPTION	92
<i>EK</i>	92
<i>Control System</i>	92
<i>Pumps</i>	92
<i>Aeration</i>	93
<i>Overall Energy Consumption</i>	93
8.5. EK - SCALING UP	94
CHAPTER 9: CONCLUSION, CONTRIBUTION & FUTURE WORK	95
9.1. CONCLUSION	95
9.2. CONTRIBUTION.....	96
9.3. FUTURE WORK	96
REFERENCES	97
APPENDIX A: ELECTRONIC & ELECTRICAL SUPPLIES	103
APPENDIX B: PUMPS LADDER DIAGRAM TASKS	104
APPENDIX C: AERATION & PURGE LADDER DIAGRAM TASKS	107

APPENDIX D:	EK & CARBON DOSING LADDER DIAGRAM TASKS	110
APPENDIX E:	P2000 & MATLAB TCP/IP.....	112
APPENDIX F:	SYSTEM IDENTIFICATION – MATLAB	114
APPENDIX G:	POWER, ENERGY & SCALE UP.....	116
APPENDIX H:	SIMPLIFIED PI CONTROLLER – GUIDELINES PROOF	117

List of Figures

Figure 1.1-1: Municipal Wastewater Treatment Levels in Canada	15
Figure 2.5-1: Membrane Fouling Factors	35
Figure 3.1-1: Automatic Closed-Loop Control.....	37
Figure 3.4-1: Performance Parameters in Step Response	41
Figure 3.5-1: Hardware Implementation.....	42
Figure 3.5-2: Continuous vs Discrete Systems (sampling at 1s)	43
Figure 3.5-3: Software Implementation – Discrete PID (Pseudocode)	43
Figure 4.1-1: MEBR Automation	45
Figure 4.2-1: MEBR System Overview.....	47
Figure 4.3-1: Luminescent Dissolved Oxygen working principle.....	50
Figure 4.4-1: Pump Controller Prototype 1 – Front & Interior Panel.....	55
Figure 4.4-2: EK Controller Prototype 2 – Front & Interior Panel.....	56
Figure 4.5-1: MEBR LAN & Remote Connectivity	59
Figure 4.5-2: MEBR Control Panel – Front & Interior	60
Figure 4.5-3: HMI – Main Menu	61
Figure 4.5-4: Control Panel Interior – Components	62
Figure 5.1-1: Water Level Control System.....	63
Figure 5.2-1: Pump Controller – Automatic Mode.....	65
Figure 5.4-1: MEBR & Feed - Water Levels over 10h on Dec 25, 2016	66
Figure 5.4-2: Feed pump auto recovery on Dec 26, 2016	67
Figure 5.4-3: System disabled from pump blockage on Dec 16, 2016	68
Figure 6.1-1: Aeration Control System.....	69
Figure 6.4-1: DO & Aeration using Rule based Control	71
Figure 6.4-2: Temperature in MEBR vs outside.....	72
Figure 7.2-1: EK Circuit Diagram	73
Figure 7.2-2: EK Simplified Circuit Diagram	73
Figure 7.2-3: RC Circuit Diagram	75
Figure 7.2-4: Effect of Sampling Rate	77
Figure 7.2-5: Optimization & Least-Square Comparison.....	77
Figure 7.3-1: EK System - Feedback Diagram.....	79

Figure 7.3-2: Comparison of Different PI Tuning Methods	80
Figure 7.3-3: Effect of Sampling rate on PI Controller	81
Figure 7.3-4: Response of Fine-Tuned PI Controller from reducing K_p	82
Figure 7.6-1: Response of Actual and Simulated System.....	83
Figure 7.6-2: Voltage Variations in MEBR	84
Figure 7.6-3: Voltage variations over EK cycle (Jan 15, 2017)	85
Figure 8.1-1: COD effluent concentration with respect to CD	87
Figure 8.1-2: PO ₄ -P effluent concentration with respect to CD	87
Figure 8.1-3: NH ₄ -N & NO ₃ -N effluent concentrations with respect to CD & Carbon Dosing..	88
Figure B-1: Pumps Water Level Task	104
Figure B-2: Pumps Automatic Task	105
Figure B-3: Pump Manual Task.....	106
Figure C-1: Aeration Task (1 of 2)	107
Figure C-2: Aeration Task (2 of 2)	108
Figure C-3: Purge Task.....	109
Figure D-1: EK Task (1 of 1).....	110
Figure D-2: EK Task (2 of 2).....	111
Figure D-3: Carbon Dosing Task.....	111
Figure E-1: MATLAB as CPoE Device	112
Figure E-2: MATLAB Task.....	112
Figure E-3: MATLAB Code for P2000 Communication	113
Figure F-1: System Identification using MATLAB.....	114
Figure F-2: FOPDT Estimation using Optimization.....	115
Figure F-3: FOPDT Estimation using Least Square	115

List of Tables

Table 4.5-1: P2000 Configuration	58
Table 4.5-2: Front Panel – Components	60
Table 4.5-3: Interior Panel – Main Components	61
Table 7.3-1: PI Tuning Methods	80
Table 8.1-1: Summary of Energy Requirements for the MEBR	93
Table A-1: List of Electronic and Electrical Supplies	103
Table G-1: Energy Consumption	116

Abbreviations

ADC	Analog to digital converter
Anammox	Anaerobic ammonium oxidation
AOB	Ammonia oxidizing bacteria
ASP	Activated sludge process
BOD	Biological oxygen demand
CAS	Conventional activated sludge
CD	Current density
COD	Chemical oxygen demand
CT	Continuous time
DAC	Digital to analog converter
DO	Dissolved oxygen
DT	Discrete time
EK	Electrokinetic
LD	Ladder diagram
LD0	luminescent dissolved oxygen
MFC	Mass flow controller
NH ₃ or NH ₃ -N	Ammonia or ammonia as nitrogen
NH ₄ or NH ₄ -N	Ammonium or ammonium as nitrogen
NO ₃ or NO ₃ -N	Nitrate or nitrate as nitrogen
NO ₂ or NO ₂ -N	Nitrite or nitrite as nitrogen
NOB	Nitrite-oxidizing bacteria
ORP	Oxidation reduction potential
OTR	Oxygen transfer rate
OUR	Oxygen uptake rate
PAC	Programmable automation controller
PI	Proportional-Integral
PID	Proportional-Integral-Derivative
PLC	Programmable logic controller
PO ₄ ³⁻ or PO ₄ -P	Orthophosphate (reactive phosphorus) or Orthophosphate as P
PV	Process variable
MEBR	Membrane electro-bioreactor
SMEBR	Submerged membrane electro-bioreactor
SP	Set-Point
TMP	Transmembrane pressure
TP	Total phosphorus
T _r	Rise time
T _s	Sampling period
t _s	Settling time
TSS	Total suspended solids
WWTP	Wastewater treatment plant
y _{ss}	Steady state output

Chapter 1: Introduction

1.1. Wastewater Treatment

Water is one of the resources essential to sustain life and has long been suspected of being the source of much human illness. It was not until approximately 150 years ago that definite proof of disease transmission through water was established (Sawyer et al., 2003). For many years following, the major consideration was to produce adequate supplies that were hygienically safe. However, sources of water such as surface water and ground water have become increasingly contaminated due to increased wastewater discharge from residential, industrial and agricultural activity.

Wastewater has always constituted a serious problem: with the development of urban areas, it became necessary, from public health and aesthetic considerations, to provide sewer systems to carry such wastes wastewaters treatment facilities (WWTP) into lakes and streams. Once WWTP facilities are operational, constant monitoring is required to maintain economical and satisfactory performance. Hence, the importance of quantitative measurements is significant. Typically, these facilities have in-house laboratories where workers perform analytical measurements to determine and control specific water quality parameters (such as pH, turbidity, dissolved oxygen, biochemical oxygen demand, etc.). The most common way to measure water quality parameters is through labour-intensive experiment: acquiring samples to measure given parameter, setting up the laboratory apparatus with the necessary instruments, calibrating such instruments, and finally completing the standardized experiment. The experimentation process may take several hours to perform and thus creates a challenging issue: WWTP are repeatedly lagging behind the parameters they must control. At the completion of the laboratory experiment, the water, from which the samples were taken hours before, is now either in a different process or has now left the facility, i.e. the wastewater reached the receiving waterbody. Fortunately, there is extensive advancement in automated measurements that allow rapid and accurate online monitoring of crucial water quality parameters. Furthermore, this innovative technology is gradually finding its way into WWTP with the objective to control more effectively and economically the water quality by minimizing the time required to analyse water quality parameters.

In Canada, WWTP are required to treat wastewater so that the effluent into the environment meets specific regulatory standards. Throughout the country, most WWTPs are only equipped with primary or primary and secondary treatment units as shown in Figure 1.1-1 (*Municipal Wastewater Treatment Indicator*, 2013). However, a tertiary treatment unit is necessary to remove nutrients through chemical or biological technologies e.g. biological nutrient removal (BNR). Tertiary treatment, like BNR, can reduce the level of nutrients such as phosphorus and nitrogen, however, this is a complex and expensive process.

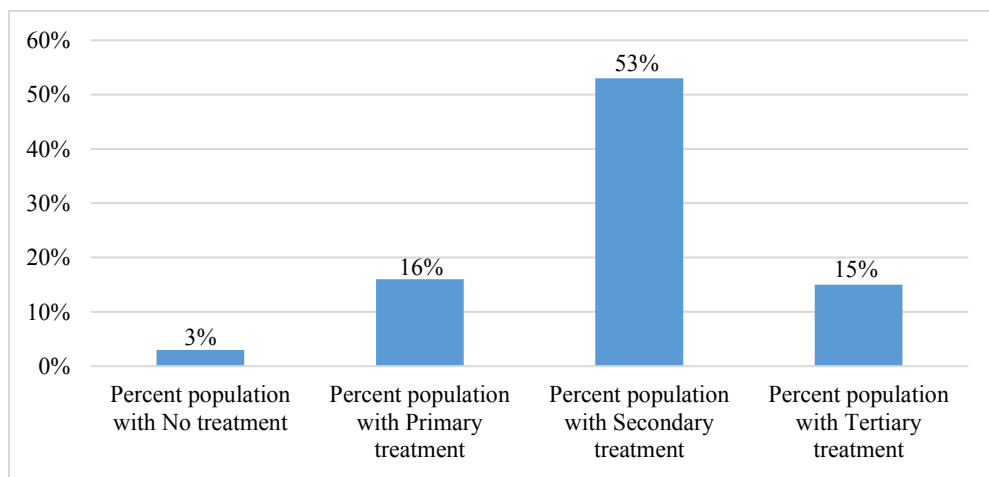


Figure 1.1-1: Municipal Wastewater Treatment Levels in Canada

1.2. Wastewater Characteristics

The assessment of the wastewater properties for this study is conducted based on the following parameters: dissolved oxygen (DO), chemical oxygen demand (COD), phosphorus (TP or PO₄-P), ammonia and nitrates.

Almost all life requires the presence of oxygen, and with respect to the aquatic world, oxygen is in the form of dissolved oxygen (DO). In aquatic systems, degradable material may be oxidized or decomposed by certain microorganisms (Sawyer et al., 2003). In nature, degradation is typically carried out by aerobic microorganisms that decompose the material while DO is needed as an electron acceptor. Dissolved oxygen depletion negatively affects several biota populations including fish, when the concentration is very low (Davis & Cornwell, 2013). Therefore, it is important to control the organic matter discharges into waterways.

The amount of DO needed by microorganisms to oxidize, or breakdown, organic matter, is known as the biochemical oxygen demand (BOD) (Davis & Cornwell, 2013). BOD is an indirect measurement of the amount of organic matter in the water because the measured variable is the amount of oxygen consumed by microorganisms. Generally, the assessment of BOD is conducted by measuring the difference in DO concentration between the 1st and 5th day of bioassay and is known as BOD₅ (APHA, 2012). However, there are also some organic matter, and some inorganic, that cannot be easily oxidized by microorganisms. In such case, a different measure of the oxygen demand is used – chemical oxygen demand (COD). COD allows to determinate of the oxygen concentration required for the full oxidation of organic compounds. The COD results are superior over BOD value assessed for the same wastewater sample. (Sawyer et al., 2003).

Phosphorus and nitrogen compounds are essential nutrients for all forms of life. When discharged into the environment, these nutrients promote growth of plants and phytoplankton while, strongly affecting the life of other aquatic organisms. Algae and cyanobacteria, being chlorophyll organisms, their growth is greatly influenced by excessive amount of phosphorus (TP) in water (Sawyer et al., 2003). Generally, phosphorus is the limiting nutrient in the growth in lakes/reservoirs aquatic systems leading to their eutrophication (Davis & Cornwell, 2013). Although eutrophication is a natural process, the process is accelerated by the release of phosphorus and nitrogen compounds in wastewater. The excessive growth of phytoplankton can lead to decreased dissolved oxygen in water. In the presence of light, phytoplankton produce oxygen using photosynthesis, however, in the absence of light, such as during the night, these organisms use oxygen – known as respiration (Davis & Cornwell, 2013). Also, when phytoplankton die, aerobic microorganisms biodegrade them which requires the consumption of dissolved oxygen. Eutrophication can be prohibited by the control of either nitrogen or phosphorus, or both. DO is also consumed by ammonia when oxidized to nitrates. Therefore, there is presently much interest in controlling the amount of phosphorus and nitrogen compounds that discharged in surface waters.

Nitrates are a common type of compound of nitrogen dissolved in water. Nitrogen content in the water is predominantly present in the organic form (proteins) and ammonia. The proteins are processed into ammonia nitrogen and under aerobic conditions, ammonia nitrogen is then oxidized to nitrite (NO_2^-) and nitrate (NO_3^-) (Davis & Cornwell, 2013). Although nitrates are essential to all

life, their presence in excess in water indicates pollution from agriculture, urban and industrial, and can lead to serious environmental problems, such as eutrophication of water bodies as mentioned earlier. Furthermore, high concentration of nitrite is toxic to animal life and high concentration of nitrate in drinking water can cause illness in humans by interacting with hemoglobin such as methemoglobinemia (Sawyer et al., 2003).

1.3. Motivation

To overcome the problems associated with conventional WWTP and to meet the future regulation of the quality of effluent being discharged into the environment while also being economically viable, innovative technologies are being developed. A particularly widespread and interesting technology is the membrane bioreactor (MBR).

The MBR combines an activated sludge (AS) reactor and membrane filtration into a single process to treat wastewater. However, instead of separating treated water and activated sludge through gravity sedimentation by using a secondary clarifier, the membrane filtration is used for the separation. Advantages of the MBR technology are that it produces very high-quality treated water however, it is unable to remove nutrients (Park et al. , 2015; Radjenović et al., 2008). In addition, membrane filtration in the MBR processes eliminates the need for gravity sedimentation tanks, which results in a smaller footprint than CAS processes (Park et al., 2015).

Nevertheless, the MBR processes on their own have limitations in terms of nutrient removal of phosphorus and nitrogen compounds. Membranes are also vulnerable to be fouled by organic and inorganic bioreactor constituents during the filtration process (Hasan, 2011; Judd, 2006; Park et al., 2015). Membrane fouling causes a decrease of the filtration, and increase transmembrane pressure. Therefore, controlling membrane fouling is essential for stable MBR operation. Various approaches have been developed to mitigate membrane fouling problems.

To overcome the above mentioned MBR disadvantages, a submerged membrane electro-bioreactor (SMEBR) was designed to improve the quality of discharged effluent discharged with respect to nutrient removal and reducing membrane fouling (Bani-Melhem & Elektorowicz, 2010; Bani-Melhem et al., 2009). The SMEBR has successfully completed a pilot test at the L'Assomption wastewater treatment plant located east of Montreal, where it was operated and optimized manually (Hasan et al., 2014). However, a different avenue has been investigated: a self-contained

membrane module (side-stream) instead of a submerged membrane as well as having completely automated processes (aeration, EK, pumps). This system is known as the membrane electro-bioreactor (MEBR). The hypothesis is that the system will provide superior effluent quality by adjusting the system's processes (aeration and EK) to varying influent conditions.

Adequate control strategies for automation purposes are required with the aim of improving the biodegradation of waste materials in addition to reducing energy consumption. Specifically, the development of an automation system will enable control the aeration and EK processes. This would be especially beneficial for WWTP found in Quebec with aeration processes, DO is the most important parameter since it affects directly both the biological treatment of wastewater as well as the energy consumption, which the latter is directly associated with the high running cost of aeration processes (Judd, 2006). By having the aeration process automated, DO would be controlled to ensure adequate treatment without excessive aeration, while also adapting to varying influent conditions. Also, having control over the EK process will enable more adequate nutrient removal, with a reduction in energy consumption, and prevent any adverse effect on the bacterial activity. Therefore, the MEBR is ready for its further development: control and automation.

1.4. Objective

The main objective of this study is to improve the treatment of wastewater by monitoring and adjusting on-line individual processes using instrumentation and control systems. Another crucial objective is to simulate a completely functional wastewater treatment facility installed in a shed beside L'Assomption's WWTP, which could potentially be implemented for a household used in remote locations, as a decentralized system, such as secluded regions of northern Canada and Quebec since it is common to not have access to a sewer network: 14% of the Canadian population use septic tanks (*Households and the Environment*, 2011). Furthermore, this study will demonstrate the steps taken in designing and implementing a control system, so that it may be applied to other processes. As the complexity of processes increase, it is difficult to guarantee their satisfactory performance; thus, this study will show how to successfully integrate a control system to ensure satisfactory performance.

Detailed objectives are:

1. Instrumentation to measure on-line process variables DO, temperature, aeration, water levels, and current density.
2. Modeling MEBR dynamic processes such as electrokinetic process.
3. Designing control algorithm by determining appropriate control strategy for each process based on specific criteria that yield satisfactory performance.
4. Automation implementation: installation of programmable controller, electronic and electrical devices (wiring, connectors, relays, breakers, fuses, etc.).
5. Process automation by creating a software that allows satisfactory operation of the system:
 - a. Measurement of process variables from sensors.
 - b. Ensure safe operation.
 - c. Data acquisition, so that process variables can be analysed over time.
 - d. Controlling automatically DO concentration and current density.
 - e. Build proper alarms to detect improper process behaviour.
6. Design a user interface was implemented to allow monitoring of MEBR through visual representation (buttons, touch panel display, switches, etc.), as well as allow the adjustment of process parameters.

The structure of this thesis follow the requirements of the project supported by NSERC “Idea to Innovation” Grant built based on the patented system (Ibeid, Elektorowicz, Oleszkiewicz, 2012).

Chapter 2: Wastewater Treatment

2.1. Conventional removal of carbon, phosphorous and nitrogen vs electro-biological

Carbon Removal - Activated Sludge Process

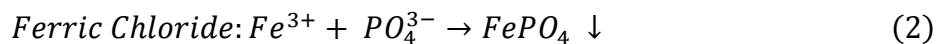
The activated sludge process (ASP) is a biological wastewater treatment technique in which a water mixture containing biomass (or microorganisms), which is agitated and aerated for the biological removal of organics. In this process, wastewater is mixed thoroughly under conditions that stimulate microorganism growth through the use of organic matter (carbon), inorganic matter (nutrients), and other micro-nutrients (Radjenović et al., 2008). Under aerobic conditions, oxygen serves as an electron acceptor where organic and inorganic matter are oxidized by microorganisms. Organic matter is generally measured as biochemical or chemical oxygen demand (BOD and COD, respectively), which are indirect measurements of organic matter concentration since both refer to the amount of oxygen utilised for oxidation of the organics (APHA, 2012; Sawyer et al., 2003). The oxygen level in aerobic process should be kept above 4 mg/L in conventional treatment facilities.

As the microorganisms grow and are mixed thoroughly due to the aeration (or mechanical motion), the individual microorganisms bundle together (flocculate) to form an active biomass, called activated sludge (AS). Activated sludge is subsequently separated from the water through membrane filtration to leave a relatively clean effluent, and its concentration within the MBR is controlled by wasting (or removing) a portion of the biomass in order to maintain an appropriate number of microorganisms to efficiently degrade organic compounds. Wasted biomass is called waste activated sludge (WAS). An equilibrium is then achieved between the growth of new biomass and their removal by wasting. The characteristics of the biomass found in membrane bioreactor (MBR) are slightly different from CAS mainly due to long sludge retention time (SRT) in MBR operation. Long SRT generates conditions where slow-growing microorganisms are favourably maintained compared with the relatively shorter SRT of CAS (Park et al., 2015). Maintaining slow-growing microorganisms is advantageous to degrade problematic organic compounds biologically (Park et al., 2015). Also, the addition of an electrokinetic process has resulted in improved COD removal through electrocoagulation (Bani-Melhem & Elektorowicz, 2010; Hasan et al., 2014), as it is described in details in section 2.2.

In MBR applications, the factors that affect the performance of an activated sludge process are: temperature, amount of dissolved oxygen (DO) available, number of organic compounds available, pH, aeration time and rate, SRT (solid retention time), HRT (hydraulic retention time), mixed liquor suspended solids (MLSS), WAS, and wastewater toxicity. This project proposes a control system for the satisfactory operation of ASP by controlling aeration time, aeration rate, SRT, HRT, and WAS while in-situ monitoring the DO concentration and temperature.

Phosphorus Removal

In conventional activated sludge (CAS) systems, a particular biomass is responsible for biological phosphorus removal - phosphorus accumulating organisms (PAO) (Davis & Cornwell, 2013). PAO accomplish this removal of phosphorus by storing the phosphorus found in the wastewater into their cell mass. This phenomenon occurs when the biomass is moved from an anaerobic to an aerobic environment. Finally, the phosphorus contained in the biomass is removed from the process with wasted activated sludge (WAS). However, the longer SRT in MBR operation, makes the removal of phosphorus limited as there is limited sludge removal (Park et al., 2015; Zuthi et al., 2013). Therefore, MBR systems generally employ chemical removal of phosphorus, known as chemical coagulation (CC). Alum or ferric salts are common chemicals used for CC. In CC, an optimal dosage is difficult and a periodic laboratory experiments are required to validate such dosage. Cations from the chemicals (Al^{3+} or Fe^{3+}) and orthophosphates (PO_4^{3-} or PO_4-P), known as soluble reactive phosphorus (SRP), react to form insoluble aluminium phosphates leading to its removal from the supernatant:



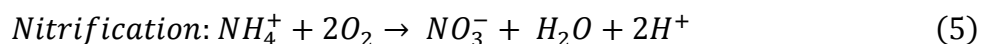
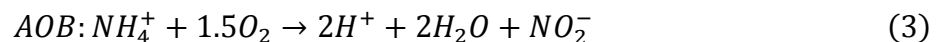
An alternative to chemical removal of phosphorus is electrocoagulation (EC) through the electrokinetic phenomena (EK) (refer to section 2.2). With EC, coagulating agents are generated *in-situ* through electrochemical reactions. EC provides high and stable effects for contaminants removal (Bektaş et al., 2004). EC is able to produce flocs over a wider range of pH values relevant to water treatment and apparently at a more rapid rate, compared to CC (Harif et al., 2012). Furthermore, Hasan et al. (2014) suggest that another mechanism of phosphorus removal in EC is electrodeposition of the non-active inorganic fractions of phosphorus, which are remaining in the wastewater instead of being absorbed by biomass. The results of the EC application into the

SMEBR (submerged membrane electro-bioreactor) have shown that its high ability of phosphorous removal (98-99%) (Bani-Melhem & Elektorowicz, 2010; Hasan et al., 2014). Moreover, EC does not use any chemical reagents and makes the process of phosphorus removal in wastewater treatment simple to automate when compared to CC. This project proposes a method of controlling and automating the EC process by manipulating current density (CD) with in-situ monitoring of applied current within the bioreactor.

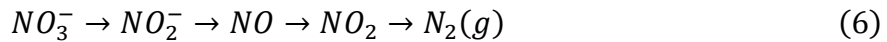
Classical Nitrogen Removal – Nitrification & Denitrification

Nitrogen compounds in the wastewater is predominantly present in the organic form (urea and fecal matter) and the first step in removal of nitrogen in wastewater involve oxidative degradation of organic matter, known as ammonification (Ward, 2013). Through hydrolysis, organic nitrogen compounds are converted to ammonium and/or ammonia. Ammonium is the ionic form of ammonia in water, where the ratio of ammonium to ammonia depends on the pH and temperature.

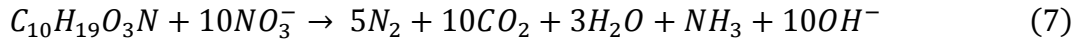
The second step in removal of nitrogen in wastewater is known as nitrification and it involves the biological conversion of ammonium to nitrate. The nitrification is a two-step process. Bacteria called ammonia-oxidising bacteria (AOB) convert ammonia and ammonium to nitrite (NO_2^-), while nitrite-oxidising bacteria (NOB) oxidize nitrite (NO_2^-) into nitrate (NO_3^-). The nitrifying microorganisms that are frequently detected in MBR plants: Nitrosomonas and Nitrosospira are the two common AOB genus, while Nitrobacter and Nitrospira are the two common NOB genus (Park et al., 2015). The reactions are generally coupled and proceed rapidly to the nitrate form; therefore, nitrite levels are usually low. These nitrifying bacteria are known as nitrifiers and they are strict aerobic bacteria, meaning they must have free dissolved oxygen to perform their work; therefore; the nitrification occurs under aerobic conditions; where the DO concentration usually needs to be 1.0–1.5 mg/L in suspended growth systems for their survival (Judd, 2006). The following are the stoichiometric equations for the nitrification process, neglecting the biomass production (Judd, 2006):



The third and final step in removal of nitrogen in wastewater involves the biological conversion of nitrate to nitrogen gas (N_2) and this is known as denitrification. Nitrate is not only a nutrient, but the substrate for the bacterial process of denitrification, by which nitrate is reduced to nitrogen gas, N_2 (Ward, 2013). Unlike nitrification, denitrification takes place when facultative heterotrophic bacteria, which normally remove BOD under aerobic conditions, are able to convert nitrates to nitrogen gas under anoxic conditions. Facultative heterotrophic bacteria, known as denitrifiers, need a carbon source and nitrate molecules. Therefore, denitrification requires a sufficient carbon source for the heterotrophic bacteria, which might be assured by adding raw, containing carbon, wastewater, then, denitrification will occur when oxygen levels are depleted resulting in nitrate becoming the primary oxygen source for microorganisms. Denitrification proceeds through a sequential reduction process involving nitrite, nitric oxide (NO), and dinitrogen oxide (NO_2), which results in the conversion of nitrate to nitrogen gas (Park et al., 2015):



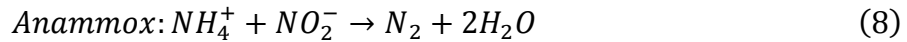
The following is the complete stoichiometric equation for the entire denitrification process (Judd, 2006):



Where $C_{10}H_{19}O_3N$ represents the wastewater, i.e. carbon source. Typically, in tertiary treatment, nitrification and denitrification is achieved by having two separate tanks: an aerobic tank where nitrification occurs, and an anoxic tank where denitrification take place. By combining a nitrification with activated sludge and recirculate activated sludge content to denitrification tank, nitrogen can be removed from the wastewater. In such case the secondary clarifier can be replaced by membrane filtration process.

Novel Nitrogen Removal - Anammox

In 1999, it was discovered that some autotrophic bacteria were responsible for **anaerobic ammonium oxidation**, called anammox bacteria (Park et al., 2015, Elektorowicz et al. 2016). This novel process is able to reduce nitrite directly into nitrogen gas, without using carbon sources for denitrification and without additional supply of air for nitrification:



Nevertheless, the process requires nitrite as the electron acceptor, in which case the nitrite is derived either from aerobic ammonium oxidation, from AOB, or partial denitrification, where nitrate is converted to nitrite. For this study, a combination of aerobic nitrification and anaerobic anammox conversion is used to improve nitrogen removal. Under oxygen limitation, aerobic nitrification and anammox reactions will occur simultaneously as demonstrated at lab scale and pilot scale in this project (Elektorowicz et al., 2017).

2.2. Electrokinetic

The electrokinetic phenomena (EK) represent a family of various processes where electrical field is applied to colloidal matrix. One of these processes related to this work is electrocoagulation. Electrocoagulation (EC) is an electrochemical process that involves the generation of coagulants in situ by dissolving electrically ions from electrodes, usually made of either aluminium or iron (Chen, 2004). The mechanisms involved in EC include coagulation, adsorption, settling or flotation.

The main reaction occurs at the anode when current is applied to the electrodes: electrolysis reactions produces cations (Fe^{2+} , Al^{3+}), depending on electrode material, and these act as coagulants (Bani-Melhem & Elektorowicz, 2010; Vasudevan et al., 2008). The release of these cations causes flocculation, or clumping, of particulates by destabilising them. The destabilisation is achieved through charge neutralisation, reduction of absolute value of zeta potential, which results in greater settling rate (Larue et al., 2003).

Additionally, there are secondary reactions involved in the process. The oxidation of water molecules produces hydrogen ion (H^+) and oxygen gas (O_2) at the anode whereas hydrogen gas (H_2) and hydrogen oxide (OH^-), from water reduction, are generated at the cathode (Bani-Melhem & Elektorowicz, 2011; Chen et al., 2000). Chlorine may also be produced and as a strong oxidant it can oxidize some organic compounds present in wastewater (Chen, 2004). Moreover, if the potential applied to the anode is sufficiently high, direct oxidation of organic compounds is also possible (Chen et al., 2000).

EC has been applied successfully to: potable water (Matteson et al., 1995; Vasudevan et al., 2008), food and restaurant wastewater (Chen et al., 2000), urban wastewater (Pouet, 1995), municipal wastewater for phosphorus removal (Bani-Melhem & Elektorowicz, 2011; Hasan et al., 2014),

sludge treatment (Elektorowicz et al., 2006; Elektorowicz & Oleszkiewicz, 2012; Ibeid et al., 2015), and membrane fouling control (Ibeid et al., 2013b).

The most frequent referred parameter, besides voltage potential and current, is current density (CD), the current per unit area of electrode, which determines the rate of EC. The CD applied to the electrodes determines the number of cations (Fe^{2+} or Al^{3+}) released from the respective electrodes. The amount of metal dissolved depends on the quantity of electricity passed through the solution. A simple relationship between current density and the amount of electrode dissolved can be derived from Faraday's law (Mollah et al., 2004):

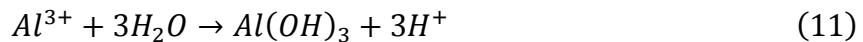
$$w = \frac{i * t * M}{n * F} \quad (9)$$

Where w is the quantity of electrode material dissolved (g of M/cm^2), i is the current density (A/cm^2), t is the electrical exposure time (seconds), M is the relative molar mass of the electrode (g of M/mole), n is the number of electrons in oxidation/reduction reaction, and F is the Faraday's constant (96,500 $\text{A}^*\text{sec}/\text{mole of electrons}$). The electrochemical reactions may be summarized as follows (Bani-Melhem & Elektorowicz, 2010; Chen, 2004):

For aluminium anode:



In acidic conditions:



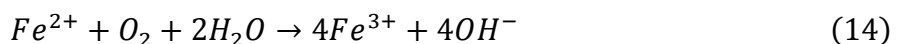
In alkaline conditions:



While for iron anode:



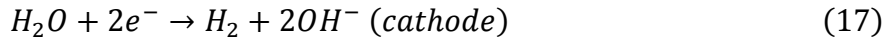
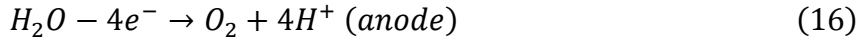
In acidic conditions:



In alkaline conditions:



Additionally, electrolysis of water produces oxygen and hydrogen gas, resulting from oxidation/reduction reaction of water.



The EC process is intrinsically associated with another important electrokinetic process, known as electro-floatation (EF) (Chen, 2004). Electro-floatation is a simple process that floats flocs to the surface of water by gas motion produced by water electrolysis.

A MBR system that combined electrokinetic processes, known as SMEBR, has been successfully used to enhance the removal of phosphorus and COD (Bani-Melhem & Elektorowicz, 2010; Elektorowicz & Oleszkiewicz, 2012; Hasan et al., 2014). Many factors influence electrokinetic, such as wastewater quality (conductivity, pH, concentration of components), temperature, electrode material and shape, electrode arrangement, flow rate, current density, charge loading and application of intermittent current (time on and off). For the SMEBR, these parameters have been investigated in previous studies, and optimal selection has been identified (Arian, 2014; Bani-Melhem & Elektorowicz, 2010; Gao, 2014; Hasan, 2011; Ibeid, 2011; Ibeid et al., 2013b). This work proposes a control system for the satisfactory and automatic operation of the electrokinetic system.

The electrokinetic (EK), previously applied to the SMEBR, enhanced organic matter and nutrient removal. Essential parameters for EK operation is current density (CD, A/m²), exposure time to DC electric field (time on and off), and electrode material. EC as an EK phenomenon has been applied for the phosphate removal in drinking water. The results showed that the maximum phosphate removal efficiency of 98% was achieved at a CD of 5A/m² and exposure time of 20 minutes for a batch cell using mild steel as the anode and stainless steel as the cathode (Vasudevan et al., 2008). For SMEBR operation, Hasan (2014) investigated EK operation with current density of 12 A/m², applied intermittently with exposure time of 5 minutes on and 10 minutes off. In that study, SMEBR achieved a reduction in membrane fouling and high removal efficiencies of

ammonia, phosphorus, and COD: 99%, 99%, and 92%, respectively. Arian (2014) similarly achieved high removal efficiencies using CD of 22 A/m² with exposure time of 5minutes on and 15minutes off. Ibeid et al. (2013a) investigated that a current density between 15 and 20 A/m² and electrical exposure times 5 minutes on and 15 minutes off, and 5 minutes on and 20 minutes off can adequately modify activated sludge characteristics in order to reduce membrane fouling. Further investigation verified membrane fouling reduction and improved removal efficiencies using that a current density of 15 A/m² and electrical exposure time 5 minutes on and 20 minutes off (Ibeid et al., 2013b). It was found that in SMEBR operation, the current density (CD) should be kept below 25 A/m² and applied at an intermittent exposure as to not significantly affect bacterial viability (Wei et al., 2011).

Consequently, the development of an effective control system for EK is essential for superior removal efficiencies, ensuring bacterial viability and contributing to the reduction of membrane fouling. The proposed control system ensures an efficient operation as to avoid over or under estimating EK by controlling CD, along with exposure time, which lead to improvement of treatment and reduction of the energy consumption.

2.3. Aeration & Dissolved Oxygen

Aeration is another essential parameter for biological wastewater treatment as it maintains sufficient DO concentration for microbial activity. In submerged membrane application, aeration is also used for reducing membrane fouling, which is known as air scouring, and is defined by the aeration intensity and the cross-flow velocity (CFV). In general, air scouring aeration is typically applied near the membranes, as well as within the bioreactor. Coarse bubble (>2 mm) aeration is generally applied for air scouring of the biomass attached to the membrane surface (De Temmerman et al., 2015). The injection of the air bubbles induces shear stress on the sludge accumulated at the membrane and resulting in prevention in surface fouling (Böhm et al. , 2012; Psoch & Schiewer, 2005).

In contrast, fine bubble (< 2 mm) aeration in the bioreactor is meant to maintain a sufficient DO concentration for organic matter (BOD/COD) removal and nitrification; even though membrane fouling increases with fine bubble aeration (De Temmerman et al., 2015). While both aeration types induce shear stress on sludge, beneficial impact has only been carefully investigated for coarse bubble aeration (Böhm et al., 2012). Aeration is a major energy consumer, often exceeding

50% of total energy consumption, with a minimum of 35% for air scouring (Judd, 2006, 2008). The significance of air scouring motivates the need for an effective control system that could lead to reduced membrane fouling and energy consumption.

As mentioned previously, aeration is essential for maintaining the acceptable DO concentration for the biological treatment process (refer to section 2.1). Making oxygen transfer from gas to liquid phase (DO) is a very energy intensive activity, a too high level of aeration is unwanted since it is costly and procures no beneficial treatment effect. At any time, the DO concentration depends on the equilibrium between oxygen transfer rate (OTR), the oxygen transferred, and oxygen uptake rate (OUR), the oxygen used by microbial activity. Accurate and precise *in-situ* measurements of the DO concentration are therefore of great importance to support meaningful wastewater treatment. Investigation of optimal DO concentration in SMEBR by Arian (2014) was determined to be 3 mg/L, while Hasan (2011) determined a required minimum concentration of at least 2 mg/L. However, it was demonstrated (Ibeid 2011, Elektrowicz et al. 2016) that maintaining a DO between 0.2 to 0.8 mg/L, would allow the simultaneous aerobic and anoxic nitrogen removal (nitrification and denitrification with anammox). Maintaining an adequate DO concentration is a great challenge for the control of aeration systems. Therefore, it is important to develop an effective aeration control system to avoid over- or under-estimating of aeration which could lead to excessive energy costs, or alternatively, to incomplete treatment.

2.4. Operational Parameters for Activated Sludge Process

Hydraulic Retention Time

Hydraulic retention time (HRT) is associated with the load and is expressed as the reactor volume divided by the influent flow rate. A low HRT results in a higher organic loading and higher biomass concentration (mixed liquor suspended solids, MLSS), therefore, increasing a potential for membrane fouling (Hasan, 2011). Generally, the biodegradation of organics in the influent becomes more stable as the HRT increases (Park et al., 2015). Food to microorganism ratio (F/M) is expressed as the ratio of food per biomass, which is directly related to HRT (Park et al., 2015):

$$\frac{F}{M} = \frac{Q * S_o}{V * X} = \frac{S_o}{\theta * X} \quad (18)$$

$$\theta = \frac{V}{Q} \quad (19)$$

Where Q is the influent flow rate (m^3/day), S_o is the influent substrate concentration ($\text{kg BOD}/\text{m}^3$), V is the bioreactor volume (m^3), θ is the HRT (day), and X is the biomass concentration ($\text{kg MLSS}/\text{m}^3$). Therefore, F/M ratio decreases as the HRT increases, which results in direct changes in microbial characteristics because the biomass growth rate strongly depends on the F/M ratio (Park et al., 2015). A low F/M ratio means that less substrate is available for the microorganisms (biomass), and results in a lower sludge production. However, a low F/M ratio also results in high MLSS concentration that can promote membrane fouling and reduce aeration efficiency, which the latter is a significant problem in terms of maintenance at high MLSS concentrations (Radjenović et al., 2008; Trussell et al., 2007). Consequently, HRT affects membrane fouling indirectly via the change in microbial characteristics. Nevertheless, with a low F/M ratio, there is a significant decrease of sludge production which reduces the cost of excess sludge handling. Carbon dosing may be used to vary the F/M ratio.

Solid Retention Time

Solids retention time (SRT), or sludge age, is associated with the time the sludge solids, or biomass, remain in the system. In the MBR systems, SRT is independent of HRT as a result of membrane separation, and therefore, SRT is expressed as the reactor volume divided by the solid, or sludge, wastage rate:

$$SRT = \frac{V}{Q_w} \quad (20)$$

Where V is the bioreactor volume (m^3), and Q_w is the solid (or sludge) wastage rate (m^3/day). Increasing SRT results in higher MLSS concentration, enhanced biodegradation and lower sludge production (Bouhabila et al., 2001). However, as mentioned previously, high MLSS is an important microbial factor affecting membrane fouling. Consequently, similarly to HRT, SRT affects membrane fouling indirectly via the change in biomass characteristics.

Previous studies on SMEBR applied SRT and HRT of 10 days and 11 hours, respectively (Hasan et al., 2014). Later, it was concluded that the SMEBR could operate at any selected HRT (between 6 and 15 hours) depending on the objective the system is trying to achieve (water quality,

membrane fouling or sludge properties). Nevertheless, superior results were achieved with increased HRT through which authors believed that the bacterial recovery occurred and contributed to the organic matter and nutrient removal efficiencies (Ibeid et al., 2012; Wei et al., 2011). Furthermore, longer HRT allowed longer exposure time of the wastewater to the electrical field thus increasing the positive impact of electrokinetic on the removal efficiency (Hasan et al., 2014). In recent investigations, SMEBR operated using a HRT of 12 hours and SRT of 15 days also demonstrated successful removal of COD and nutrients (Elektorowicz et al. 2014, Arian, 2014). The significance of SRT and HRT on process behaviour motivates the need for an effective control system that could lead to reduced membrane fouling and enhanced biological treatment.

2.5. MBR

Membrane Filtration

Membrane filtration is the process in which a membrane acts as a semi-permeable barrier that separates substances when a driving force, or pressure difference, is applied across the membrane (Hai & Yamamoto, 2011). The membrane has minuscule pores that allow only very small particles, such as water and solutes, to permeate through the membrane while retaining (or rejecting) larger particles inside the bioreactor. Therefore, the primary mechanism of membrane filtration is size exclusion. Membrane filtration processes are categorized into four categories based on particle size: Microfiltration (MF), Ultrafiltration (UF), Nanofiltration (NF) and Reverse Osmosis (RO).

Microfiltration can separate small particles from 0.1 to 10 μm in size such as suspended solids and bacteria. Ultrafiltration (UF) can separate smaller particles like viruses and endotoxin that range in size from 0.01 to 0.1 μm . Nanofiltration can be used to remove small particles that range in size from 0.001 to 0.01 μm like pesticides and herbicides. Finally, reverse osmosis can separate the smallest particles, size less than 0.001 μm like metal ions and acids (Hai & Yamamoto, 2011; Zhang et al., 2012). Unlike microfiltration, UF or smaller membranes do not have an absolute micron rating because all pores are not the same size. Instead, they use a nominal molecular weight cut-offs that are a measure of the pore size distribution across the membrane surface, typically the unit is in kilodaltons (kD). In spite of solids separations, MBR are not capable of retaining phosphorus and nitrogen compounds. Additional technologies have to be applied to remove nutrients in MBR systems.

Membrane: Material, Modules & Configuration

There are mainly two different types of membrane material: organic (polymers such as polyvinylidene difluoride (PVDF), polyethylenesulphone (PES), polyethylene (PE), polypropylene (PP) and inorganic (ceramic) (Judd, 2006; Zhang et al., 2012). Organic membranes are more commonly used in water and wastewater treatment because they have good chemical, mechanical and thermal stability as well as being more flexible and providing higher surface area per volume (Hasan, 2011). However, current polymer membranes suffer from the low fouling resistance due to the intrinsic hydrophobic property of the polymers (Judd, 2006). Membrane modules come in two different modules: side-stream, or self-contained, and open immersion. Side-stream modules have an external housing around the membrane, where the feed water must be circulated continuously while the permeate exits by passing through the membrane – these are used externally, or as a side-stream, of a bioreactor. Open immersion membranes are submerged in the bioreactor with the membrane exposed to the feed water. There are three main type of membrane configuration found in MBR applications: plate and frame, tubular and hollow fibers (Hasan, 2011; Judd, 2006).

Plate and frame membrane consists of two flat sheets of membrane material, typically an organic polymer, stretched across a thin frame. Several plates may be arranged in a stack formation, which are immersed in the feed water. The driving force needed for filtration is provided by placing the inner membrane sheets under vacuum. Tubular membrane consists of an outer and inner tube: the outer tube is the housing and the inner tube is the membrane. Tubular membranes are typically made of inorganic materials like ceramic. Unlike the previous two types, the driving force is not based on the vacuum since the materials are separated at high velocity under pressure causing a transverse force to drive the water through the membrane while rejecting the large particles. These types of membranes can be arranged in either feed water flow direction: from the inside to the outside, or vice versa. This configuration is typically used in self-contained modules. Hollow fibers membrane consists of long strands of hollow extruded membrane, typically made of organic polymers. One side of the fibers are mounted on a supporting structure, which serves as a manifold for the permeate. The other side of the fiber is not fixed; by having a free end, the membrane is able to move freely around which reduces membrane fouling. This type of profile may be used in a self-contained or open immersion module. For this profile, the driving force needed for filtration is provided by placing the supporting structure, and therefore the inner hollow membrane, under

vacuum. To conclude this section, MEBR achieves membrane filtration by using tubular membrane operating as a side-stream.

Membrane Operational Parameters

The key parameters in any membrane operation are the transmembrane pressure (TMP), permeate flux (J), critical flux (J_c), total resistance (R_t), permeability (K), and specific aeration demand (SAD) (Field, Wu, Howell, & Gupta, 1995; Hasan, 2011; Judd, 2006). TMP is defined as the pressure difference across the membrane: the difference in pressure on the feed water side and permeate side, and is considered as a driving force behind the filtration process. Critical flux is defined as the flux below which a decline of flux with time does not occur and above it, fouling is observed (Field et al., 1995). Permeability is calculated as permeate flux per unit of TMP. The permeate flux is defined as the permeate volumetric flow rate per unite area and may be described by:

$$J = \frac{TMP}{\mu * R_t} \quad (21)$$

Where J is the permeate flux, μ is the dynamic viscosity of the permeate, and R_t is the total resistance. The general approach to describing the total resistance is given by (Chang et al., 2002; Hasan, 2011; Radjenović et al., 2008):

$$R_t = R_m + R_c + R_f \quad (22)$$

Where R_m is the intrinsic membrane resistance, R_c is the resistance from the cake layer, and R_f is the fouling resistance. It is necessary to clean the membrane unit in an MBR by removing solids from the membrane surface. Cleaning achieved by scouring, or scrubbing by aeration, the membrane, which is supplied using coarse bubble diffusers. Specific aeration demand (SAD) is the air flow necessary for the cleaning of the membrane and it may be represented either as the ratio of air flow to membrane unit area (SAD_m) or to permeate unit volume (SAD_p) (Judd, 2006). Membrane aeration values are typically based on suppliers' recommendation for aeration rate or based experimentally. SAD is an essential parameter for the design and operation of submerged MBR because it allows optimal permeate flux by reducing membrane fouling, while also being a key contributing factor to energy demand in submerged systems (Judd, 2006).

Fouling

Membrane fouling (MF) is a major problem encountered during MBR operation in water and wastewater treatment. Undesired deposition and accumulation of foulants (microorganisms, colloids, and solutes) onto a membrane surface or into the membrane pores impairs the proper functioning of the filtration process – this phenomenon is known as membrane fouling. MF causes a decrease of the permeation through a membrane. MF is affected by many factors such as the feed water quality, membrane characteristics, MBR operational conditions, and membrane cleaning methods. Therefore, the success of MBR operation is largely dependent upon how to manage or control MF (Flemming, Schaule, Griebel, Schmitt, & Tamachkiarowa, 1997; Park et al., 2015).

MF causes an increase in the resistance to filtration process and may be perceived as a decrease in permeate flux or an increase in TMP, and therefore leads to greater energy demand while also accelerating membrane deterioration. Given that MF represents the main limitation to membrane process operation, it is unsurprising that the majority of membrane research and development conducted is dedicated to understanding membrane fouling and its reduction (Judd, 2006; Meng et al., 2009; Oh et al., 2012). MF may occur due to the following mechanisms: adsorption of solutes and/or colloids within/on membrane, deposition of sludge flocs onto membrane surface, formation of a cake layer on the membrane surface, detachment of foulants attributed mainly to shear forces, and spatial and temporal changes of the foulant composition during long-term operation (changes in bacterial community and components in cake layer) (Meng et al., 2009).

Reliable operation of MBR systems requires careful management of MF and recent developments in fouling control technologies have led to improved membrane lifespan and significantly reduced overall maintenance and operational costs. Fouling control includes all kinds of implementation strategies to maintain the flux as high as the design requirement. Fouling can be classified into three groups: reversible, irreversible, and irrecoverable (Judd, 2006; Park et al., 2015). Reversible fouling can be removed by physical cleaning, such as air scouring, back flushing or MBR relaxation. Irreversible fouling cannot be removed by physical cleaning but can be removed using chemical cleaning. Irrecoverable cannot be removed with either physical or chemical cleaning, membrane replacement is necessary (Meng et al., 2009).

There are numerous methods of fouling control that have are practiced in MBR: applying appropriate pre-treatment to the feed water, employing appropriate physical or chemical cleaning,

reducing flux, increasing air scouring, chemically or biochemically modifying the mixed liquor, or others (membrane and module development) (Hasan, 2011; Judd, 2006).

Pre-treatment helps reduce MF by removing coarse particles in size (typically >1mm) that are susceptible to foul membrane, such has hair which combine and clog both the membrane pores and aeration outlets (Judd, 2006). Chemically cleaning membranes certainly restores membrane filtration performance. Strong acids and/or oxidizing agents recover the membrane's deteriorated performance nearly completely. However, chemical cleaning incurs operational downtime and cannot avoid secondary contamination, which is the generated waste chemicals that require further treatment and eventual disposal. Moreover, safety regulations for the transport, storage, and usage of chemicals have become stringent nowadays, so that alternative cleaning options are encouraged instead of chemical cleaning. Physical cleaning methods are preferred and recommended as they do not produce secondary contaminants that require further treatment. Physical cleaning refers to backwashing, air scouring and membrane relaxation. However, frequent backwashing leads membrane damage, backwashing incurs operational downtime. Air scouring, such as coarse bubble aeration, is widely practiced in submerged MBR systems but is an energy intensive process.

Most operation and maintenance (O&M) costs in MBR plants are attributed to the electrical energy consumption of the blower supplying coarse air to the membrane surfaces. Reducing the flux to the critical flux always reduces fouling but obviously then impacts directly on capital cost through larger membrane area or additional MBR systems (Judd, 2006). Critical flux is defined as the flux below which a decline of flux with time does not occur and above it, fouling is observed (Field et al., 1995). Modifying mixed liquor generally refers to the addition of chemicals: coagulant agents. Coagulant agents such as ferric chloride and aluminium sulphate (alum) have both been studied to improve membrane fouling because these agents increase flocculation and hence the settling rate of flocs formed. As an alternative of adding coagulants from chemical solutions, electrocoagulation (EC) is an innovative technology used for the generation of coagulants in-situ by dissolving electrically ions from electrodes, usually made of either aluminium or iron (Chen, 2004).

Many factors affect membrane fouling: membrane properties, sludge properties and operating conditions have significant impacts on membrane fouling (Figure 2.5-1) (Zhang et al., 2012).

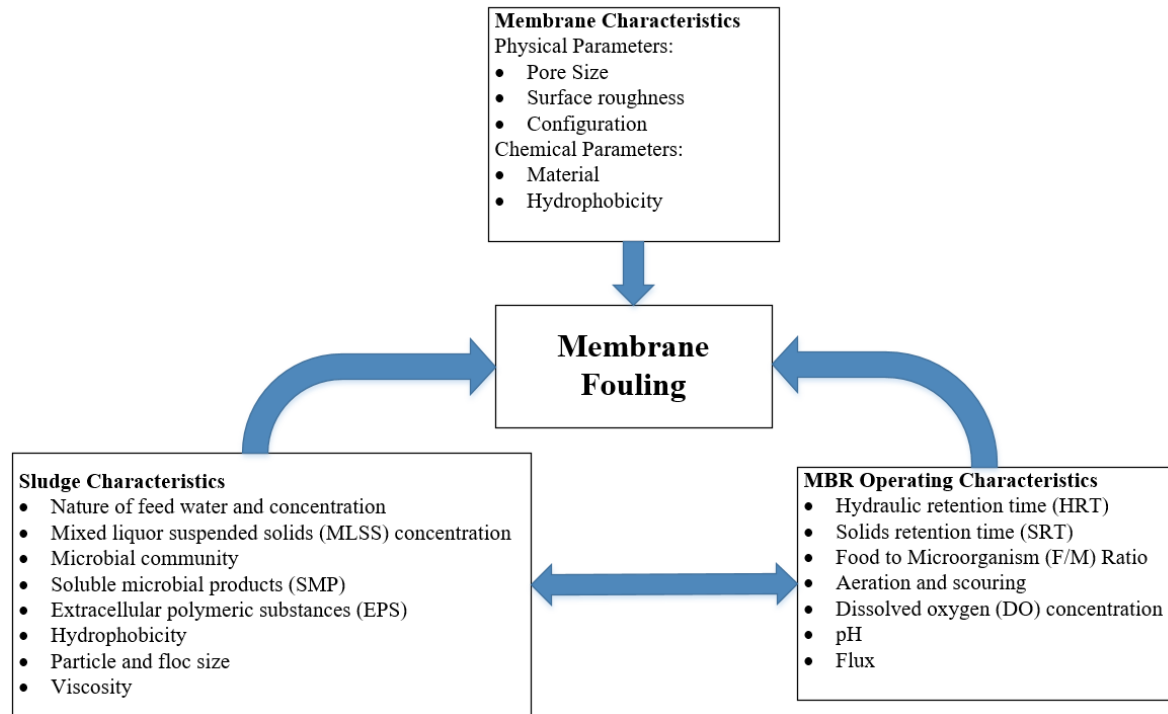


Figure 2.5-1: Membrane Fouling Factors

MBR process parameters such as solid retention time (SRT), hydraulic retention time (HRT), dissolved oxygen (DO) concentration and food to microorganism ratio (F/M) have no direct impact on membrane fouling; but they determine the sludge characteristics and the variation of those parameters can modify the characteristic of activated sludge; thus, indirectly impacting membrane fouling (Meng et al., 2009). An accurate control of electrokinetic electrical parameters will allow to influence wastewater properties and decrease membrane fouling (Hasan et al., 2012; Ibeid et al., 2013a, 2015; Wei et al., 2011)

Chapter 3: Process Control

3.1. Introduction to Process Control

Control in process industries refers to the automatic control of all aspects of a process. A process, as used in process control, is a method of transforming an input into a desired output; all processes have at least one input and one output, known as single input single output (SISO) system, while more complex systems may have multiple inputs and multiple outputs (MIMO system). For example, a SISO system may be a water heater tank where the input is a voltage applied to the heating element and the output is the resulting water heating. This type of control is known as open-loop control. Open-loop control is useful when it is not critical to have strict control over the output.

In the case where tight control of the process is necessary (i.e. a specific temperature), it becomes necessary to introduce feedback by measuring the output parameter (or process variable). The term feedback refers to a situation in which two (or more) dynamical systems are connected together such that each system influences the other and their dynamics are thus strongly coupled (Åström & Murray, 2012). Thus, the output and process are interconnected in a cycle and this is known as closed-loop control. By introducing feedback, the process may be set at a specific set-point, as long as the process remains constant and there are no external disturbances. However, in reality, dynamic processes do not remain constant and there are always disturbances that affect the system's response. Therefore, in the event of disturbances, some sort of compensation is necessary to keep the process at the set-point.

In order to compensate for external disturbances or changes in system's behavior, automatic closed loop control is essential. Automatic control is achieved by the addition of a controller algorithm. The controller monitors the operation of a system by measuring the process variable (PV) that needs to be controlled, compares the output against the desired set-point (SP), computes corrective actions and actuates the process to successfully get the desired PV (Figure 3.1-1). This basic feedback loop of sensing, computation and actuation is the central concept in control (Åström & Murray, 2012). The main advantages of an automatic closed-loop control system are its ability to reduce a system's sensitivity to external disturbances and increase the system responsiveness or performance; thus, allowing control on the system as any changes in the feedback signal will result

in compensation by the controller. Consequently, the objective becomes how to successfully design a control system to meet satisfactory results.

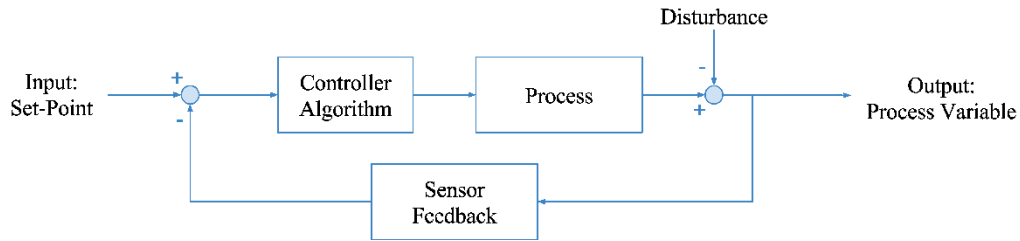


Figure 3.1-1: Automatic Closed-Loop Control

A control system is the framework which guarantees a process will meet specific requirements with respect performance and safety. The effective design of a control system can be divided into 4 essential elements: process modeling, system identification, controller design, and implementation.

3.2. Process Modeling

Modeling of physical system is a key element in the design and analysis of control systems. A model is a precise mathematical representation of a system's dynamics describing how it will behave. The dynamic behaviour of a system is generally described by differential equations which are obtained by applying physical laws that are known to govern the behaviour of the system (Dorf & Bishop., 2011). By analyzing the relationship between the system variable: inputs and outputs variables, a mathematical model of may be defined. The model can be defined in continuous time (CT) through differential equations and transformed into the Laplace domain (reduces differential equations into an algebraic equations). The system may also be defined in discrete time (DT) using difference equations or Z-transform.

In practice, the complexity of systems and the ignorance of all the relevant factors necessitate the introduction of assumptions concerning the system operation (Dorf & Bishop., 2011). After defining the mathematical model, a solution may be obtained describing the operation of the system. To guarantee a satisfactory model has been developed, model validation is necessary and can be performed by comparing the actual system with the model under identical inputs. Mathematical models can be solved using popular software packages like MathWorks (MATLAB and Simulink) or Microsoft Office (Excel). For certain systems, it may prove to be difficult or time

consuming to define an adequate mathematical model. As an alternative, it may be suitable to define a model based on the actual system, known as system identification.

3.3. System Identification

System identification is an experimental procedure and is used to determine particular models for systems based on observed inputs and outputs (Garnier & Wang, 2008; Johnson & Moradi, 2005; Liu & Gao, 2012). This is particularly useful for modest systems (controlling a motor, a pump, etc.); however, for more complex systems, a satisfactory model may be defined through approximation. A model approximation may be achieved by representing a system using only first or second order plus dead time (FOPDT or SOPDT) models (Liu & Gao, 2012). A FOPDT is similar to the plant transfer developed previously except that it includes the concept of ‘dead time’: any delay in measuring, controller action or system response, and has the following form where L represents the delay:

$$FOPDT(s) = e^{-L*s} \frac{K}{\tau s + 1} \quad (23)$$

The problem is now to find the optimal parameters: K , τ , and L that best fit the response of the system. A simple method to generate experimental data may be using the open loop response, i.e. no feedback or controller, of the system with zero initial conditions to a step input of magnitude U and output response Y . Typically, this data is generated as discrete time (DT) system, the sampling rate may be fast enough to be approximated by a continuous time (CT) system. Applying the Z-Transform to the FOPDT model results in the following discrete form, where T_s is the sampling period:

$$FOPDT(z) = \frac{Y(z)}{U(z)} = \frac{z - 1}{z} * Z \left\{ \frac{FOPDT(s)}{s} \right\} = \frac{K \left(1 - e^{-\frac{T_s}{\tau}} \right) z^{-1}}{1 - e^{-\frac{T_s}{\tau}} z^{-1}} * z^{-\frac{L}{T_s}} \quad (24)$$

The difference equation may be derived from the discrete form:

$$Y(z) \left(1 - e^{-\frac{T_s}{\tau}} z^{-1} \right) = U(z) K \left(1 - e^{-\frac{T_s}{\tau}} \right) * z^{-\frac{L}{T_s}} \quad (25)$$

$$y(n) = e^{-\frac{T_s}{\tau}} y(n-1) + K \left(1 - e^{-\frac{T_s}{\tau}} \right) u \left(n - 1 - \frac{L}{T_s} \right) \quad (26)$$

Where n represents the sample number of the data. An optimization problem may be defined by expressing a predictor, parameter vector, and predictor error (Garnier & Wang, 2008):

$$\text{Predictor: } \hat{y}(t, \theta) = G_p(t, U, \theta) \quad (27)$$

$$\text{Parameter vector: } \theta = [K \tau L]^T \quad (28)$$

$$\text{Minimize (output error)}^2 = \arg \min_{\theta \in [0, \infty)} \varepsilon^2 = \arg \min_{\theta \in [0, \infty)} (y - \hat{y})^2 \quad (29)$$

Solving optimization problems is tedious; however, various software packages offer mathematical solvers that implement known optimization algorithms: MATLAB (Interior-point, Quasi-Newton Method), and EXCEL (GRG Nonlinear). The problem may also be solved through linear least-square (LS) estimation if the delay term can be determined experimentally or is deemed unnecessary (i.e. no observable delays or neglecting it). A complex method exists to solve the LS problem with the delay term by using a two stage LS (Garnier & Wang, 2008). For the moment, the optimization problem may be defined into a linear LS estimation by removing delay term and rewriting the difference equation into matrix form:

$$\text{Linear system: } Y = X * \theta \rightarrow y(n) = [y(n-1) \ u(n-1)] \begin{bmatrix} \theta_1 \\ \theta_2 \end{bmatrix} \quad (30)$$

$$\text{Parameter vector: } \theta = [\theta_1 \ \theta_2]^T = \left[e^{-\frac{T_s}{\tau}} \ K \left(1 - e^{-\frac{T_s}{\tau}} \right) \right]^T \quad (31)$$

Where matrix X represents the previous states of the output Y and input U , and vector Y represents the current states of the output. Solving for the parameter vector may be done directly through matrix manipulation, the result is known as the normal equations:

$$Y = X\theta \rightarrow X^T Y = X^T X \theta \rightarrow (X^T X)^{-1} X^T Y = (X^T X)^{-1} X^T X \theta = \theta \quad (32)$$

$$\theta = (X^T X)^{-1} X^T Y \quad (33)$$

$$\text{Therefore: } K = \frac{\theta_2}{1 + \theta_1}, \tau = -\frac{T_s}{\ln(\theta_1)} \quad (34)$$

For cases where matrix X is singular, LS can be solved using Moore-Penrose pseudoinverse.

3.4. Control Strategy – PID Control

Mathematical models allow the understanding of a system and make predictions about how a system will behave. With this knowledge, a control algorithm may be designed to take advantage of the system's dynamics to enhance performance, provide stability to the process, and ensure safe operations. The physical unit of a controller will be discussed in the implementation section: from physical implementation, measuring the process variable, to computing corrective actions and actuating the process. The control algorithm is the logic of the controller and the most popular control strategy is the Proportional-Integral-Derivative (PID) controller, approximately 95% of all control loops in the world (Åström & Hägglund, 2005). Essentially, PID controller compares the set-point (SP) with the process variable (PV), known as the error signal, and computes a controller output based on the following equation:

$$\text{Error} = e(t) = SP(t) - PV(t) \quad (35)$$

$$\text{PID Controller Output} = u(t) = K_p \left(e(t) + \frac{1}{T_i} \int e(t) dt + T_d \frac{de(t)}{dt} \right) \quad (36)$$

This controller algorithm is called a PID controller in standard form because it contains a **P**roportional, an **I**ntegral and **D**erivative term represented by K_p , T_i and T_d . The logic for the proportional term is in essence the following: it applies an effort, or signal, in proportion to how far the set-point is from the process variable: the larger the error, the larger the controller output and vice versa. For the integral term, a controller considers the history of the error, essentially how long and how far has the output been from the set-point over time. The integral term is especially useful to eliminate error when the system is in steady-state. The derivative term gives a controller additional control action when the error changes constantly. In many situations, the derivative term will include a low-pass filter in order to eliminate high frequency noise amplification, caused by differentiation, known as derivative kick (Johnson & Moradi, 2005).

The design of a PID controller requires an adequate selection of the parameters K_p , T_i and T_d . A common method to designing any controller is to define satisfactory performance specifications such as settling time, rise time, overshoot. A sample step response is shown in Figure 3.4-1. The steady-state value (y_{ss}) of a step response is the final level of the output, assuming it converges. Settling time (T_s) is the time required for the response to reach and stay within a range of certain

percentage (usually 2%) of the final steady-state value, rise time (T_R) is the time required for the response to rise from 10% to 90% of its final steady-state value and the overshoot (M_p) is the percentage of the final value by which the response initially rises above the final value (Åström & Murray, 2012).

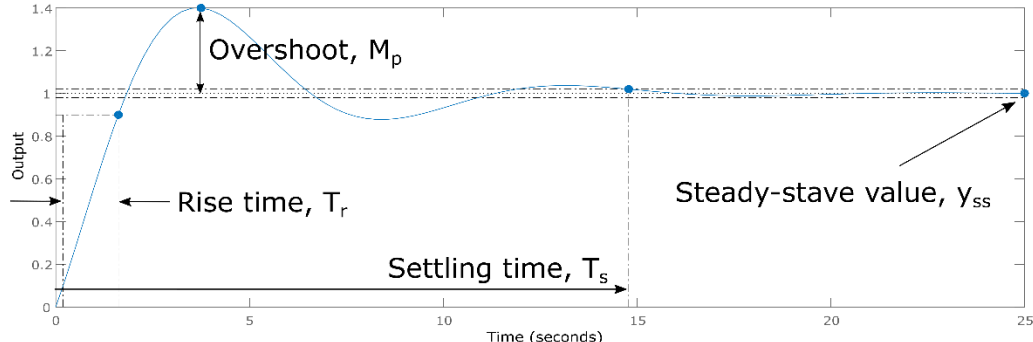


Figure 3.4-1: Performance Parameters in Step Response

With the selection of satisfactory performance specifications, a controller may be designed using one of the several methods (frequency domain methods, pole-placement, Ziegler–Nichols tuning method, Åström-Hägglund, Skogestad, optimization tuning, etc.) (Åström & Hägglund, 2005; Chen, 2006; Ziegler & Nichols, 1942). Ziegler and Nichols were pioneers in the field of control theory for their significant contributions. They presented the Ziegler-Nichols tuning method which proved to be a simple and elegant method for adjusting PID parameters by approximating the response of a system. Skogestad (2001) and Åström-Hägglund (2005) present another experimental method for tuning PI controllers and is compared to the standard method: Ziegler-Nichols. The method demonstrated to result in improved stability and robustness over Ziegler-Nichols' method. It would be interesting to investigate this method as they are relatively simple to design and implement. Once the controller has been designed, further manual tuning on the physical system may be performed to precisely adjust the controller, particularly when the system model is an approximation and doesn't capture all system's dynamics.

3.5. Implementation

The first part of implementing a control system is related to the hardware, from measuring the process variable to actuating the process. A wide range of sensors are available to measure process variables: flow meter for a pump, level gauge for a tank, etc. Sensors have various parameters that must be selected carefully in order to accurately measure and capture the process variables, here are the main parameters: range, accuracy, and precision, resolution and response time. The range

of a sensor is the maximum and minimum values of process variables that can be measured. The accuracy is the maximum difference that will exist between the actual value and the indicated value of the sensor. Precision refers to the degree of reproducibility of a measurement. Resolution refers to the smallest detectable incremental change of a process variable that can be detected by the sensor. Finally, response time refers to the time taken by a sensor to approach its true output. Other important parameters must also be wisely chosen such as sensor output (digital or analog), operating environmental conditions, material selection, calibration frequency, etc. After that, the controller need to be able to modify the input to the process by using an actuator: pump, motor, control valves, etc. Typically, actuators receive an input from the controller and are programmed to respond according to the input. A controller is physically integrated into a digital computer, which in process control is normally a programmable logic controller (PLC) or programmable automation controller (PAC). A touch panel (in the control jargon it is referred to as a human machine interface (HMI)), may be implemented to provide graphical user interface that allows an operator to observe and modify process parameters. The controller algorithm is programmed inside the PLC/PAC memory, the sensors' measurement outputs are connected to the PLC/PAC inputs, and actuators inputs are connected to the PLC/PAC outputs (Figure 3.5-1).

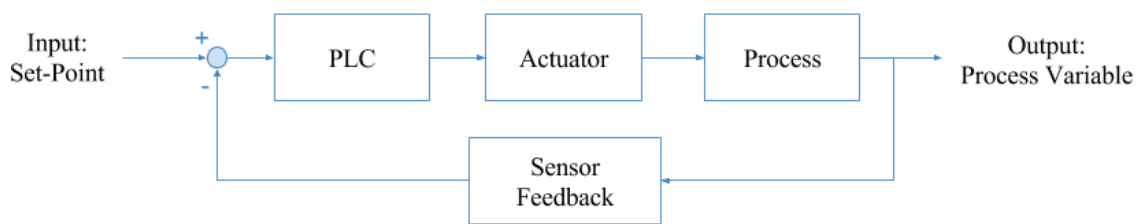


Figure 3.5-1: Hardware Implementation

The second part of implementing a controller is the digital implementation: developing the software algorithm to perform the control action. The PID control structure shown below is considered to be continuous-time: the error and output signal are changing continuously.

$$PID = u(t) = K_P \left(e(t) + \frac{1}{T_i} \int e(t) dt + T_d \frac{de(t)}{dt} \right) \quad (37)$$

However, digital computers are not continuous systems but rather discrete systems. The difference between the two systems are that discrete systems have finite states at specific intervals, or

sampling period; therefore, a discrete system may approximate a continuous system by having an infinitely small sampling period (Figure 3.5-2).

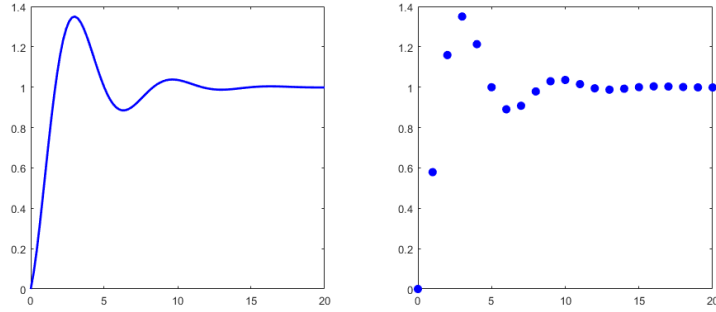


Figure 3.5-2: Continuous vs Discrete Systems (sampling at 1s)

Conversely, a continuous-time system may be represented by a discrete-time system through discretization. For a PID controller, discretization can be performed with the application of Euler's method (Franklin et al., 1997). A discrete PID controller in standard form using Euler's forward method has the following form (Franklin et al., 1997):

$$PID_{discrete} = u[n] = u[n - 1] + K_p \left(1 + \frac{T_s}{T_i} + \frac{T_d}{T_s} \right) e[n] - K_p \left(1 + \frac{2T_d}{T_s} \right) e[n - 1] + K_p \left(\frac{T_d}{T_s} \right) e[n - 2] \quad (38)$$

Where T_s is the sampling period, and the index n refers to the sample number. In discrete form, the PID controller may easily be implemented to any digital computer with pseudocode in Figure 3.5-3.

```

Initialize:
e_{n-1} = 0
e_{n-2} = 0

Loop:
yinput = set-point
youtput = read measurement from sensor
en = yinput - youtput
un = un-1 + Kp (1 + Ts/Ti + Td/Ts)en - Kp (1 + 2Td/Ts)en-1 + Kp(Td/Ts)en-2
en-2 = en-1
en-1 = en
Send un to actuator
Repeat Loop

```

Figure 3.5-3: Software Implementation – Discrete PID (Pseudocode)

The information provided in this work describes the fundamental steps to designing a successful automatic control system. It is important to understand the behaviour of the system so that a controller may be designed to meet satisfactory performance specifications. Finally, the controller may be implemented with appropriate sensors and actuators to allow satisfactory control of the process. An essential step in implementing a PID controller is the selection of the sampling rate and understanding its impact on the system's response. A digital PID algorithm requires an amount of time to perform the computations and, in most cases, other tasks need to be completed in conjunction by the programmable controller, such as controlling pumps. Therefore, it is important to leave an interval of time, known as the sampling period, between PID computations for these other tasks. By definition, the sampling rate is the number of sampling periods per second.

Chapter 4: Automation of the MEBR

4.1. Automation Overview

By definition, automation is allowing a system to operate without the intervention of a person. Automation is typically achieved by integrating computer electronics with electrical and mechanical devices that are controlled by predefined control logic. The automation of MEBR can be viewed as followed:

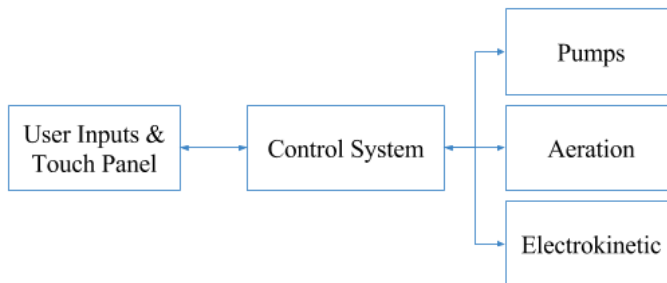


Figure 4.1-1: MEBR Automation

Where ‘User Inputs & Touch Panel’ controls and displays the settings for the parameters, ‘Control System’ refers to how the inputs interact with various processes, and ‘Pumps’, ‘Aeration’ and ‘Electrokinetic’ refers to the processes used in the MEBR (Figure 4.1-1). This chapter will first outline the MEBR processes, and then demonstrate the automation of each processes.

4.2. MEBR System Overview

The fundamental MEBR design was based on a patent by Elektorowicz et al (2015). One of the objectives of this project is to simulate a completely functional and automated wastewater treatment for a household that could potentially be used in remote locations; therefore, the system had to fit in a convenient facility: a common shed (10ftx8ftx8ft). The general guidelines for the system were the following:

- Continuously treat 2000L of wastewater per day (HRT of 12h, SRT of 20days).
- 1000L MEBR tank (830L effective) and 100L feed tank.
- 4 pairs of electrodes: 80cm by 60cm, with 40%-hole perforation. Material for anode is aluminum and cathode is stainless steel, distance between electrodes of 5cm.
- 4 membrane modules in series with a cross flow velocity of 3-4m/s. Based on membrane module diameter, this resulted in:

- Circulation loop flow rate required is 10,000L/h.
 - Circulation feed flow rate required is 1,000L/h.
- Instrumentation:
 - Water levels (feed and MEBR).
 - DO and temperature.
 - Aeration and air flow control.
 - EK power supply and current measurement.
- Automated system:
 - Filling of both feed and MEBR tanks, using water level sensors in combination with MEBR and feed pumps, with observable and adjustable levels from HMI.
 - Automatic circulation feed and circulation pumps based on level in bioreactor.
 - Adjustable aeration & air compressor purging based on DO.
 - Electrokinetic: control for current density with adjustable exposure time, as of now it is 5minutes on time and 15minutes off time.
 - Data acquisition of current density, DO, temperature, and air flow rate at desired intervals (10sec or 1min).
 - Safety verifications (short circuits, power, clogged pumps).

The system overview is shown in Figure 4.2-1, it shows the flow of wastewater in MEBR system, no control panels and wiring are shown here beside electrodes connection.

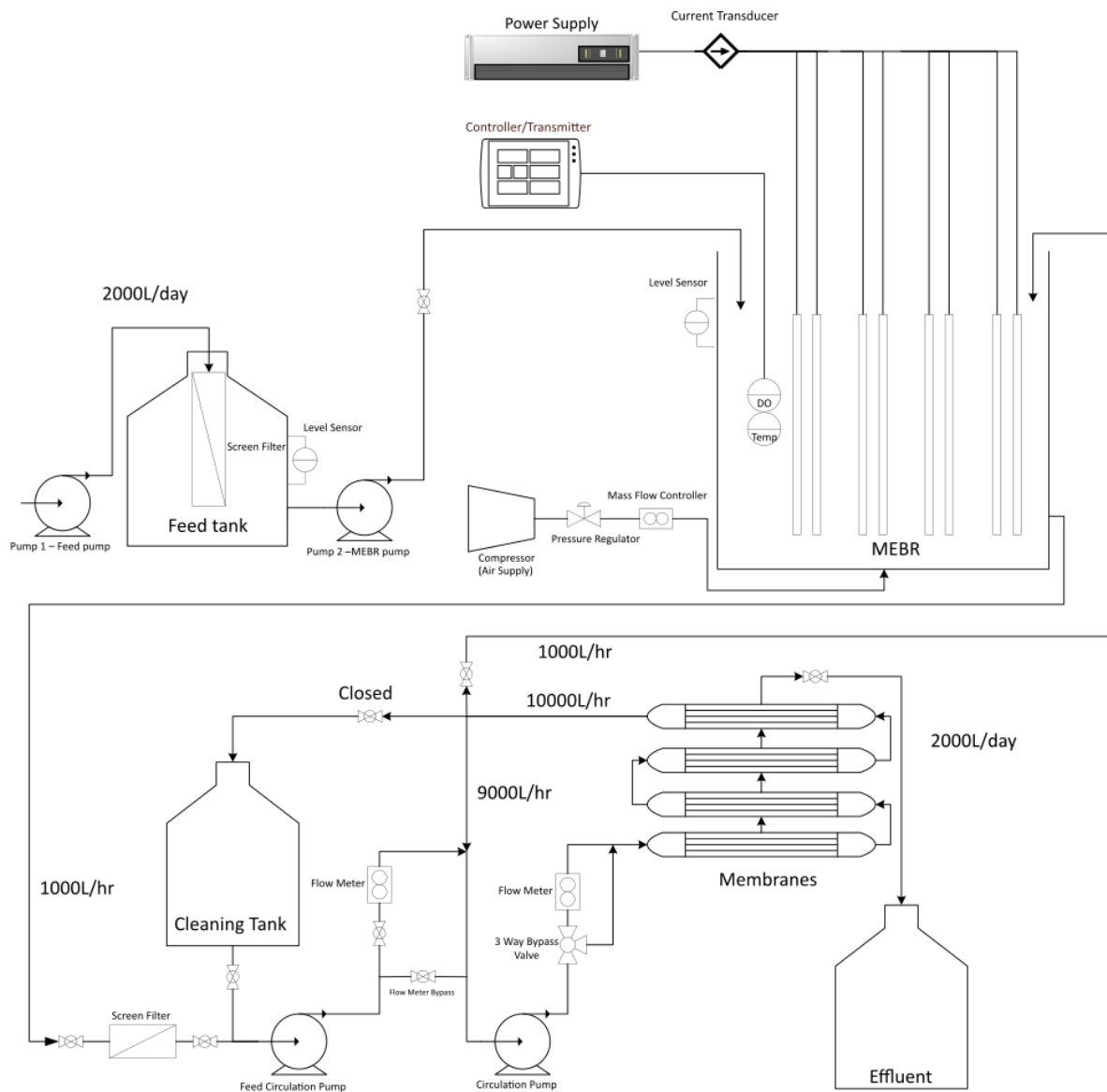


Figure 4.2-1: MEBR System Overview

The wastewater is pumped into the feed tank using a submerged pump, known as the feed pump. The feed pump is located within one of the two pre-treatment channels inside L'Assomption WWTP. The pump is located directly after screening but before grit removal; therefore, besides screening, no other treatments are performed on the wastewater pumped to the feed tank. The reason for installing the feed pump after screening is because no screening system is available on the market for a project this size and for a reasonable price. It was attempted to install the feed

pump before screening; however, the feed pump was clogged in a matter of minutes because of large debris like toilet paper.

The wastewater is pumped into the feed tank that has a screen filter to remove debris that may have passed screening. Without this filter, the rest of the pumps would be clogged within half a day. The wastewater is then pumped in the MEBR using the MEBR pump. Inside the MEBR, air is injected through fine bubble diffusers located at the bottom of the tank. After the MEBR, wastewater enters the circulation loop for the membrane filtration process. Another screen filter is used at the beginning of the circulation loop as a safety precaution to protect the circulation pumps, this filter might be removed in the future. The circulation feed pump flow rate is set to 1000L/h, by using a ball valve and mechanical flow meter. The circulation loop flowrate is 10,000L/h to ensure the cross-flow velocity of 3-4m/s inside the membrane modules. After the membranes, 1/10th of the flow (1000L/h) returns to the bioreactor and the remaining (9000L/h) is returned in the circulation loop. Water permeating through the membrane, the effluent, is returned to the WWTP. The effluent flow rate is set by ball valve. By-pass valves were added as a precaution of fouling occurring in the mechanical flowmeters.

4.3. Instrumentation

In order to have a completely automated system, it is important to measure process variables in real time. In the case of the MEBR, the following instruments are required:

- Water level sensors
- DO and temperature probes
- Aeration and air flow control
- EK power supply and current measurement

Water Level Sensors

There are many different types of water level sensors available: mechanical floats, ultrasonic, optical or magnetic switches. An ultrasonic level transmitter was selected because it may be easily programmed for any desired levels and tank shapes. As there is no physical interaction unlike floats or switches, this means effectively no maintenance is required. Furthermore, the accumulation of foam could be an issue for the other types of sensors, and for this project, there is foam being produced. The selected ultrasonic sensor is the Omega LVCN414, which is simply a

rebranded Flowline Echopod DL14. It has the following specifications (“LVCN414 Level Sensor,” 2017):

- Range: 0-1.25m
- Accuracy: $\pm 3\text{mm}$.
- Resolution: $\pm 0.5\text{mm}$.
- Dead band: 5cm.
- Water level signal output: 4-20mA (loop powered and selectable range).
- Loop fail-safety.
- 4 SPST relays rated at 1A with relay fail safety.
- Automatic temperature compensation: -35-60°C.
- PVDF Housing material.
- Programmed via free PC software.

Dissolved Oxygen & Temperature

Monitoring of dissolved oxygen is critical for the activated sludge process, especially for the MEBR. It is critical to ensure that there is sufficient DO in the bioreactor for the biological activity to take place in order to ensure waste biodegradation. Insufficient oxygen will slow down or kill off the very aerobic organisms the bioreactor is designed to cultivate. On the other hand, if DO levels are too high, it can result in excessive power consumption (increased operating costs). Generally, there are two types of in-situ, or on-line, probes for DO measurement: galvanic membrane or optical probes (Kiser, 2012).

Galvanic membrane probes essentially consist of an electrochemical cell with a DO-selective membrane, which allows oxygen to migrate to the cell. By doing so, the probe measures the electric current created as oxygen is being reduced. Membrane probes are less expensive than optical probes; however, they are known for measurement error due to the contamination of the membrane or due to the depletion of oxygen at the membrane, they also require frequent membrane replacement (Kiser, 2012; Sawyer et al., 2003). Optical probes were developed to overcome these issues. Optical probes are fundamentally based on luminescence (Figure4.3-1). The probe has a luminescent coating located on its surface. Blue light emitted from a light emitting diode (LED) is transmitted to the surface which excites the coating. As this coating relaxes, it emits red light. The

time from when the blue light was sent and the red light is emitted correlates to the oxygen concentration. The more oxygen present, the shorter the time it takes for the red light to be emitted. To ensure repeatability, an internal red LED is used as an internal reference between flashes of blue light (HACH, 2011; Kiser, 2012).

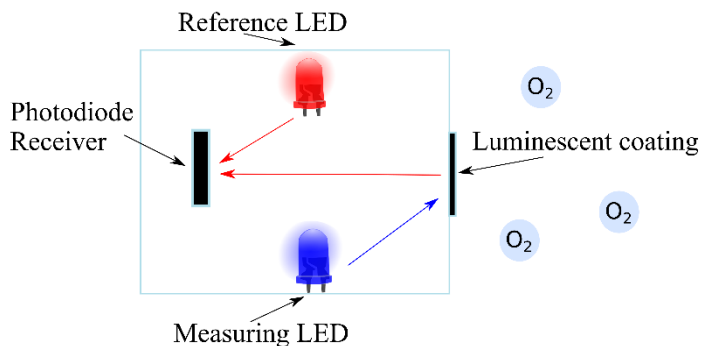


Figure 4.3-1: Luminescent Dissolved Oxygen working principle

For this work, various luminescent dissolved oxygen (LDO) probes were assessed. Many available LDO probes have similar specifications in terms of resolution, range, response time and sizes; however, all available sensors, except for one, had their housing made of stainless steel and this was considered a major concern. The sensor would be immersed near electrodes and stainless steel may have corroded too fast. Therefore, the choice of the LDO sensor was limited to the HACH LDO 2 Saltwater, where the housing is made of Noryl, which has excellent corrosion resistance. Another advantage of the HACH LDO 2 sensor is that it has higher accuracy than other sensors in low DO concentration. The HACH LDO 2 also includes a temperature probe. Here are the important specifications (“HACH LDO 2,” 2017):

- Accuracy:
 - $\pm 0.05\text{mg/L}$ below 1 mg/L
 - $\pm 0.1\text{mg/L}$ below 5 mg/L
 - $\pm 0.2\text{mg/L}$ above 5 mg/L
- Range: 0 to 20.00 mg/L
- Resolution: $\pm 0.01\text{mg/L}$
- Repeatability: $\pm 0.1\text{mg/L}$
- Integrated temperature and correction: $\pm 0.2^\circ\text{Celsius}$
- Temperature range: -5 to 55 $^\circ\text{Celsius}$.
- Response time, $t_{95} < 60\text{seconds}$.

Like most LDO probes, the HACH LDO requires a controller to calibrate the instrument, view and transmit the data. The SC200 Controller was chosen so that two sensors can be used with this unit, even though only the LDO is used at the moment. An additional probe could always be added later in the project (pH, ORP, conductivity or Ammonia). Other benefits of using this controller is that the data (DO and temperature) may be transmitted on analog signals (4-20mA). Also, direct data acquisition is possible using an SD card.

Aeration & Air Flow Control

With DO concentration being measured in real time, a mass flow controller (MFC) is necessary to measure and control the aeration within the bioreactor. An MFC allows the simultaneous measurement and control of the air flow rate integrated into one instrument. Various MFC are available in the market with similar specifications. The final choice was the Sierra SmartTrak 50 as it met all design specifications, while also being in the most economical. Here are the important specifications (“Sierra SmartTrak 50,” 2017):

- Accuracy: $\pm 1\%$ full scale. Full scale is 200sLPM: $\pm 2\text{sLPM}$.
- Range: 0-200sLPM.
- Repeatability: $\pm 0.25\%$.
- Response time, $t_{90} = 0.3\text{s}$.
- Set-point signal: 4-20mA (sourcing).
- Process variable signal: 4-20mA (sourcing).
- Inlet max pressure: 150psi.
- Differential pressure requirement: 30psi.

To supply the aeration process, a quiet and capable air compressor was required. As this project was being setup inside a small shed, noise was a major concern. Similarly, to reduce maintenance, an oil-less air compressor was chosen. The final choice was the California Air Tools 4620A, which has the following specifications.

- 180sLPM max (non-continuous) air flow rate at 40psi.
- Outlet pressure can be regulated from 70kPa (10psi) to 620kPa (90psi).
- Only 70 decibels with a 2hp motor.

- 20Litre air tank. This allows the motor to turn off when the tank pressure is between 620 and 820kPa (90 and 120psi).
- Low start amp draw: 14Amps. For a 2hp motor, this was critical because it is connected on a standard 15A/20A outlet (common household outlets in Canada).

Another concern with air compressors is that they need to be purged frequently when used during extended periods of time because of water build-up in the air tank, which may cause premature corrosion. Therefore, the original manual purge valve was removed and replaced with a solenoid valve that is connected to the main control system. The control system purges the air tank every 30 minutes with a sequence of two 2 seconds on-off purges.

EK Power Supply and Current Measurement

The EK process is operated with a programmable AC-DC power supply with a current transducer as a feedback sensor. The power supply used for this project is the XP Power HDS1500PS24, and the HDS series is truly exceptional for the price and specifications (“HDS1500 Datasheet,” 2017):

- Output power = 1500W, 24Volts at 62.5Amps.
- High efficiency = 91%.
- Power density = 9.7W/in³.
- Programmable output voltage and current: 0 to 105% of rated values (24V, and 62.5A). Fully programmable output voltage and current.
- Zero minimum load, 1%-line regulation and 1% peak-peak ripple and noise.
- Rise time of 120ms maximum at full load.
- Overvoltage, overload, and over temperature protection.
- Short circuit protection with auto recovery.
- Remote sense is available, can be used to compensate for losses in transmission cables.
- Easy to scale up to 5 units can be current shared (in parallel) for a total power of 7500W.

For current measurement, AcuAMP DCT current transducer was chosen. It has the following specification (“AcuAMP DCT,” 2017):

- Fixed core transducer with 0-50, 0-75, or 0-100A jumper-selectable input ranges.

- Accuracy: $\pm 1\%$ full scale, at the moment the selected input range is 0-50A resulting in an absolute accuracy of $\pm 0.5\text{A}$.
- Repeatability: $\pm 1\%$ full scale.
- Response time, t_{90} : 0.02seconds.
- Output signal: 4-20mA (sourcing).

It may seem strange at first to use a current transducer when the power supply can control both the voltage and current. This project requires constant current, one way it could have been achieved is by setting the power supply is constant current mode. A reason why this is not desirable is that there is no feedback information on applied voltage, which means there is no way to know the actual power used. This could have been resolved by purchasing a voltage transducer. However, from a safety perspective, this is not ideal as there is no way to detect a short circuit. Fortunately, this power supply has short circuit protection with auto recovery, but if a short circuit exists, the power supply will continuously loop in short circuit and auto recovery. Instead, it is preferred to have a true current feedback from a current transducer:

- Actual short circuit detection.
- More accurate current measurements.
- Easier to calibrate power supply voltage output, as opposed to current output.

For additional short circuit protection, each anode of the EK process are fused with 30A fuses.

4.4. Prototyping & Arduino

Prototyping

An important stage in developing in any projects is assessing the requirements, which is no easy feats in automation as there is a long journey between the concept and the actual building of a control system. In many cases, the requirements of a project may not be well known in the early stages of a project and it may not be evident on which approach works best. Consequently, prototyping resolve these issues early in the development. It also provides a better understanding of the problem, allows one to gather more accurate and additional requirements, and it is relatively inexpensive. Therefore, building prototypes was considered a must especially since it was possible to start controlling different aspects of the project early on.

Arduino

To implement a control logic that can interact with the real world, electronic components must be used. Arduino is an open-source electronic platform that seamlessly integrates hardware and software in order to make electronics more accessible for anyone to interact with both the digital and physical world, which is ideal for prototyping. Arduino have established a trend in the electronic world for low-cost microcontroller and several companies now offer similar microcontrollers for various price ranges. A microcontroller (MCU or μ C) is essentially a small computer than can interact with the real world with various inputs and outputs, whether be digital (switches/buttons, displays) or analog (sensors). The greatest advantage with the Arduino environment is the open source nature, where users around the world share pieces of codes (libraries, algorithms) to interact with many peripherals (i.e. LCD display), which greatly reduces prototyping time and errors in programming. Additionally, the programming language for microcontrollers is C and/or C++, which is very popular and vast amount of information is available online. Two controller prototypes were built to assess the requirements for controlling the entire MEBR: a prototype controller for the pumps, and a prototype controller for EK. These prototypes were implemented and tested from September to December 2016.

Prototype 1 – Pump Control System

The first prototype built was for controlling the pumps (Figure 4.4-1). This allowed to get the system running automatically, enabling the bacteria to stabilise before applying EK. The pump controller prototype was built upon the Arduino Nano board which uses the popular Atmega328p microcontroller. This board was selected for its small size and number of inputs and outputs (I/O) available: digital I/O pins = 14, analog I/O pins = 8.

The controller prototype performed the following task:

- Read input for manual or automatic mode.
- Acquire wastewater levels from ultrasonic sensors.
- Control four pumps accordingly.
- Control two LED indicators (green and red) for pump controller status.
- Display information to LCD (water levels). Also, displays errors if they occur.
- Emergency stop button (turns off all four pumps through by-passing pump controller).

In Figure 4.4-1 is a picture of the front and interior panel for the pump controller. Note that the circulation and circulation feed pump relays are not located in this control panel, instead in the prototype 2.

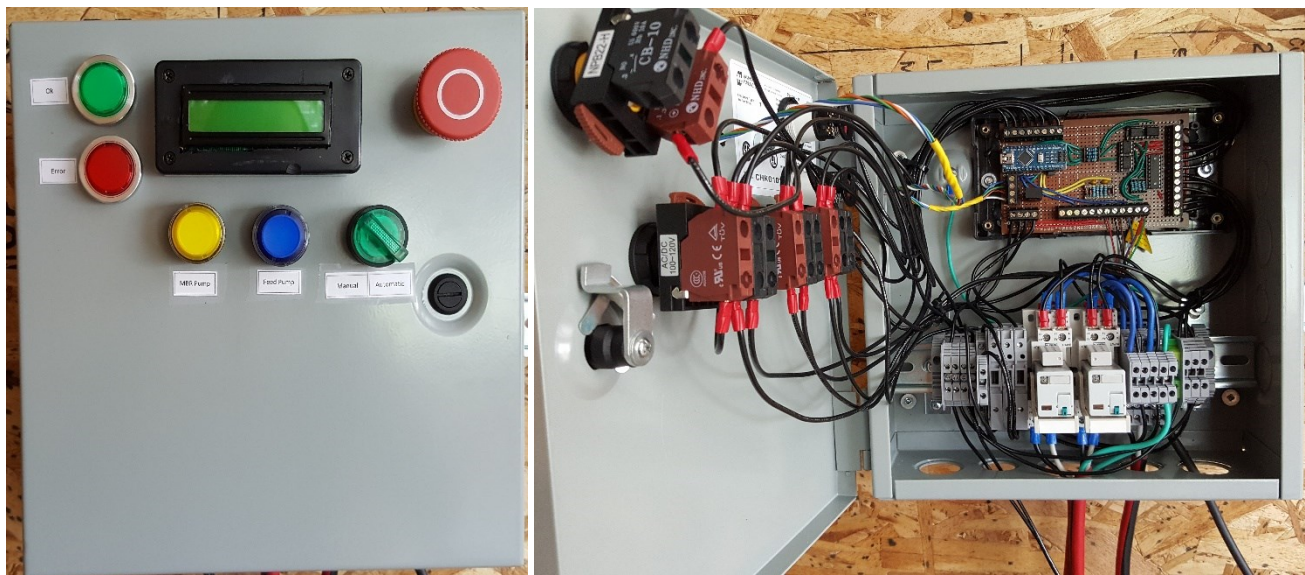


Figure 4.4-1: Pump Controller Prototype 1 – Front & Interior Panel

Prototype 2 – EK Control System

The pump controller prototype was built upon the Arduino Mega2560 board which uses the Atmega 2560 microcontroller (Figure 4.4-2). This board was selected for its large number of inputs and outputs (I/O) available: digital I/O pins = 54, analog I/O pins = 16.

The controller prototype performed the following task:

- Control CD through PI controller, and allow different CD, and ON and OFF times.
- Acquire measurements: CD, applied voltage, DO, temperature and time, which were logged to an SD card. Time was provided using a real-time clock module.
- Purge the air compressor at desired intervals through solenoid valve.
- Display information to LCD (CD, V, DO, Temp and time). Also, displays errors.
- Emergency stop button (turns off power supply).

In Figure 4.4-2 is a picture of the front and interior panel for the EK controller. Note that the circulation and circulation feed pump relays are located in this control panel.

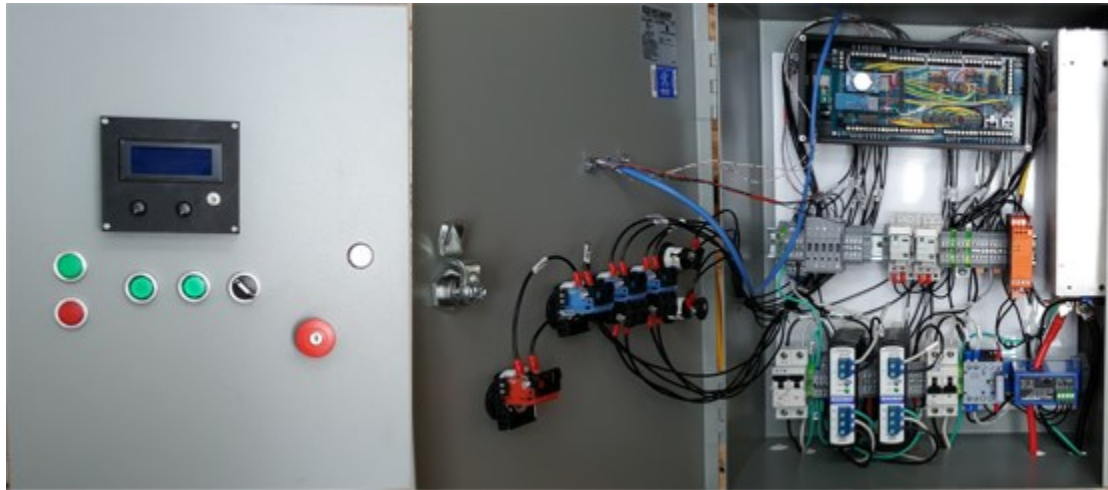


Figure 4.4-2: EK Controller Prototype 2 – Front & Interior Panel

A manually tuned PI controller algorithm has been implemented to simply assess how to get started in controlling CD. The PI controller was able to achieve acceptable performances: reasonably fast settling time: <10sec, little to no observable overshoot, and no steady state errors. The reason why it was possible to manually tune the PI controller is due to the direct relationship between voltage applied by the power supply and current density. However, as will be discussed in a later section, a proper PI controller will be designed.

Arduino Software Implementation

Using the Arduino platform, the programming language used to implement the controller algorithm is C++, which is an object-oriented programming language. Therefore, the first step was to develop the appropriate classes, or objects, that would be used in the software. Next was developing the necessary control algorithms.

4.5. Industrial Automation

Arduino is a great platform for prototyping for the reasons enumerated previously; however, they are not adequate for industrial automation. Industrial automation requires more robust solution due to harsh environments, and typical automation requires safe, reliable and continuous operations. Industrial automation is commonly achieved using programmable controllers, either programmable logic controllers (PLC) or more recently programmable automation controllers (PAC). The PAC can be thought of an improved PLC: allowing more advanced communications (Ethernet), advanced control algorithms, better data handling, and multitasking operations. PLC/PAC may be programmed based on the IEC 61131-3 standard, which defines 5 programming languages:

- Ladder diagram (LD)
- Function block diagram (FDB)
- Structured text (ST)
- Instruction list (IL)
- Sequential function chart (SFC)

The programming language supported on a specific PLC/PAC is vendor specific but most of them, if not all, support LD. LD, sometimes referred as ladder logic, is the preferred language in many cases because it's a graphical (as opposed to text based) language and electricians/technicians are typically learn it and are quite familiar with it, therefore greatly simplifies code maintenance when issues occurs.

Programmable Controller

After successful prototyping, an industrial programmable controller was necessary to ensure robust automation. For this purpose, the Productivity 2000 (P2000) from *AutomationDirect* was selected for the following reasons:

- Powerful CPU: sub-millisecond scan times
- Vast communication possibilities: RS232, RS485, Modbus RTU, Modbus TCP/IP, Ethernet/IP, and TCP/UDP
- Tag name database that can be directly exported to an HMI
- Remote monitoring and programming
- Built-in data logging, with remote connectivity to access data logs
- Built-in PID algorithm, even for cascade PID control
- Up to 4000 inputs and outputs per controller
- Free programming software and technical support

A touch panel, also known as human machine interface (HMI), was also acquired from *AutomationDirect*, C-More Micro 6”, to locally monitor and modify the system’s processes. The P2000 can be configured with various modules for different types of I/O depending on the project needs. Based on the two prototypes built previously, those requirements were identified. The P2000 was configured as show in Table 4.5-1.

Table 4.5-1: P2000 Configuration

Component	Description	Model	Qty.
P2000 CPU	CPU	P2-550	1
Base	7-slot base for modules, CPU and power supply	P2-07B	1
Power Supply	110VAC input based power supply	P2-01AC	1
Discrete input	16-point, 12-24VDC	P2-16ND3	1
Discrete output	16-point, 12-24VDC	P2-16TD1P	1
Relay output	16-point, 6-24VDC/6-240VAC, 2 isolated commons	P2-16TR	1
Analog input	8-channel, 16bit resolution, 0-20mA	P2-08AD-1	1
Analog output	8-channel, 16bit resolution, 0-10VDC	P2-08DA-2	1
Analog output	4-channel, 12bit resolution, 0-20mA	P2-08DA-2	1
Filler	Module for protecting empty base slots	P2-FILL	1

To setup and program the P2000 and the HMI, the free programming software offered by *AutomationDirect* were used: *Productivity Suite v2.4.0.16* and *C-More Micro v4.10*. The industrial automation has been operational since December 13, 2016 with a data logging interval of 10seconds.

Remote Connectivity & Network

A local area network (LAN) was built using a wireless router (D-Link 825) and an Ethernet switch from *AutomationDirect* (SE-SW5U), which links the router to the P2000 and HMI to the router, see Figure 4.5-1. In order to permit remote connectivity to the P2000 and HMI from outside the LAN, it is important to port forward their respective internal access ports to the router. The P2000 offers different ports for various features: programming/remote access, web server for data logs, SMTP for emails, MODBUS, and Ethernet/IP.

The programming software for the P2000 and the HMI allow the system to be monitored and programmed remotely (Figure 4.5-1). The P2000 can also create an internal web server where the data logs can be found and downloaded. In addition to allowing for remote monitoring of the process and bring modifications, the P2000 software may also override parameters by forcing them to any value. For this project, the following ports were forwarded in the router:

- P2000 programming/remote access port (UDP port 9999, not configurable),
- Web server port to remote access to data logs (TCP port configurable and set to 80).
- HMI programming port (UDP port 9999, not configurable).

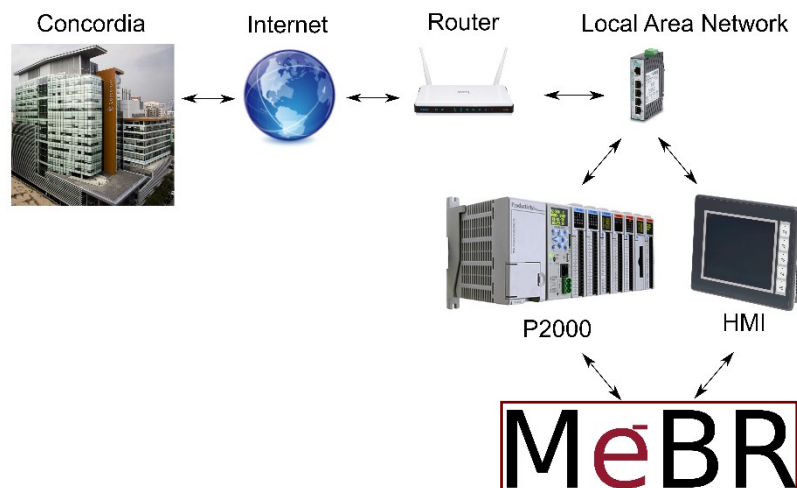


Figure 4.5-1: MEBR LAN & Remote Connectivity

Control Panel

All components (P2000, HMI, relays, fuses, power supplies, etc.) were installed in a control panel for added protection. The router is installed on top of the control panel. The Figure 4.5-2 shows the front and interior of the enclosure.

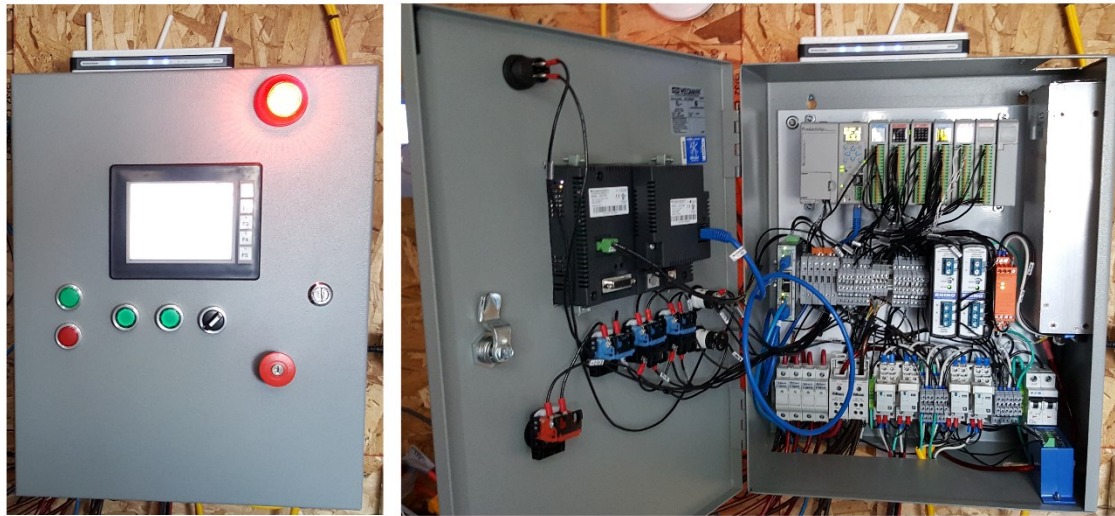


Figure 4.5-2: MEBR Control Panel – Front & Interior

The following components are installed on the front panel:

Table 4.5-2: Front Panel – Components

Component	Description	Model	Qty.
Green LED	Indicator	DR22E3L-E3GZA	1
Red LED	Indicator	DR22E3L-E3RZA	1
Green Push button	Pumps & EK Activation	AR22F5L-10E3GZA	2
Selector Switch	Enable or disable system	AR22PR-210BZA	1
Emergency Stop	Stop system	AR22V7R-01R	1
Red signal beacon	Power indicator	20610000 & 95584035	1
HMI	Touch screen panel	C-More Micro EA3-T6CL	1

The green and red LED are used as indicators. Two green pushbuttons are used:

1. Pumps automatic mode when pressed, or manual mode when depressed.
2. EK enabled mode when pressed, or disabled when depressed.

A selector switch and emergency stop are both connected to a safety relay within the enclosure. These are used in combination to enable or remove power going to the relays, which provide power to the pumps when activated, and EK power supply. The rotary switch is useful to quickly remove or restore power when verifying connections in the enclosure, while the emergency stop is used for quicker power removal and the switch can only be restored to its active state by using a key, which is located beside the enclosure. Red signal beacon (top right) is used to indicate that the safety relay is energized, meaning the relays and EK power supply can be activated. The HMI is used to monitor and modify process parameters. Figure 4.5-3 shows a close-up of the HMI's main menu.



Figure 4.5-3: HMI – Main Menu

The Table 4.5-3 shows main components installed on the inside the panel.

Table 4.5-3: Interior Panel – Main Components

Component	Description	Model	Qty.
P2000	Programmable Controller	P2000	1
Ethernet switch	Link P2000 & HMI to router	SE-SW5U	1
Fuses (6x 2Amps)	Used to protect P2000, HMI and Sensors	KN-F10-10 & GMA2	6
EK fuses (4x30Amps)	Used to protect electrodes	EHCC2DIU-6 & HCLR30	4
Relays	Used to activate pumps, including diode reverse protection	782-2C-SKT, 782-2C-24D, AD-BSMD-250	4
EK power supply	Programmable power supply	HDS1500	1
Safety relay	Provides power to relays and EK power supply	Dold LG5924-48-61-24	1
Relay power supply	24V power supply, 60W	PSB24-060S-P	1
Logic power supply	24V power supply, 60W	PSB24-060S-P	1
Breaker	Used to remove AC power to power supplies	FAZ-B15-2	1
Current Transducer	Measure current output from EK power supply	DCT100-42-24-F	1

Note: a complete list of all components is given in Appendix A.

The Figure 4.5-4 shows a close-up of the interior of the panel.

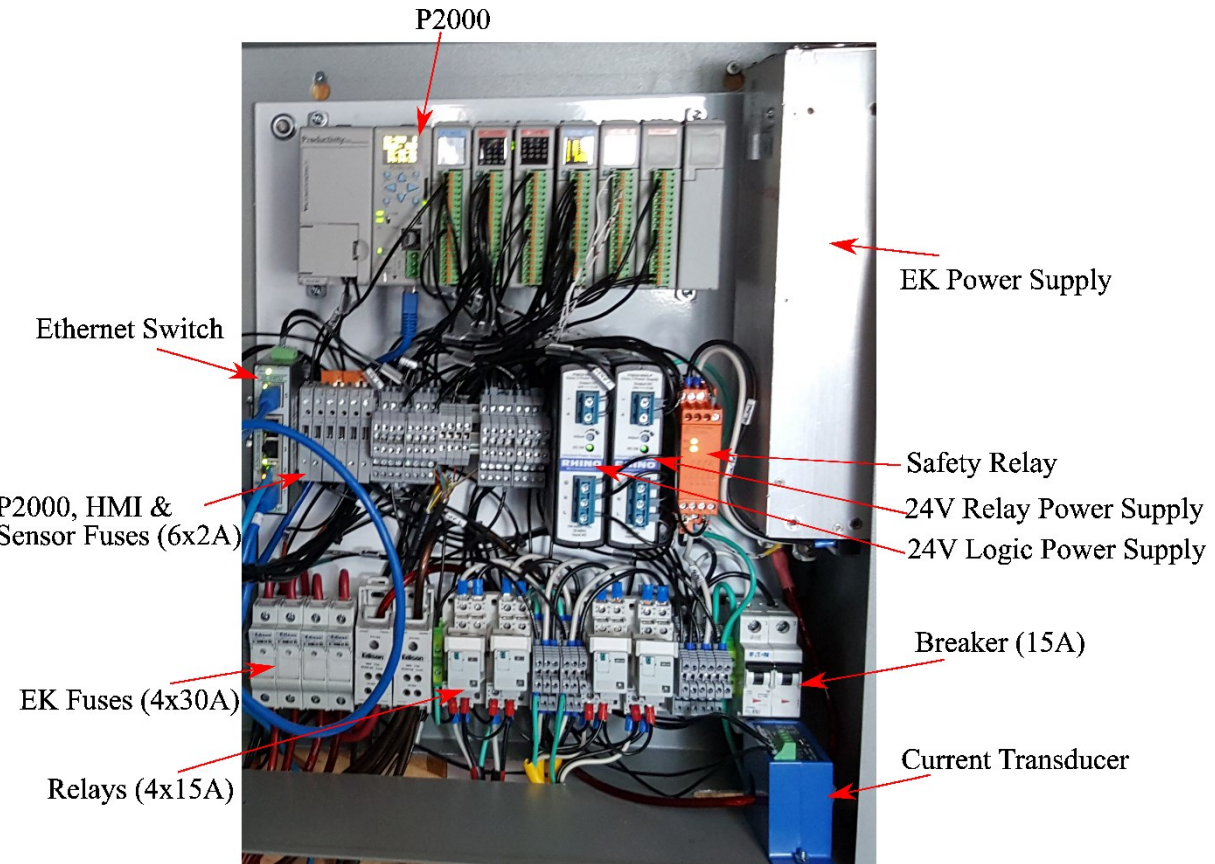


Figure 4.5-4: Control Panel Interior – Components

Chapter 5: Pump Control System

5.1. Overview

To ensure autonomous operation, it is critical to have two water level sensors for the bioreactor and feed tank working together. This will allow the pump control system to know when to turn on the respective pumps and provide safe operations; when the level reaches a low or too high critical level, the control system can turn on or off any of the system pumps. This proved to be quite useful to protect the circulation and feed circulation pumps, when either the feed pump or MEBR pump were clogged. Below, in Figure 5.1-1 the feedback diagram for the control system is demonstrated.

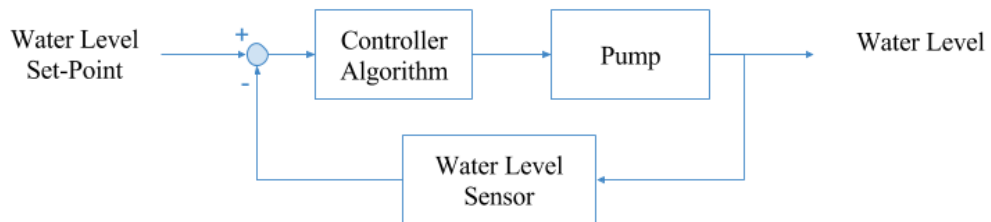


Figure 5.1-1: Water Level Control System

5.2. Pump Controller Algorithm

For both feed and MEBR, an on-off controller algorithm had been implemented. The wastewater levels were decided based on the geometry of the tanks.

Feed tank (100L):

- Minimum level = 30cm.
- Maximum level = 55cm.
- Critical low = 15cm.
- Critical high = 60cm.

MEBR (1000L):

- Minimum level = 79.8cm.
- Maximum level = 80cm.
- Critical low = 60cm.
- Critical high = 85cm.

A small difference in water level in MEBR was judged necessary as to simulate a nearly continuous system. Based on the dimensions of the MEBR tank and the difference in minimum and maximum levels, the MEBR feed pump turns on for ~1minutes to fill the tank back to 80cm. It will turn on again ~2minutes after it turns off, which ensures there is sufficient carbon for the various biological processes. Ideally, this pump should be always on; however, controlling the MEBR pump flowrate using a ball valve has caused some issues due to clogging (debris were getting trapped due to smaller orifice). A better suited pump could resolve this issue.

The critical levels are used to ensure safe operations. Conditions for critical levels (low or high) may occur in the following situations:

- Critical high level may occur if one of the relays controlling the pump fails and the normally open contacts fuse together. To overcome this possible issue as well as to ensure that no overflow occurs, overflow weirs were added to the feed and MEBR tanks.
- Critical low level may occur if a pump or valve has a blockage; for example, if the feed pump is clogged, the feed tank level will eventually drop below the minimum level as the controller algorithm will try to maintain the water level in MEBR tank. Another possibility for a critical low level is if the MEBR pump is blocked but both circulation pumps remain turned on, the MEBR tank will eventually drop below the minimum level.

To ensure satisfactory operations, all four pumps and both level sensors are controlled with the following simplified controller algorithm (Figure 5.2-1). A manual mode was also added which allows the operator to stop automatic operations of all four pumps and manually turn them on, which proved useful for cleaning the membrane modules. The automatic mode ensures that MEBR and feed tank levels are within specified range; if they are not, i.e. blockage, it will take the appropriate action. Finally, the software verifies if the water level sensors working within their range (4-20mA) and when an error occurs, the system will alert the operator and stop the particular pump accordingly.

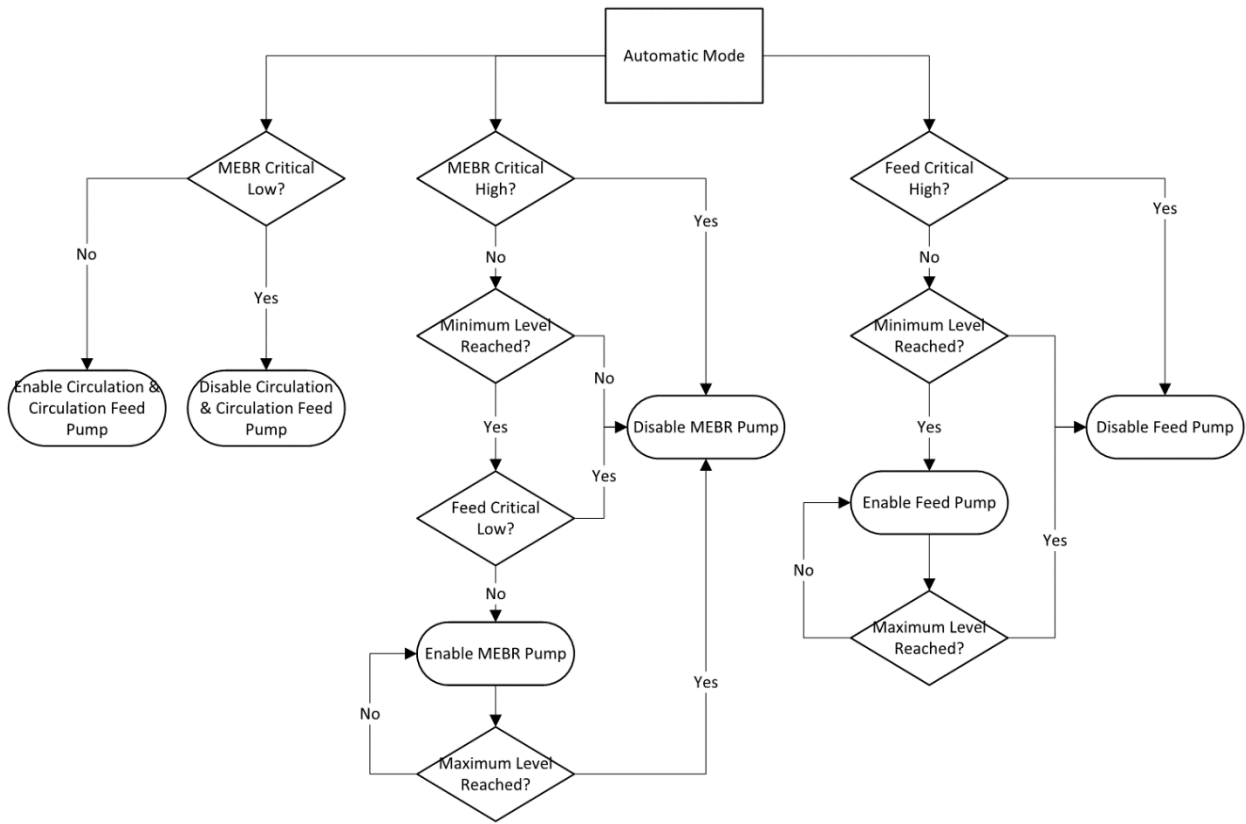


Figure 5.2-1: Pump Controller – Automatic Mode

5.3. Software Implementation

The algorithm along with the safety features were implemented in the P2000 in three different tasks.

The *Pumps_Water_Level* task performs the following functions:

- Checks the sensor to make sure they are reading in the valid range (4-20mA)
- Read water level sensors, converts the signal to centimeters, and performs a moving average
- Debounce the pushbuttons to make sure the input is valid and determine whether to run the pumps in automatic or manual mode.

The *Pumps_Automatic* task performs the following functions:

- Upon the start of the automatic mode, it will enable the circulation feed pump and wait 5 seconds to enable the circulation pump. By doing so, it lets the circulation feed pump to prime the circulation pump and reduces current surges as not to reset the control breaker.
- Verifies if the water levels are within the limits, if not it turns the respective pumps.
- Verifies if there is an issue with either the MEBR or Feed pumps, the software will take corrective actions, explained in the ‘Results & Analysis’ Section.

The *Pumps_Manual* task performs the following function:

- Allows any pumps to be enabled or disabled manually. It will also disable MEBR or Feed pump if the level reaches the maximum level to ensure no overflow if the operator is not actively present.

The manual pump task is especially useful for the cleaning process of the membrane modules. The LD program for these tasks are shown in Appendix B.

5.4. Results & Analysis

MEBR & Feed – Water Levels

The following Figure 5.4-1 demonstrates how the control system operates over a 10hour period.

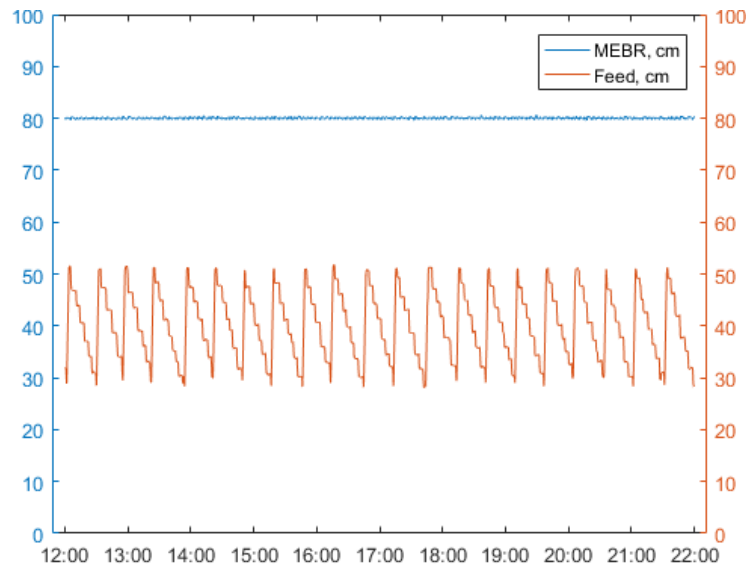


Figure 5.4-1: MEBR & Feed - Water Levels over 10h on Dec 25, 2016

Notice the small decreasing steps in the Feed Water level, these occur when the MEBR pump is enabled. The large increasing steps are when the Feed Pump is enabled.

Safety

Since the beginning of the start-up period of the MEBR, there has been issues with the feed and MEBR pump blocked. To ensure safe operation, two timers are also used to check if either pump, MEBR or Feed, is blocked, or perhaps if wastewater is not present. Once a minimum level is reached, the timer is started. If the timer reaches a specified period of time before the water level reaches at the very least the minimum level, then it is considered as clogged. The period of time for each timer is determined based on how long it should take to fill each respective tank. If the software detects either pump is blocked, it will wait one minute and try to fill the tank again. By doing so, a pump will not overheat if it is clogged, and will try recover on next attempt. By looking at the water level data, it can be observed the Feed pump had an issue on December 26, 2016 at 9:15AM but was able to recover automatically without affecting the MEBR level since there is a nice margin between the low and critical low level of the Feed tank (Figure 5.4-2).

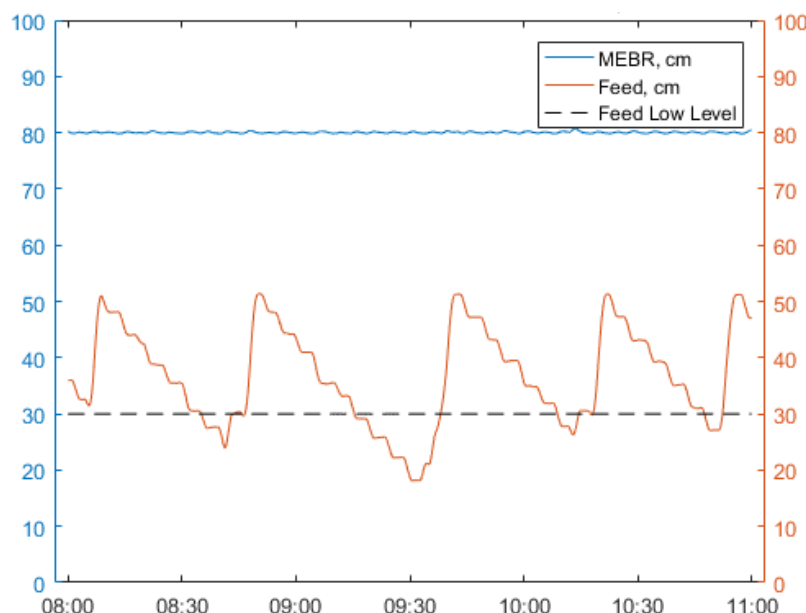


Figure 5.4-2: Feed pump auto recovery on Dec 26, 2016

Another critical safety feature of the system is that it will turn off the required pumps once either the Feed or MEBR level reaches a critical low. This is necessary to make sure the pumps do not run dry and overheat, but also to not destroy the bacteria in the MEBR. Once the Feed level goes below 15cm, which is almost the height of the outlet to the MEBR pump, the system will not allow the MEBR to turn on as to ensure the pump will not run dry and thus overheat. As for the MEBR, once the level goes below 60cm, the system will turn off both the circulation feed and circulation pump. This situation occurred on December 16, 2016 (Figure 5.4-3). It can be observed that the Feed level reached the critical low level at around 2:30AM, which disabled the MEBR pump. Soon after the water level in the MEBR started dropping, and when the MEBR critical low was reached, both circulation feed and circulation pump were disabled. After inspection of the Feed pump, it was observed that toilet paper had blocked the inlet.

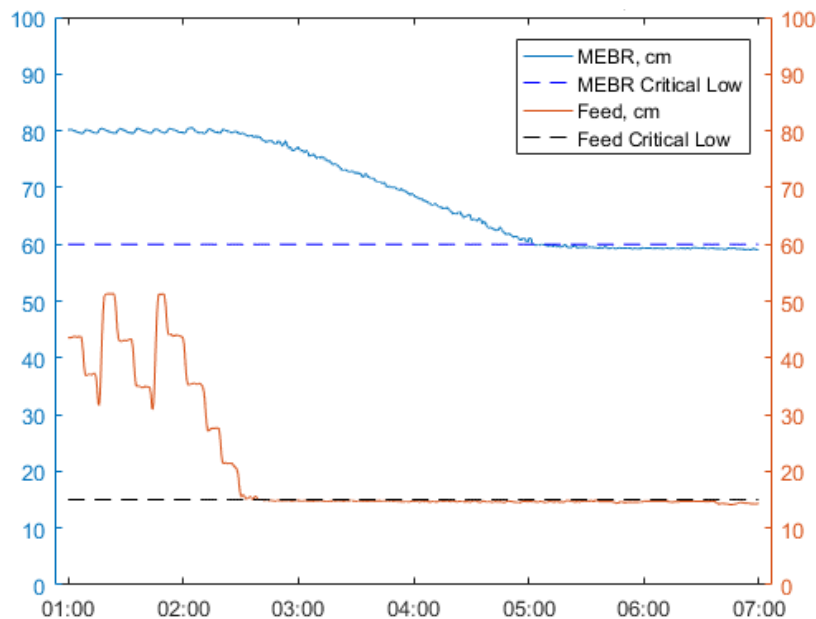


Figure 5.4-3: System disabled from pump blockage on Dec 16, 2016

Chapter 6: Aeration Control System

6.1. Overview

Aeration is a critical process for the MEBR as the DO concentration directly impacts the effectiveness of the wastewater treatment. Controlling DO is rather complex because there are two time varying parameters that are critical in understanding the dynamics of DO: oxygen transfer rate (OTR) and oxygen uptake rate (OUR). First, DO may only be increased through aeration and the OTR is simply nonlinear. Second, the microorganism activity combined with the current presence of carbon, nitrogen and EK process has a great influence on OUR. Even more so, having both aerobic and anoxic conditions within a single bioreactor requires DO concentration to be at a critical level. Previous laboratory results demonstrated DO concentrations in the range 0.2-0.8mg/L offers high nutrient removal as long as there was sufficient COD in the influent (Ibeid, 2011, Ibeid et al. 2012). In these conditions, it allows the simultaneous aerobic and anoxic nitrogen removal (nitrification and denitrification with anammox). For automating the MEBR aeration process, a rule based control was successfully implemented, Figure 6.1-1 is the feedback diagram for the control system.

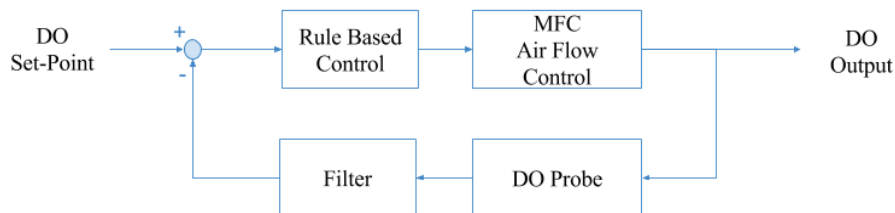


Figure 6.1-1: Aeration Control System

Alongside controlling the DO concentration, an automatic purge and mixing cycles were implemented. The purge is required to remove the water collected in the air compressor tanks as to minimize corrosion. The mixing cycle consists of frequent sudden increase in aeration flow rate.

6.2. Aeration Controller Algorithm

Rule based control refers to using a set of rules, or guidelines, that determine what the output should be based on the input in the form of IF-THEN statements. An advantage to using rule based control is that it is simple to implement and the parameters may be optimized during operation of the MEBR. The current rules were based on the analysis of nitrogen and phosphorus concentration and they are:

- **If** ($DO_{now} \leq DO_{lowlow}$) **then** set aeration high until $DO \geq DO_{low}$
- **If** ($DO_{low_low} < DO_{now} \leq DO_{low}$) **then** set aeration to normal
- **If** ($DO_{now} \geq DO_{high}$) **then** set aeration low

Where the parameters are set to:

- $DO_{lowlow} = 0.12\text{mg/L}$
- $DO_{low} = 0.16\text{mg/L}$
- $DO_{high} = 0.35\text{mg/L}$
- Aeration high = 50SLPM
- Aeration normal = 35SLPM
- Aeration low = 15SLPM

The purge and mixing cycles set on two separate timers where the interval and activation times can be set on the HMI. The purge cycle consists of *two* consecutive 2s ON- 2s OFF, set with an interval of 30min. The mixing cycle sets the aeration to 100SLPM for 10seconds, set with an interval of 10min. All of these parameters may be modified through HMI.

6.3. Software Implementation

The aeration algorithm has been implemented in two different tasks: *Aeration* and *Purge*.

The *Aeration* and *Purge* tasks performs the following functions:

- Acquires, scales, and averages DO and Temperature measurement from DO probe.
- Perform rule based control based on the previously established rules, which can be modified in HMI.
- Checks if it is time for mixing cycle. If so, will override rule based control.
- Checks if it is time for purging.

The LD program for these tasks are shown in Appendix C.

6.4. Results & Analysis

Dissolved Oxygen & Aeration

The rule based control has been implemented on January 15, 2017. Before that time, the aeration was running in manual mode. Figure 6.4-1 shows the DO concentration and aeration flow rate from the latest data.

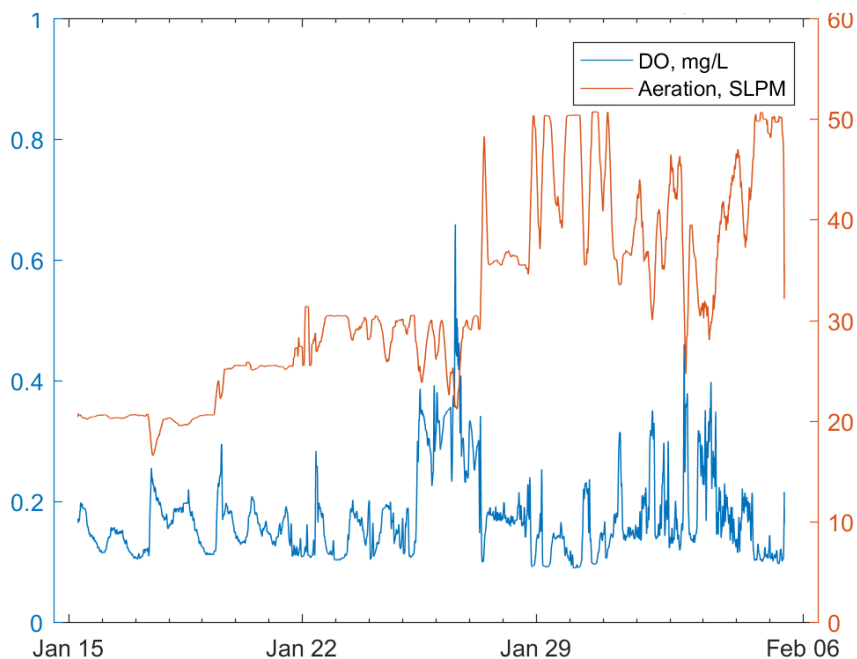


Figure 6.4-1: DO & Aeration using Rule based Control

The objective of maintaining adequate DO through rule based control was achieved. The fluctuations in aeration, observed above, were necessary to keep the DO fluctuating within those rules, which indicate that the system is adjusting automatically to different influent conditions in real-time. It can be observed that the rules were changed on January 22nd, and again on January 27th, where the normal aeration flowrate was increased from 20 to 30SLPM, and then from 30 to 35SLPM respectively. The average DO concentration and aeration flowrate in this period was 0.17mg/L and 32SLPM respective. Therefore, volumetric aeration flowrate is evaluated to be 40SLPM/m³ of wastewater.

Temperature

As the DO probe provides temperature measurement, it is interesting to compare the MEBR temperature with the outside average temperature, as shown in Figure 6.4-2 (EnvironmentCanada, 2017). The short and rapid declines of temperature occur when the researchers were entering the shed, and typically the door would be left slightly open because of the warm interior temperatures:

- MEBR $T_{avg} = 24^{\circ}\text{C}$
- Outside $T_{avg} = -7^{\circ}\text{C}$

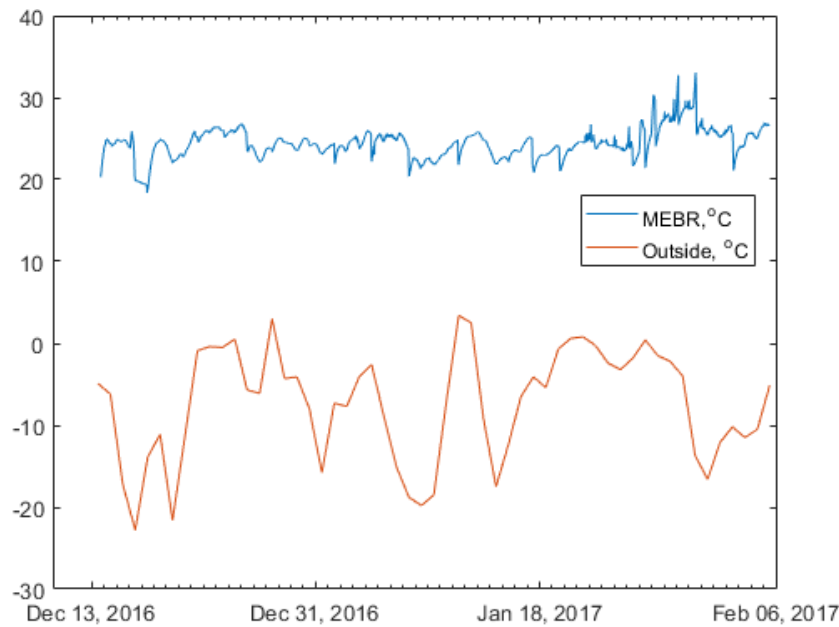


Figure 6.4-2: Temperature in MEBR vs outside

There is one major and two minor sources of heat generation: air compressor, and circulation feed and circulation pump respectively. This result is interesting from two perspectives. Previous laboratory results demonstrated that temperatures greater than 18°C was beneficial for microorganism activity and, therefore, resulted in improved nutrient removal (Ibeid, 2011). From a remote location perspective, even in cold weather, it is possible to maintain adequate temperatures MEBR temperatures without external heating.

Chapter 7: EK Control System

7.1. Overview

From the Arduino prototype, it was clear that a PI controller algorithm was adequate for controlling CD within the MEBR. The prototype demonstrated a reasonable settling time (<10sec), and no steady state errors which was largely due to a direct relationship between the voltage applied and CD. However, having a proper programmable controller, like the P2000, with various communication capabilities unlocked new possibilities: modelling and validation with system identification. Capturing the dynamics of the system allows one to understand the intricate properties and adopt an appropriate control strategy.

7.2. Modelling & System Identification

Modelling EK Process

The objective in modelling the EK process is to understand how the process responds and that will allow the design of a controller to control precisely the CD by varying the applied voltage. The theoretical model can be developed by observing the circuit diagram (Figure 7.2-1):

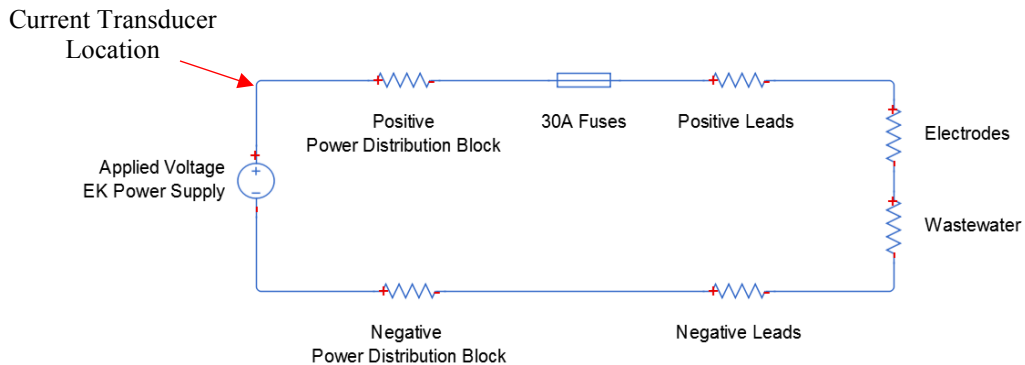


Figure 7.2-1: EK Circuit Diagram

Each component beside the power supply act as a resistor in the loop. The distribution blocks are used to split the 1 output from the power supply to 4 outputs to connect to the electrodes. Because we are interested in controlling CD, the circuit diagram can be simplified (Figure 7.2-2)

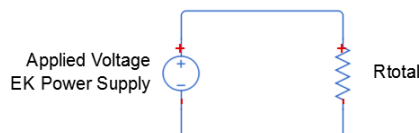


Figure 7.2-2: EK Simplified Circuit Diagram

Where the total resistance is the sum of each individual components. The applied voltage across the electrodes is still unknown: the applied voltage at the power supply will not be the same at the electrodes due to voltage drops at each component. Luckily, there are two ways to solve this situation: software compensation or use the remote sense feature of the EK power supply which may compensate up to 0.5V. The latter was selected for this project since the compensation was on the order of 0.1V when measured using a multimeter. The corresponding model is now the following:

$$V_a(t) = i(t) * R_t(t) \quad (39)$$

Where $V_a(t)$ is the applied voltage across the electrodes, $i(t)$ is the total current, and $R_t(t)$ is a function of time since the electrodes and wastewater resistances vary over time. From a modelling perspective, it can be assumed that the total resistance is constant, it will be observed later that this is not true but the controller can compensate for these variations which will be discussed later in the disturbance rejection section. The relationship between the total current and CD is simply:

$$CD(t) = \frac{i(t)}{n * A_s} \quad (40)$$

Where n is the number of electrodes and A_s is defined as the surface area of the electrode. Therefore, the model is now:

$$V_{applied}(t) = \frac{R_t}{n * A_s} * CD(t) \quad (41)$$

Taking the Laplace transform of this equation and rearranging the terms gives the following transfer function:

$$L\{V_{applied}(t)\} = L\left\{\frac{R_t}{n * A_s} * CD(t)\right\} \quad (42)$$

$$V_a(s) = \frac{R_t}{n * A_s} CD(s) \quad (43)$$

$$G_{EK}(s) = \frac{CD(s)}{V_a(s)} = \frac{n * A_s}{R_t} = K = constant \quad (44)$$

Where $G_{EK}(s)$ is the EK transfer function. The result is that the relationship between CD and V_a is simply a constant K , which can be viewed as an indicator of conductivity since it is inversely proportional to the resistance. There is another underlying assumption in this model: the EK power supply can instantaneously supply the desired voltage. By looking at the datasheet, the HDS1500 power supply has a maximum rise time of 120ms at maximum load. The power supply can be modelled as a simple resistor-capacitor (RC) circuit (Fig 7.2-3).

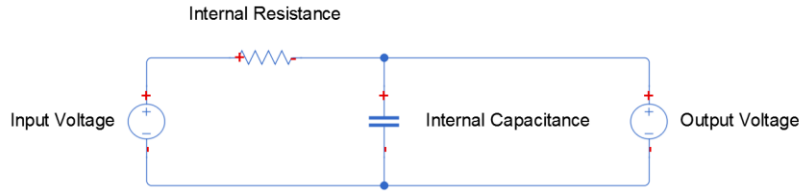


Figure 7.2-3: RC Circuit Diagram

By applying Kirchhoff's circuit laws (KVL and KCL), the transfer function of the circuit results in (Dorf & Bishop., 2011):

$$V_{in}(t) = V_R(t) + V_{out}(t) = i_C(t) * R + V_{out}(t) \quad (45)$$

$$i_c(t) = C \frac{dV_{out}(t)}{dt} \quad (46)$$

$$L\{V_{in}(t)\} = L\left\{RC \frac{dV_{out}(t)}{dt} + V_{out}(t)\right\} \quad (47)$$

$$V_{in}(s) = RC * sV_{out}(s) + V_{out}(s) = (RCs + 1)V_{out}(s) \quad (48)$$

$$G_{PS}(s) = \frac{V_{out}(s)}{V_{in}(s)} = \frac{1}{RCs + 1} = \frac{1}{\tau s + 1} \quad (49)$$

Where $G_{PS}(s)$ is the power supply transfer function, and τ is known as the time constant of the power supply. From the definition of the rise time (time from 10-90%), the time constant of a first order system can be calculated as followed (Dorf & Bishop., 2011):

$$\tau = \frac{T_r}{\ln(9)} \cong \frac{T_r}{2.2} = \frac{120ms}{2.2} = 55ms = 0.055sec$$

Combining the EK and power supply transfer functions results in what is known in control theory the plant transfer function:

$$G_p(s) = G_{PS}(s) * G_{EK}(s) = \frac{CD(s)}{V_a(s)} = \frac{K}{\tau s + 1} \quad (50)$$

With the obtained plant transfer function, the parameter K , often named the process gain, reflects the conductivity of the wastewater and electrode remains unknown but will be determined through system identification. Note: the process gain K is the ratio between the voltage applied and resulting current density once steady state has been reached.

Data Acquisition – P2000 & MATLAB TCP/IP Communication

It is important to acquire measurements at a fixed sampling rate for generating data for system identification and validation. The P2000 is capable of data logging very quickly, so it would be possible to run a step response and record the CD at a fixed interval, for example 0.1sec. However, it would be tedious to access the P2000 web server and download the Excel file every time and load the data in another software for analysis. Instead, the P2000 offers TCP/IP communication which can directly communicate with various engineering software (MATLAB, Python, and Octave). TCP/IP thus allows to send and receive data between the P2000 and a computer. Within the *Productivity Suite*, this feature is enabled by setting up a ‘Custom Protocol over Ethernet Device’, CPoE. In this work, the P2000 as a server was setup as a server and MATLAB was setup to be the client in the TCP/IP communication. Appendix E shows how to create a CPoE device in the *Productivity Suite*, note this is only available on v.2.4.0.16 and later. Appendix E also demonstrates the LD and MATLAB code to send and receive data over TCP/IP.

System Identification for EK Process

During the early stages of system identification and designing the PI controller, it was apparent that the selection of the sampling rate was important. Figure 7.2-4 shows a unit step response at two different sampling periods:

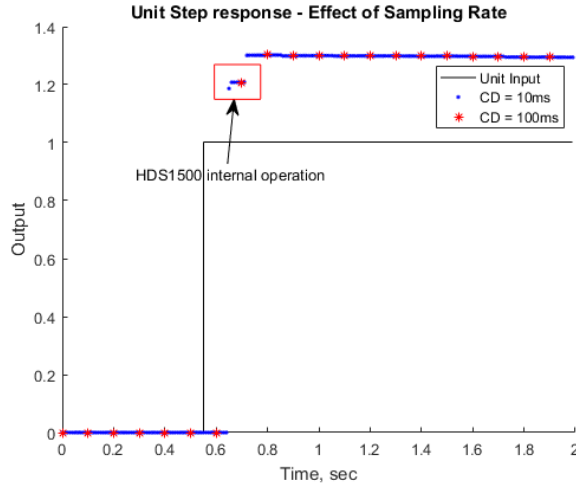


Figure 7.2-4: Effect of Sampling Rate

Sampling at 10ms, the internal operation of the power supply can be observed, where the power supply's internals operation is increasing the output voltage in order to meet the set-point voltage. It is also observed at 100ms but to a lesser extent. Another observable factor is the delay, approximately 90ms. From the generated open-loop step response, the optimization problem and least-square estimation may be used to identify parameters K and τ . Figure 7.2-5 provides the comparison of both methods with respect to the actual step response, the MATLAB script and functions to calculate the parameters are given in Appendix F.

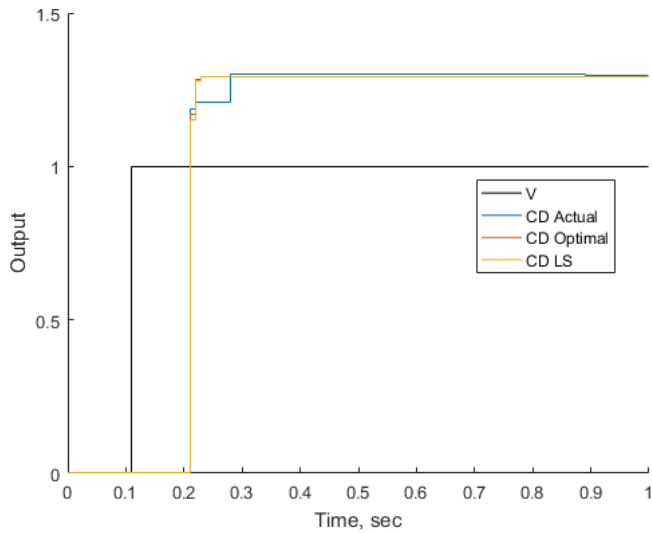


Figure 7.2-5: Optimization & Least-Square Comparison

$$G_{P_{optimal}}(s) = \frac{1.3}{0.0041s + 1} e^{-0.09s} \quad (51)$$

$$G_{P_{LS}}(s) = \frac{1.3}{0.0045s + 1} e^{-0.09s} \quad (52)$$

The shape of the output response to both methods are similar to the actual response. The slight differences come from the non-linearity of the power supply, and since a linear model was assumed, this difference is to be expected but negligible. Thus far, the least-square estimation presented has ignored the possibility that the data might be subject to noise; however, the actual noise observed experimentally is insignificant compared to the signal (signal to noise ratio >50dB).

7.3. Controller Design

P2000 – PID Controller Implementation

Before designing a controller for the EK process, it is essential understanding how the PID controller is implemented in the P2000. Upon looking at the documentation of the *Productivity Suite*, an important information is missing: it doesn't mention how they managed the discretization of the PID controller. Fortunately, they provide the algorithm used which can be reversed engineered:

$$M_n = K_p * e_n + K_i \sum_{i=1}^n e_i + K_d(e_n - e_{n-1}) \quad (53)$$

Where M_n is the PID controller output and e_n is the error at sample n . The summation operator may be eliminated as followed:

$$M_{n-1} = K_p * e_{n-1} + K_i \sum_{i=1}^{n-1} e_i + K_d(e_{n-1} - e_{n-2}) \quad (54)$$

$$M_n - M_{n-1} = K_p(e_n - e_{n-1}) + K_i(e_n) + K_d(e_n - 2e_{n-1} + e_{n-2}) \quad (55)$$

$$M_n = M_{n-1} + (K_p + K_i + K_d)e_n - (K_p + 2K_d)e_{n-1} + K_d e_{n-2} \#(56)$$

This is in the parallel form, therefore transforming it into standard form demonstrates that *AutomationDirect* have used Euler's forward method to discretize the P2000 PID controller:

$$PID_{P2000} \rightarrow M_n = M_{n-1} + K_p \left(1 + \frac{T_s}{T_l} + \frac{T_d}{T_s} \right) e_n - K_p \left(1 + 2 \frac{T_d}{T_s} \right) e_{n-1} + K_p \left(\frac{T_d}{T_s} \right) e_{n-2} \quad (57)$$

Design of PI controller

The PI controller may be designed with the plant transfer function acquired through LS and understanding how the PID controller is actually implemented in the P2000. There is a simple reason why a PI controller is selected instead of a PID: it is simply not necessary to achieve stable and robust control for a first order system, as indicated by the various tuning methods found in literature, refer to section 3.2. Given below are the continuous time transfer functions of the plant and PI controller.

$$G_{PLS}(s) = \frac{K}{\tau s + 1} = \frac{1.3}{0.0045s + 1} \quad (58)$$

$$PI(s) = K_p \left(1 + \frac{1}{T_i s} \right) \quad (59)$$

In order to reduce current transducer variations, a low pass filter is implemented in the P2000, which has the following transfer function, cut off frequency selected is 15Hz (corresponding time constant is 10ms).

$$G_f(s) = \frac{Av g_{out}}{Sensor_{in}} = \frac{1}{\tau_f s + 1} = \frac{1}{0.01s + 1} \quad (60)$$

The resulting feedback diagram is provided in Figure 7.3-1.

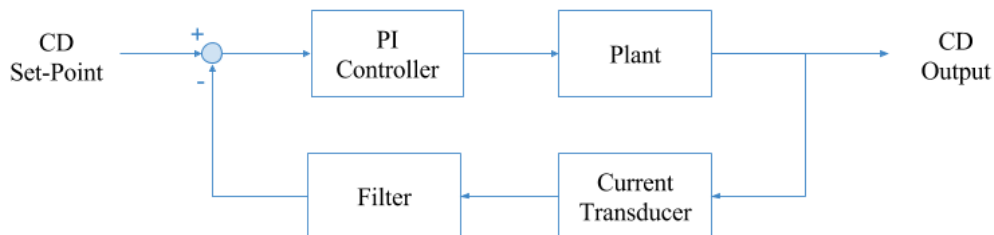


Figure 7.3-1: EK System - Feedback Diagram

The designer must now establish the desired specifications for the PI controller. For this project, the following specifications were desired:

- Settling time, $t_s \leq 5\text{sec}$
- Zero steady state error, $CD_{SP} - CD_{ss} = 0$
- No overshoot, $M_p = 0$ (as not to affect microorganisms from high current outputs)

There are numerous available tuning methods to design a PI controller: Ziegler-Nichols, Åström-Hägglund, Skogestad. Manual tuning is achievable but it's generally only worthwhile once a range of PI parameters (K_p and T_i) are known. The Table 7.3-1 shows the PI tuning rules for the aforementioned methods (Åström & Hägglund, 2005; Skogestad, 2001; Ziegler & Nichols, 1942):

Table 7.3-1: PI Tuning Methods

PI Tuning Method	K_p	T_i
Ziegler-Nichols (Z-N)	$\frac{0.9\tau}{K\theta} = 0.035$	$3\theta = 0.27$
Åström-Hägglund (AH05)	$\frac{0.15\theta + 0.35\tau}{K\theta} = 0.13$	$\theta * \frac{0.15\theta + 0.35\tau}{0.46\theta + 0.02\tau} = 0.03$
Skogestad	$\frac{0.5\tau}{K\theta} = 0.02$	$\tau \leq T_i \leq 8\theta = 0.005 \leq T_i \leq 0.72$

Observing the following step responses, Z-N and Skogestad ($T_i = 8\theta$) methods do not meet the settling time criteria, and Skogestad ($T_i = \tau$) has a slight overshoot (8%). While AH05 meets all criteria with a settling time of 0.5sec. The PI parameters from AH05 will serve as a comprehensive starting point to manually fine-tune the PI controller (Figure 7.3-2).

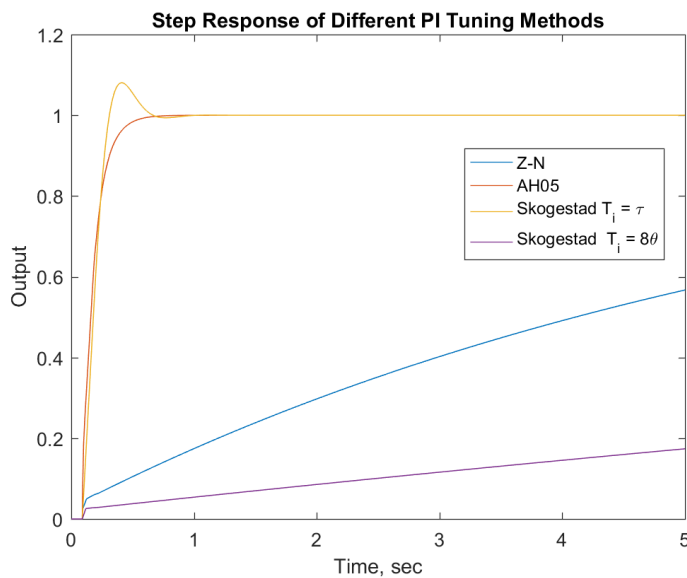


Figure 7.3-2: Comparison of Different PI Tuning Methods

Selection of Sampling Rate & PI Fine-Tuning

The effect of the sampling rate on the output response becomes apparent when looking at step response of the system using a digital PID (PI_{AH05} and plant). Changing the sampling period from 10ms to 100ms causes the system to overshoot (20%) (Figure 7.3-3).

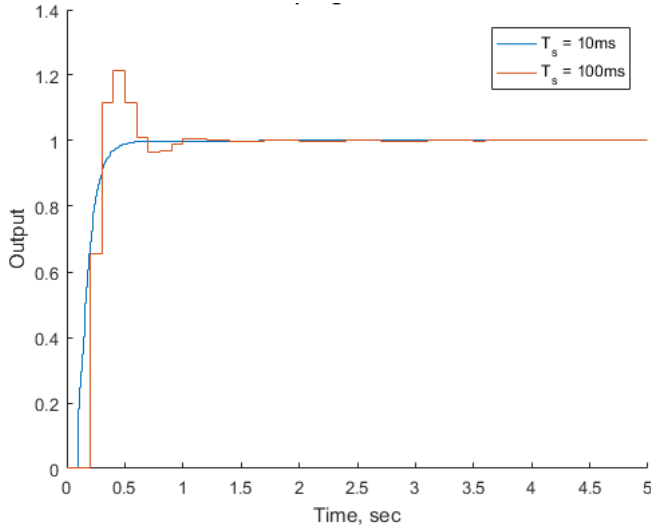


Figure 7.3-3: Effect of Sampling rate on PI Controller

The $\text{PI}_{\text{AH}05}$ controller may definitely be implemented with a 10ms sampling period; however, in practice, sampling every 10ms will cause the P2000 to perform 100 PID calculations per second, as opposed to 10 when sampling every 100ms. For a system with a rise time on the order of 1sec, it is typical to choose a sample rate of 10 to 20Hz in order to provide some smoothness in the response and limit the change in magnitude of the control steps (Franklin et al., 1997). By definition, the rise time is always less than the settling time ($\leq 5\text{sec}$); therefore, it is satisfactory to sample at 10 Hz (every 100ms) as long as the PI parameters are tuned accordingly to meet the specifications. Besides, increasing the sampling period from 10ms to 100ms would alleviate the P2000 from many redundant PID calculations, allowing it to perform other time critical tasks.

Starting with the $\text{PI}_{\text{AH}05}$ controller, fine-tuning the controller can be achieved by simply decreasing the proportional gain K_p . It is possible since the PI controller is in standard form, meaning that changing K_p will also have a direct consequence on the integral action (T_i) of the controller. After decreasing K_p manually, a satisfactory PI controller has been achieved: $K_p = 0.03$, T_i remained the same. Shown below is the fine-tuned $\text{PI}_{\text{AH}05}$ controller and its new response compared to its previous response. It can be observed that the response has no overshoot and is now smoother (Figure 7.3-4).

$$\text{PI}_{\text{Fine-Tuned}}(s) = K_p \left(1 + \frac{1}{T_i s} \right) = 0.03 \left(1 + \frac{1}{0.03s} \right) \quad (61)$$

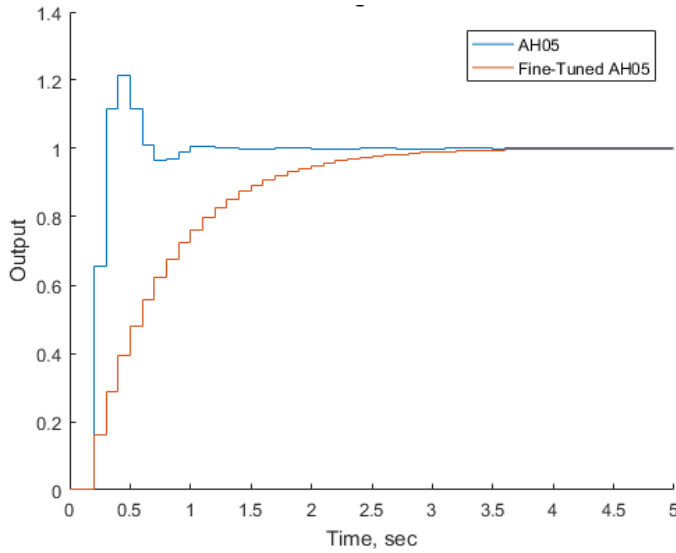


Figure 7.3-4: Response of Fine-Tuned PI Controller from reducing K_p

7.4. Carbon Dosing

Later in the project, a carbon dosing pump was installed for testing the effect of adding carbon (as sucrose) during the EK process. Three parameters are used to control the dosing:

- Dosing flow rate (L/day)
- Offset time: time to wait after EK is active
- Extra time: time to continue after EK went inactive

7.5. Software Implementation

The EK and carbon dosing algorithm has been implemented in two different tasks: *Electrokinetic* and *Carbon Dosing*.

The *Electrokinetic* and *Carbon_Dosing* tasks performs the following functions:

- Acquire, scale, and average current measurement from current transducer. Checks also for short circuits and stops the EK if it detects one.
- Cycles the EK ON and OFF based on the desired times.
- When EK is active, the PID controller is active to ensure satisfactory control over CD.
- Checks if it is time for carbon dosing.

The LD program for these tasks are shown in Appendix D.

7.6. Results & Analysis

PI Controller

The PI controller has been implemented on the P2000 and validated. A comparison between the actual and simulated system response was generated using MATLAB to communicate to the P2000 over TCP/IP, as shown in Figure 7.6-1. The difference between the actual and simulated systems are from the assumption that the power supply model is linear, even though it was shown earlier that this was not entirely valid but the approximations work well (Figure 7.6-1).

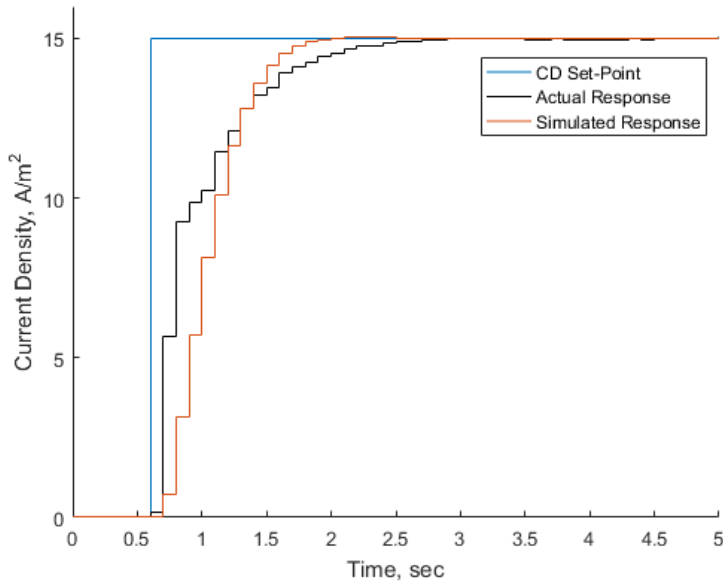


Figure 7.6-1: Response of Actual and Simulated System

Fluctuating Conditions

Controlling CD over time in the EK process is challenging because of varying conditions: DO concentrations, wastewater conductivity, and passivation of electrodes. A PI controller is required to ensure the CD is at the desired set-point during varying conditions. The importance of the PI controller may be observed over the 2-month period in operation, shown in Figure 7.6-2 the application of EK continuously (December 23, 2016). The tendency for the increasing of voltage is mainly from electrode passivation and deposition (Ibeid, 2011). On February 2nd, 2017, the electrodes were cleaned to remove the passivation and deposition layers (Figure 7.6-2).

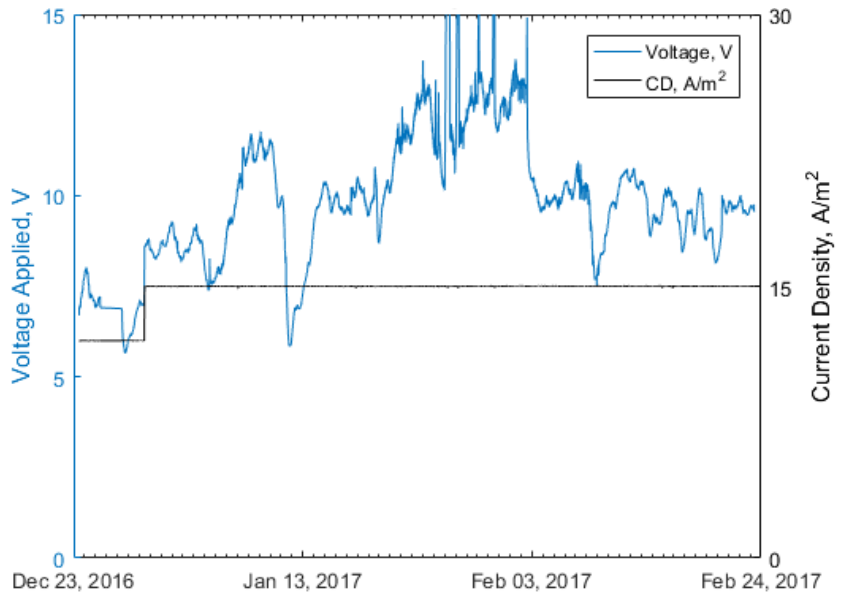


Figure 7.6-2: Voltage Variations in MEBR

Furthermore, for the first time in this research group, the varying conditions during an EK cycle have been observed, as shown in Figure 7.6-3. It is assumed that the increase in voltage ($\sim 0.8\text{V}$ over a single cycle) to keep constant CD is caused from the combination of the following: gas production at the electrodes, bacteria responding to electric field, and formation of flocs from dissolution of aluminum ions. Clearly demonstrating the necessity for having a PI controller for maintaining true constant CD during the EK. Several previous studies have neglected validating if the CD was truly constant during an EK cycle, instead relied either by setting the power supply in constant voltage mode and hoped the CD wouldn't vary or by setting the power supply in constant current mode but then voltage is free to vary. The voltage is free to be varied by the PI controller but its value is being monitored and measured in real-time.

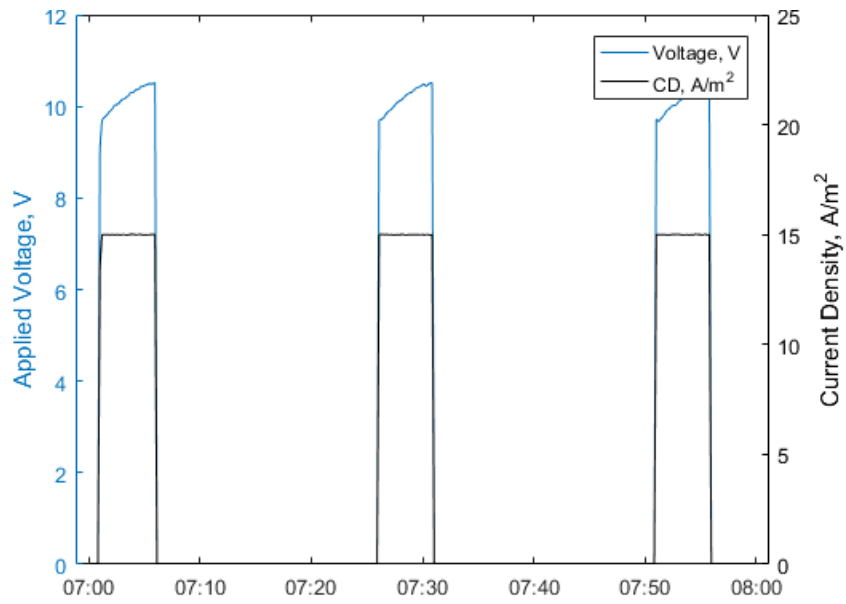


Figure 7.6-3: Voltage variations over EK cycle (Jan 15, 2017)

Chapter 8: Discussion

8.1. Wastewater Treatment

Influent & Operating Conditions

The feed pump was installed in a sanitary wastewater only channel such that the influent would not be affected by rain water or water resulting from melt of ice. The pump was also installed right after a fine screen system; therefore, no other treatment has altered the conditions of the wastewater. The average influent conditions were (Elektorowicz et al., 2017):

- COD: 170mg/L.
- Orthophosphates (PO₄-P): 3.1mg/L.
- Ammonium (NH₄-N): 26mg/L.

The following MEBR operating conditions were applied:

- HRT: 12h.
- SRT: 20days.
- CD: 12-15A/m² with 3 to 4 electrode pairs, electrode distance = 5cm.
- Exposure time: 5min ON, 15min OFF.
- Denitrification: with and without carbon dosing.
- Aeration: continuous aeration with different flowrates.
- DO average concentration: 0.2mg/L

Carbon Removal

Removal of COD was high from the beginning of the MEBR start-up: removal efficiency $\geq 99.6\%$ (Elektorowicz et al., 2017). This result suggests that provided electrical mode operation did not have detrimental effect on the microbial activity. Low DO concentrations did not impede the biological treatment, which is exceptional since many MBR operate with high DO concentrations to ensure aerobic conditions (Judd, 2006). The COD effluent concentration over a one month period may be observed in Figure 8.1-1 , where the effluent COD concentration is adapted from Elektorowicz et al., 2017.

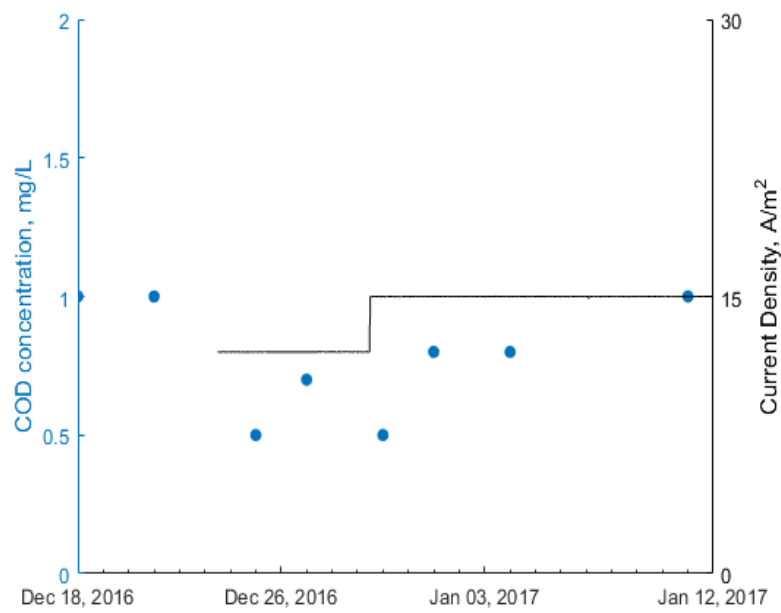


Figure 8.1-1: COD effluent concentration with respect to CD

Phosphorus Removal

Removal of phosphorus improved after two weeks in the project: removal efficiency $\geq 95.2\%$ (Elektorowicz et al., 2017). The increase in removal is in accordance with the application of EK (December 23, 2016) and in accordance with the increasing of the CD from 12 A/m^2 to 15 A/m^2 (occurred on December 29), refer to Figure 8.1.2 and Figure 7.6-2. With the application of the EK process, coagulants were beginning to be created, so it took a few days for the system to have enough coagulants in order to remove phosphorus. The phosphorus concentration ($\text{PO}_4\text{-P}$) in effluent over a one month period may be observed in Figure 8.1-2 (effluent concentration is adapted from Elektorowicz et al., 2017)).

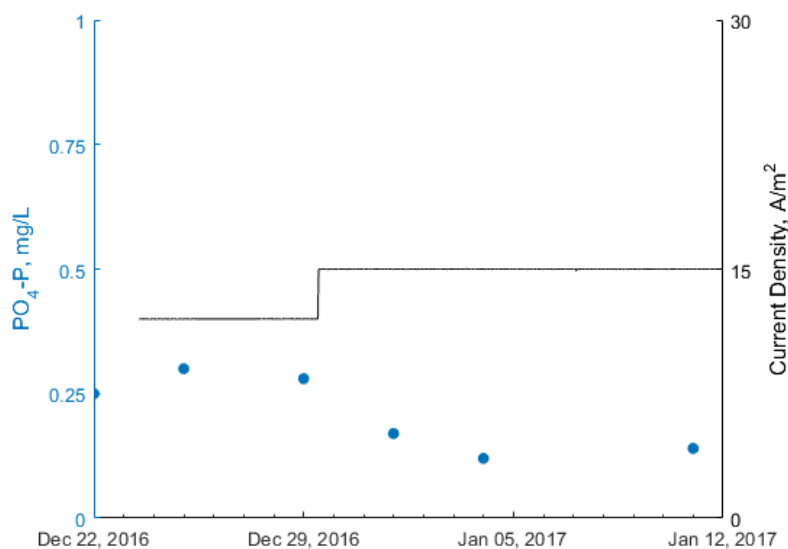


Figure 8.1-2: $\text{PO}_4\text{-P}$ effluent concentration with respect to CD

Nitrogen Removal

Removal of nitrogen improved with CD and carbon dosing, where 7 minutes of carbon dosing resulted in: $TN \geq 79.3\%$ removal. At first no carbon dosing was applied, 5 minutes was then applied to see how it would improve denitrification. A clear improvement in denitrification and hence lower TN concentration in effluent (higher removal) was observed, refer to Figure 8.1-3. By having simultaneous control over EK and carbon dosing, denitrification was improved. The ammonia and nitrate effluent concentrations over a one month period may be observed in Figure 8.1-3 (the effluent concentrations are adapted from Elektorowicz et al., 2017).

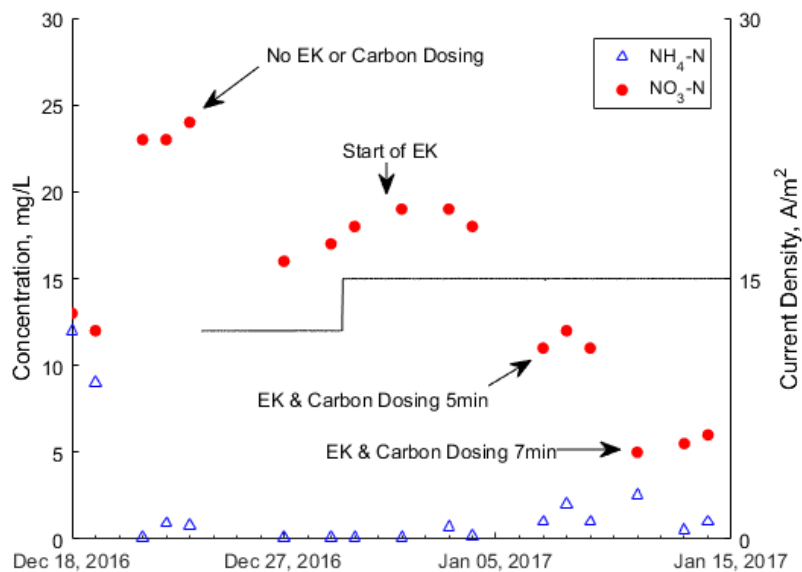


Figure 8.1-3: $\text{NH}_4\text{-N}$ & $\text{NO}_3\text{-N}$ effluent concentrations with respect to CD & Carbon Dosing

8.2. Flexibility of the MEBR

Pumps

The first part for automating the MEBR was controlling the pumps. One of the objective of the project was to build a wastewater treatment for a household; therefore, it was necessary to use standard pumps so that it would be affordable and readily available. Given that the automation and pumps may be easily decoupled, the pump system may easily be adapted to different circumstances without having any consequence on the automation, merely changing the system's parameters.

By using a programmable controller, like the P2000, allows effortless adjustment of the system for carbon dosing in cases where the influent is lacking COD for the EK process. Moreover, the system

could be enhanced by incorporating pumps for automatic membrane backwashing or chemical cleaning, and sludge wasting.

Aeration & DO Control

Similarly, adjusting the aeration and DO concentration may easily be adapted to different circumstances. Besides, the system could be easily enhanced by incorporating nitrogen or phosphorus on-line measurements, which would allow the programmable controller to better respond to influent variations and, therefore, offer higher removal of TP and nitrogen, and possibly lower even further aeration demand (Ingildsen, 2002). Other studies has demonstrated the feasibility and shown improved nutrient removal and reduced energy consumption. (Åmand, Olsson, & Carlsson, 2013; Benedetti, Baets, Nopens, & Vanrolleghem, 2010; Bilodeau & DeSilva, 2015). Nonetheless, having DO measurement has proved to be quite beneficial in terms of aeration, (see section 8.4).

Temperature Control

Under the current conditions, the MEBR has shown to be able to maintain adequate temperature throughout the project, refer to 6.4. However, this may not be the case for remote locations that experience extreme cold or warm weather. Nevertheless, incorporating a heating, ventilation and air conditioning (HVAC) system would permit the system to be expanded for these extreme conditions. It may also be connected to the programmable controller if it doesn't have its own internal controller.

Membrane Filtration

A side-stream membrane filtration units were used in the MEBR; however, submerged membrane filtration could have also been used. As will be discussed in the energy section of this chapter (section 8.4), the side-stream membrane filtration was the most energy intensive process in the MEBR, representing 71% of all energy consumption. Therefore, careful consideration is necessary when selecting side-stream versus submerged membrane application.

EK & CD Control

Using a PI controller opens new possibilities in applying EK process. It may perform waveform tracking or become a function of parameters: where the set-point may vary according to a function

that may be dependent on: time (i.e. sinusoidal, saw tooth), the DO concentration, or even phosphorus or nitrogen concentrations if the information is available (sensors or laboratory tests).

Although the EK process demonstrated in this project is applied in a bioreactor, it may be applied for many any other situations that would benefit from electrokinetic processes such as submerged membrane bioreactors for reducing membrane fouling, CAS systems, and industrial wastewater treatment. Controlling CD over time in the EK process is challenging because of varying conditions; however, this work has provided all required information so that any EK process may be controlled as desired.

MEBR

The project has achieved something quite unique in the field of wastewater treatment: innovative and complete automatic wastewater treatment that easily fits inside an everyday shed. MEBR may, for example, be installed as a decentralized system in remote locations to improve the quality of life for the secluded population of Northern Canada and Quebec, where it may be remotely monitored and controlled through wireless communication from mobile or satellite networks. Treated water could even be recovered for other purposes such as domestic water recovery (i.e. toilet water), and agriculture or industrial purposes. The MEBR may well find its purpose into the military and mining (bases or camps). Finally, it is conceivable to develop mobile MEBR units, perhaps travelling on semi-trailer truck, which could be deployed in catastrophic situations (flooding, forest fires, or refugee camps).

8.3. Simplified PI design guidelines for EK

A complete framework has been offered in section 7.3 for designing a satisfactory PI controller for controlling CD in the EK process. However, these simplified guidelines may provide enough information for the inexperienced to successfully implement a PI controller. For the intrigued, these guidelines are generally valid assuming the sampling period is larger than the response time (rise time and delay) of a power supply because the system will behave as a zeroth order system, see Appendix H.

1. Determine the process gain K : the ratio between the voltage applied and resulting current density once steady state conditions has been reached (i.e. wait until the power supply voltage has reached the desired CD).

2. Determine power supply response time from datasheet, or, if possible, time constant (τ), rise time (T_r), and delay (θ). Note: $\tau = \frac{T_r}{2.2}$.
3. Determine desired settling time (i.e. 10sec), set the sampling period accordingly:

$$\text{Sampling Period, } T_s \rightarrow \frac{t_s}{20} \leq T_s \leq \frac{t_s}{10}$$

Or conceivably start with 1sec, ideally must be close or larger than the response time of the power supply. For more details, refer to selection of sampling rate in section 7.5.

4. Use the regular AH05 tuning rules to determine PI parameters (K_p and T_i). If only the power supply response time information is not available, or AH05 doesn't yield satisfactory PI controller, use the next steps.
5. From AH05 tuning rules, two assumptions can be made: let's assume the time delay that is usually larger than the rise time (or time constant): $\tau \ll \theta$, and that the sampling period is larger than the power supply response time, so let $\theta = T_s$ in the calculation of T_i . The first assumption may not need to be true since it is more conservative than either $\tau \approx \theta$ or $\tau \gg \theta$; therefore, it will always lead to a smaller K_p . This results in the following modified AH05 tuning rules:

- $K_p = \frac{0.15\theta + 0.35\tau}{K\theta} \cong \frac{0.15}{K} = \frac{1}{7K} \approx \frac{1}{10K}$ for more conservative
- $T_i = \theta * \frac{0.15\theta + 0.35\tau}{0.46\theta + 0.02\tau} \cong \frac{\theta}{3} = \frac{T_s}{3} \approx \frac{T_s}{2}$ for more conservative

6. The PI may then be fine-tuned to improve the system's response:
 - If the system is unstable, increase sampling period (decrease sampling rate) and/or decrease K_p .
 - If the system overshoots, decrease K_p .
 - If the system responds too slowly:
 - Start by decreasing T_i
 - Increase K_p
 - Decrease sampling period (increase sampling rate), unless experiencing instability
 - If current sensor fluctuates, implement low pass filter.

Refer to Appendix H for proofs why these guidelines result in a satisfactory PI controller.

8.4. Power & Energy Consumption

A detailed power and energy consumption table is given in Appendix G.

EK

The EK process fluctuates a lot in terms of voltage applied; therefore, it is useful to look at both daily average and peak consumption, refer to Appendix G: G.

- Average consumption: energy = 0.31 kWh/m^3
 - $V_{avg} = 9.7V$, $CD_{avg} = 14.4 \text{ A/m}^2$.
- Peak consumption: energy = 0.39 kWh/m^3 .

Notes: V_{avg} reflects the average voltage applied from the start of the EK, while CD_{avg} reflects average CD from the start of the EK, where it started at 4 electrode pairs with 12A/m^2 and later it was 3 electrode pairs and CD increased to 15A/m^2 , when 1m^3 reactor was used.

Control System

The entire control system (sensors, controllers, relays) is working on two power supplies, except for the HACH SC200 controller (for DO and temperature probe), which is connected directly to an AC outlet. From the datasheets of all the equipment used, the complete control system daily energy consumption is:

- Control system: energy = 2.12 kWh/m^3 .

Pumps

There are 5 pumps in the MEBR, and using datasheet information along with their ON-OFF time ratio, the individual daily energy consumptions may be evaluated:

- Feed pump: energy = 0.12 kWh/m^3 .
- MEBR feed pump: energy = 0.36 kWh/m^3 .
- Feed circulation pump: energy = 10.5 kWh/m^3 .
- Circulation pump: energy = 12.1 kWh/m^3 .
- Dosing pump: energy = 0.18 kWh/m^3 .

This results in a daily pump energy consumption of 23.3kWh/m^3 .

Aeration

During the period the rule based control has been implemented, the average aeration flowrate is 32SLPM. The daily energy consumption for the air compressor is based on the time it takes to fill versus the time it takes to empty:

- Air compressor: energy = 6.1 kWh/m³

Overall Energy Consumption

Table 8.1-1 shows a summary of the results for the MEBR energy consumption (Appendix G).

Table 8.4-1: Summary of Energy Requirements for the MEBR

Equipment	Daily Energy (kWh/m ³)	%Demand
Control System	2.12	6.7
Feed pump	0.14	0.4
MBR pump	0.36	1.1
Feed circulation pump	10.5	32.9
Circulation pump	12.1	38.1
Aeration	6.1	19.0
EK (power supply)	0.39	1.2
Dosing pump	0.18	0.6
Total	31.87	

As mentioned in the literature review (section 2.3), aeration in activated sludge or MBR processes is a major energy consumer, often exceeding 50% of total energy consumption (Judd, 2006, 2008). In this project, aeration has only accounted for 19% of all energy demand because the DO concentration was maintained at adequately low concentration of around 0.2mg/L. A reduction in energy consumption for the aeration process in the future may be achieved by using an air blower with a variable frequency drive instead of using an air compressor. However, for the moment such solution is too costly for the magnitude of this project. The membrane filtration process was discovered to be the most energy intensive process because of the pumping requirements (feed circulation and circulation pumps). Implementing a decentralized MEBR system based on these results indicates that the peak power requirement is 2.1kW/m³, while peak daily energy requirement is 32kWh/m³. The energy requirement of the MEBR would dramatically be reduced from scaling up since more efficient pumps and aeration methods are available at larger scale.

8.5. EK - Scaling Up

Previous smaller scale lab study, where submerged membrane was used and synthetic wastewater applied, has demonstrated that EK process performed quite well for (Elektorowicz et al. 2014, Arian, 2014):

- Flowrate of 40L/day
- Total Current per Volume (TC/L): 0.1-0.11A/L.
- Energy requirement: 0.6kWh/m³

Whereas this project has demonstrated lower energy consumption values under varying influent conditions with side-stream membrane filtration:

- Flowrate 2000L/day
- TC/L: 0.016A/L (formula in Appendix G)
- Energy requirement: 0.31(average) to 0.39 (peak) kWh/m³.
- Average electrical cost for EK: ¢1.01/m³ to ¢1.54/m³. (Hydro Québec Rate L & M)
- Electrode cost achieved was ¢57 /m³ per pairs (over a 7month period).
- Power supply footprint required per reactor volume is 270cm³/m³.

The operating electrical cost may be evaluated by using the latest Hydro Québec rate *Large and Medium Power Customers* (Appendix G). The electrical operational cost for the EK could be further reduced either by optimizing the EK active time or by frequent cleaning of the electrodes as to reduce or remove the passivation and deposition layers.

As mentioned in the selection of the EK power supply, special attention was already given for scaling up the EK process. The selected power supply has a high power density and high efficiency resulting in a very low footprint, allowing it to be easily implemented in WWTP or other treatment facilities (i.e. industrial). A controller specific for the EK process could also be developed using this study method, so scaling-up will be done in a modular fashion (i.e. standard building block to be easily scaled-up). Also, with a low EK energy consumption observed, alternative sources of energy are possible, for example solar panels. This enables the EK technology to be applied in remote locations, or even replace chemical coagulations since both transport of chemicals and fuels are costly.

Chapter 9: Conclusion, Contribution & Future Work

9.1. Conclusion

This study successfully simulated a completely functional wastewater treatment pilot facility, which was located in a self-standing shed. Then, the project has proven potential implementation of the MEBR for decentralized MEBR wastewater treatment facilities. Subsequently, it might contribute system in remote regions to improve the quality of life for the secluded population of Northern Canada and Quebec.

The control and automation of the MEBR pilot facilities demonstrated the treatment of wastewater to a level even higher than lab scale preliminary tests. Treated water from MEBR may be considered for water recovery (domestic, agricultural, industrial). Such achievement was possible due to monitoring and adjusting on-line individual treatment processes.

Automated aeration ensured biological treatment with a reduction in aeration, fluctuating low dissolved oxygen concentrations allowed for simultaneous aerobic and anoxic conditions without inhibiting biological treatment. Automated control of the electro-bioreactor operation improved nutrient removal, where biological treatment was not inhibited by the application of EK.

This study designed a flexible automated system to control pumps, bioreactor aeration and intermittent electrokinetic process. Such work also included remote connectivity and data logs for all MEBR processes, including safety verifications. A human machine interface was implemented to allow easy on-site monitoring and operation, by allowing the adjustment of process parameters.

The treatment facilities can contain a completely automated MEBR with a simple interface allowing non-highly-qualified personnel to operate MEBR. Additionally, the system can be controlled remotely through the Internet.

Automated aeration ensured biological treatment with a reduction in aeration, fluctuating low dissolved oxygen concentrations allowed for simultaneous aerobic and anoxic conditions without inhibiting biological treatment. Automated control of the electro-bioreactor operation improved nutrient removal, where biological treatment was not inhibited by the application of EK.

This study permitted to designing of a PI controller for regulating CD in the EK process, which also can be applied to any wastewater characteristics and where guidelines were provided for successfully designing a PI controller. Finally, this study also showed precisely variations of the applied voltage during operation and during a single intermittent EK cycle.

Furthermore, a significant energy reduction was achieved by controlling EK process; EK demonstrated lower than previously observed daily energy consumption: 0.31 (average), 0.39 (peak) kWh/m³ (1.2% of all energy demand), and equivalent to ¢1.01/m³ to ¢1.54/m³.

9.2. Contribution

The achieved contribution can be summarized as follows:

- Designing and implementation of automation to a novel MEBR pilot facility, which demonstrated the feasibility of scaling-up of the system. Thus, make possible local and remote monitoring which enable exciting possibilities for MEBR applications such to decentralized systems.
- Development of EK control system through monitoring current density, by using a current transducer, and adjusting applied voltage by implementing a PI controller. Thus, make possible to change the mode of operation, carbon dosing, varying CD in order to track specific waveform or function of parameters.
- Development of the DO control system using the state of art sensors for DO and aeration, for achieving alternate aerobic and anoxic conditions in electro-bioreactor.

9.3. Future Work

- Investigation of more energy efficient side-stream membrane filtration (i.e. membrane modules and pumps) and aeration (i.e. blower and diffusers).
- Investigation of the MEBR control system's sensitivity to different influent conditions.
- Developing automatic systems for raw feed sewage screening, wasted sludge discharge, and electrode cleaning.
- Designing PID for simultaneous ammonia and DO control.

References

- AcuAMP DCT. (2017). Retrieved July 20, 2003, from
<https://cdn.automationdirect.com/static/specs/acuampdct.pdf>
- Åmand, L., Olsson, G., & Carlsson, B. (2013). Aeration control – a review. *Water Science & Technology*, 67(11), 2374. <https://doi.org/10.2166/wst.2013.139>
- APHA. (2012). *Standard Methods for the Examination of Water and Wastewater* (22nd ed.). American Public Health Association, American Water Works Federation, Water Environment.
- Arian, Z. (2014). *New configuration of submerged electro-bioreactor (SMEBR) for nutrient removal in water recovery*. Concordia University.
- Åström, K. J., & Hägglund, T. (2005). *Advanced PID Control*. ISA - The Instrumentation, Systems, and Automation Society.
- Åström, K. J., & Murray, R. M. (2012). *Feedback Systems - An introduction for scientists and engineers* (2nd ed.). Princeton University Press.
- Bani-Melhem, K. Q., & Elektorowicz, M. (2010). Development of a novel submerged membrane electro-bioreactor (SMEBR): Performance for fouling reduction. *Environmental Science and Technology*, 44(9), 3298–3304. <https://doi.org/10.1021/es902145g>
- Bani-Melhem, K. Q., & Elektorowicz, M. (2011). Performance of the submerged membrane electro-bioreactor (SMEBR) with iron electrodes for wastewater treatment and fouling reduction. *Journal of Membrane Science*, 379(1–2), 434–439. <https://doi.org/10.1016/j.memsci.2011.06.017>
- Bani-Melhem, K. Q., Elektorowicz, M., & Oleszkiewicz, J. A. (2009). Wastewater Treatment System and Method. US Patent 8147700 A1. Retrieved from <http://www.google.com/patents/US8147700>
- Bektas, N., Akbulut, H., Inan, H., & Dimoglo, A. (2004). Removal of phosphate from aqueous solutions by electro-coagulation. *Journal of Hazardous Materials*, 106B, 101–105. <https://doi.org/10.1016/j.jhazmat.2003.10.002>
- Benedetti, L., Baets, B. De, Nopens, I., & Vanrolleghem, P. A. (2010). Multi-criteria analysis of wastewater treatment plant design and control scenarios under uncertainty. *Environmental Modelling & Software*, 25(5), 616–621. <https://doi.org/http://dx.doi.org/10.1016/j.envsoft.2009.06.003>
- Bilodeau, K., & DeSilva, V. (2015). Ammonia-Based Aeration Control On-Line Probes to Save Energy Cost and Meet Compliance. In *WEFTEC 2015* (pp. 435–442).
- Böhm, L., Drews, A., Prieske, H., Bérubé, P. R., & Kraume, M. (2012). The importance of fluid dynamics for MBR fouling mitigation. *Bioresource Technology*, 122, 50–61. <https://doi.org/10.1016/j.biortech.2012.05.069>

- Bouhabila, E. H., Ben Aïm, R., & Buisson, H. (2001). Fouling characterisation in membrane bioreactors. *Separation and Purification Technology*, 22–23, 123–132. [https://doi.org/10.1016/S1383-5866\(00\)00156-8](https://doi.org/10.1016/S1383-5866(00)00156-8)
- Chang, I., Le Clech, P., Jefferson, B., & Judd, S. (2002). Membrane fouling in membrane bioreactors for wastewater treatment. *Journal of Environmental Engineering-Asce*, 128(11), 1018–1029. [https://doi.org/10.1061/\(asce\)0733-9372\(2002\)128:11\(1018\)](https://doi.org/10.1061/(asce)0733-9372(2002)128:11(1018))
- Chen, C. (2006). *Analog and Digital Control System Design* (1st ed.). Oxford University Press.
- Chen, G. (2004). Electrochemical technologies in wastewater treatment. *Separation and Purification Technology*, 38(1), 11–41. <https://doi.org/10.1016/j.seppur.2003.10.006>
- Chen, G., Chen, X., & Yue, P. L. (2000). Electrocoagulation and Electroflotation of Restaurant Wastewater. *Journal of Environmental Engineering*, 126(September), 858–863.
- Davis, M. L., & Cornwell, D. A. (2013). *Introduction to Environmental Engineering* (5th ed.). McGraw-Hill.
- De Temmerman, L., Maere, T., Temmink, H., Zwijnenburg, a., & Nopens, I. (2015). The effect of fine bubble aeration intensity on membrane bioreactor sludge characteristics and fouling. *Water Research*, 76(0), 99–109. <https://doi.org/10.1016/j.watres.2015.02.057>
- Dorf, R. C., & Bishop., R. H. (2011). *Modern control systems* (12th ed.). Pearson.Elektorowicz M, Arian Z, Ibeid S, 2014. Submerged membrane electro-bioreactor for water recovery, Membranes and Membrane Processes in Environmental Protection. Monographs of the Environmental Engineering Committee. Monograph of Polish Academy of Sciences. vol. 119: 93-98, ISBN 978-83-63714-18-5
- Elektorowicz M., Oleszkiewicz J, Ibeid S, 2017, NSERC I2I Final Report, Internal document.
- Elektorowicz, M., Habibi, S., & Chifrina, R. (2006). Effect of electrical potential on the electro-demulsification of oily sludge. *Journal of Colloid and Interface Science*, 295(2), 535–41. <https://doi.org/10.1016/j.jcis.2005.08.042>
- Elektorowicz M, Hoseini F, Ibeid S. 2016. Anammox membrane electro-bioreactor. Architecture, Civil Engineering, Environment. 9 (3): 123-128
- Ibeid S, Elektorowicz, M., & Oleszkiewicz, J. A. (2012). Processes and apparatuses for removal of carbon, phosphorus and nitrogen. Canadian Patent Application No. 2,894,617
- Elektorowicz, M., & Oleszkiewicz, J. A. (2012). Method of Treating Sludge Material using Electrokinetics. US Patent 8329042 B2. Retrieved from <http://www.google.com/patents/US8329042>
- Environment Canada. (2017). Historical Climate Data. Retrieved February 10, 2017, from http://climate.weather.gc.ca/historical_data/search_historic_data_stations_e.html?searchType=stnName&timeframe=1&txtStationName=L%27Assomption&searchMethod=contains&

[optLimit=yearRange&StartYear=2016&EndYear=2017&Year=2017&Month=2&Day=9&selectedRowPerPage=25](#)

Field, R. W., Wu, D., Howell, J. A., & Gupta, B. B. (1995). Critical flux concept for microfiltration fouling. *Journal of Membrane Science*, 100(3), 259–272. [https://doi.org/10.1016/0376-7388\(94\)00265-Z](https://doi.org/10.1016/0376-7388(94)00265-Z)

Flemming, H. C., Schaule, G., Griebe, T., Schmitt, J., & Tamachkiarowa, a. (1997). Biofouling - the Achilles heel of membrane processes. *Desalination*, 113(2–3), 215–225. [https://doi.org/10.1016/S0011-9164\(97\)00132-X](https://doi.org/10.1016/S0011-9164(97)00132-X)

Franklin, G. F., Powell, J. D., & Workman, M. L. (1997). *Digital Control of Dynamic Systems - Franklin.pdf* (3rd editio). Prentice Hall.

Gao, Y. (2014). *Enhancement of wastewater treatment under low carbon/nitrogen ratio by using submerged membrane electro-bioreactor (SMEBR)*. Concordia University.

Garnier, H., & Wang, L. (2008). *Identification of Continuous-time Models from Sampled Data* (Vol. 1). London: Springer London. <https://doi.org/10.1007/978-1-84800-161-9>

HACH. (2011). Hach Method 10360 Luminescence Measurement of Dissolved Oxygen in Water and Wastewater and for Use in the Determination of BOD 5 and cBOD 5, (October), 1–13.

HACH LDO 2. (2017). Retrieved from <https://www.hach.com/hach-ldo-model-2-optical-process-dissolved-oxygen-probe/product?id=10182183350>

Hai, F. I., & Yamamoto, K. (2011). Membrane Biological Reactors. *Treatise on Water Science*, 571–613. <https://doi.org/10.1016/B978-0-444-53199-5.00096-8>

Harif, T., Khai, M., & Adin, A. (2012). Electrocoagulation versus chemical coagulation: Coagulation/flocculation mechanisms and resulting floc characteristics. *Water Research*, 46(10), 3177–3188. <https://doi.org/10.1016/j.watres.2012.03.034>

Hasan, S. W. (2011). *Design and Performance of a Pilot Submerged Membrane Electro-Bioreactor (SMEBR) for Wastewater Treatment*. Concordia.

Hasan, S. W., Elektorowicz, M., & Oleszkiewicz, J. A. (2012). Correlations between trans-membrane pressure (TMP) and sludge properties in submerged membrane electro-bioreactor (SMEBR) and conventional membrane bioreactor (MBR). *Bioresource Technology*, 120, 199–205. <https://doi.org/10.1016/j.biortech.2012.06.043>

Hasan, S. W., Elektorowicz, M., & Oleszkiewicz, J. A. (2014). Start-up period investigation of pilot-scale submerged membrane electro-bioreactor (SMEBR) treating raw municipal wastewater. *Chemosphere*, 97, 71–77. <https://doi.org/10.1016/j.chemosphere.2013.11.009>

HDS1500 Datasheet. (2017). Retrieved from http://xppower.com/Portals/0/pdfs/SF_HDS1500.pdf?ver=2016-05-26-135546-300

Households and the Environment. (2011). Statistics Canada.

Ibeid, S. (2011). *Enhancement of the submerged membrane electro-bioreactor (SMEBR) for*

- nutrient removal and membrane fouling control.* Concordia University.
- Ibeid, S., & Elektorowicz, M. (2017). *MEBR - Idea to Innovation Report*.
- Ibeid, S., Elektorowicz, M., & Oleszkiewicz, J. A. (2013a). Modification of activated sludge properties caused by application of continuous and intermittent current. *Water Research*, 47(2), 903–10. <https://doi.org/10.1016/j.watres.2012.11.020>
- Ibeid, S., Elektorowicz, M., & Oleszkiewicz, J. A. (2013b). Novel electrokinetic approach reduces membrane fouling. *Water Research*, 47(16), 6358–6366. <https://doi.org/10.1016/j.watres.2013.08.007>
- Ibeid, S., Elektorowicz, M., & Oleszkiewicz, J. A. (2015). Electro-conditioning of activated sludge in a membrane electro-bioreactor for improved dewatering and reduced membrane fouling. *Journal of Membrane Science*, 494, 136–142. <https://doi.org/10.1016/j.memsci.2015.07.051>
- Ingildsen, P. (2002). *Realising full-scale control in wastewater treatment systems using in situ nutrient sensors*. Department of Industrial Electrical Engineering and Automation. PhD Dissertation, Lund University.
- Johnson, M. A., & Moradi, M. H. (2005). *PID Control: New Identification and Design Methods*. Springer.
- Judd, S. (2006). *The MBR book: Principles and Applications of Membrane Bioreactors in Water and Wastewater Treatment*. Elsevier. Elsevier Ltd. <https://doi.org/10.1016/B978-185617481-7/50005-2>
- Judd, S. (2008). The status of membrane bioreactor technology. *Trends in Biotechnology*, 26(2), 109–116. <https://doi.org/10.1016/j.tibtech.2007.11.005>
- Kiser, P. Advances in On-Line Dissolved Oxygen Measurement Using Luminescent Technology (2012). Retrieved from <http://www.hach.com/hach-ldo-model-2-optical-process-dissolved-oxygen-probe/product-downloads?id=10182183350>
- Larue, O., Vorobiev, E., Vu, C., & Durand, B. (2003). Electrocoagulation and coagulation by iron of latex particles in aqueous suspensions. *Separation and Purification Technology*, 31, 177–192. [https://doi.org/10.1016/S1383-5866\(02\)00182-X](https://doi.org/10.1016/S1383-5866(02)00182-X)
- Liu, T., & Gao, F. (2012). *Industrial Process Identification and Control Design*. Springer. <https://doi.org/10.1007/978-0-85729-977-2>
- LVCN414 Level Sensor. (2017). Retrieved from http://www.omega.ca/pptst_eng/LVCN414.html
- Matteson, M. J., Dobson, R. L., Glenn, R. W., Kukunoor, N. S., Waits, W. H., & Clayfield, E. J. (1995). Electrocoagulation and separation of aqueous suspensions of ultrafine particles. *Colloids and Surfaces A: Physicochemical and Engineering Aspects*, 104(1), 101–109. [https://doi.org/10.1016/0927-7757\(95\)03259-G](https://doi.org/10.1016/0927-7757(95)03259-G)
- Meng, F., Chae, S.-R., Drews, A., Kraume, M., Shin, H.-S., & Yang, F. (2009). Recent advances in membrane bioreactors (MBRs): Membrane fouling and membrane material. *Water*

Research, 43(6), 1489–1512. <https://doi.org/10.1016/j.watres.2008.12.044>

Mollah, M., Morkovsky, P., Gomes, J. A. G., Kesmez, M., Parga, J., & Cocke, D. L. (2004). Fundamentals, present and future perspectives of electrocoagulation. *Journal of Hazardous Materials*, 114(1–3), 199–210. <https://doi.org/10.1016/j.jhazmat.2004.08.009>

Municipal Wastewater Treatment Indicator. (2013). Environment Canada. Retrieved from <https://www.ec.gc.ca/indicateurs-indicators/default.asp?lang=En&n=2647AF7D-1>

Oh, H. S., Yeon, K. M., Yang, C. S., Kim, S. R., Lee, C. H., Park, S. Y., ... Lee, J. K. (2012). Control of membrane biofouling in MBR for wastewater treatment by quorum quenching bacteria encapsulated in microporous membrane. *Environmental Science and Technology*, 46(9), 4877–4884. <https://doi.org/10.1021/es204312u>

Park, H., Chang, I., & Lee, K. (2015). *Principles of Membrane Bioreactors for Wastewater Treatment*. CRC Press.

Pouet, M. (1995). Urban wastewater treatment by electrocoagulation and flotation. *Water Science and Technology*, 31(3–4), 275–283. [https://doi.org/10.1016/0273-1223\(95\)00230-K](https://doi.org/10.1016/0273-1223(95)00230-K)

Psoch, C., & Schiewer, S. (2005). Long-term study of an intermittent air sparged MBR for synthetic wastewater treatment. *Journal of Membrane Science*, 260(1–2), 56–65. <https://doi.org/10.1016/j.memsci.2005.03.021>

Radjenović, J., Matošić, M., Mijatović, I., Petrović, M., & Barceló, D. (2008). Membrane Bioreactor (MBR) as an Advanced Wastewater Treatment Technology. In *Emerging Contaminants from Industrial and Municipal Waste* (Vol. 5, pp. 37–101). Berlin, Heidelberg: Springer Berlin Heidelberg. https://doi.org/10.1007/978_5_093

Sawyer, C., McCarty, P., & Parkin, G. (2003). *Chemistry for Environmental Engineering and Science* (5th ed.). McGraw-Hill.

Skogestad, S. (2001). Probably the best simple PID tuning rules in the world. *Journal of Process Control*, xx, 1–27.

Sierra SmartTrak 50. (2017). Retrieved from <http://www.sierrainstruments.com/products/50series.html>

Trussell, R. S., Merlo, R. P., Hermanowicz, S. W., & Jenkins, D. (2007). Influence of mixed liquor properties and aeration intensity on membrane fouling in a submerged membrane bioreactor at high mixed liquor suspended solids concentrations. *Water Research*, 41(5), 947–958. <https://doi.org/10.1016/j.watres.2006.11.012>

Vasudevan, S., Sozhan, G., Ravichandran, S., Jayaraj, J., Lakshmi, J., & Sheela, M. (2008). Studies on the Removal of Phosphate from Drinking Water by Electrocoagulation Process. *Industrial & Engineering Chemistry Research*, 47(6), 2018–2023. <https://doi.org/10.1021/ie0714652>

Ward, B. B. (2013). Nitrification. *Reference Module in Earth Systems and Environmental Sciences*, (March), 1–8. <https://doi.org/10.1016/B978-0-12-409548-9.00697-7>

- Wei, V., Elektorowicz, M., & Oleszkiewicz, J. A. (2011). Influence of electric current on bacterial viability in wastewater treatment. *Water Research*, 45(16), 5058–5062. <https://doi.org/10.1016/j.watres.2011.07.011>
- Zhang, T. C., Surampalli, R. Y., Vigneswaran, S., Tyagi, R. D., Ong, S. L., & Kao, C. M. (2012). *Membrane Technology and Environmental Applications* (Vol. 82). Environmental and Water Resources Institute (EWRI) of the American Society of Civil Engineers (ASCE).
- Ziegler, J. G., & Nichols, N. B. (1942). Optimum Settings for Automatic Controllers. *ASME Transactions*, 64, 759–765. <https://doi.org/10.1115/1.2899060>
- Zuthi, M. F. R., Guo, W. S., Ngo, H. H., Nghiem, L. D., & Hai, F. I. (2013). Enhanced biological phosphorus removal and its modeling for the activated sludge and membrane bioreactor processes. *Bioresource Technology*, 139, 363–374. <https://doi.org/10.1016/j.biortech.2013.04.038>

Appendix A: Electronic & Electrical Supplies

Table A-1: List of Electronic and Electrical Supplies

Component	Description	Model	Qty.
P2000 CPU	CPU	P2-550	1
Base	7-slot base for modules, CPU and power supply	P2-07B	1
Power Supply	110VAC input based power supply	P2-01AC	1
Discrete input	16-point, 12-24VDC	P2-16ND3	1
Discrete output	16-point, 12-24VDC	P2-16TD1P	1
Relay output	16-point, 6-24VDC/6-240VAC, 2 isolated commons	P2-16TR	1
Analog input	8-channel, 16bit resolution, 0-20mA	P2-08AD-1	1
Analog output	8-channel, 16bit resolution, 0-10VDC	P2-08DA-2	1
Analog output	4-channel, 12bit resolution, 0-20mA	P2-08DA-2	1
Filler	Module for protecting empty base slots	P2-FILL	1
Ethernet switch	Link P2000 & HMI to router	SE-SW5U	1
Fuses	2Amps. Used to protect P2000, HMI and Sensors	KN-F10-10 & GMA2	6
EK fuses	30Amps. Used to protect electrodes	EHCC2DIU-6 & HCLR30	4
Relays	Used to activate pumps, including diode reverse protection	782-2C-SKT, 782-2C-24D, AD-BSMD-250	4
EK power supply	Programmable power supply	HDS1500	1
Safety relay	Provides power to relays and EK power supply	Dold LG5924-48-61-24	1
Relay & Logic power supply	24V power supply, 60W	PSB24-060S-P	1
Breaker	Used to remove AC power to power supplies	FAZ-B15-2	1
Current Transducer	Measure current output from EK power supply	DCT100-42-24-F	1
Green LED	Indicator	DR22E3L-E3GZA	1
Red LED	Indicator	DR22E3L-E3RZA	1
Green Push button	Pumps & EK Activation	AR22F5L-10E3GZA	2
Selector Switch	Enable or disable system	AR22PR-210BZA	1
Emergency Stop	Stop system	AR22V7R-01R	1
Red signal beacon	Power indicator	20610000 & 95584035	1
HMI	Touch screen panel	C-More Micro EA3-T6CL	1
Control Wiring	20AWG Wiring, 500' roll	MTW20BK	1
Terminals	Konnect-It terminal blocks	KN-T12GRY KN-D12X	20 20

Appendix B: Pumps Ladder Diagram Tasks

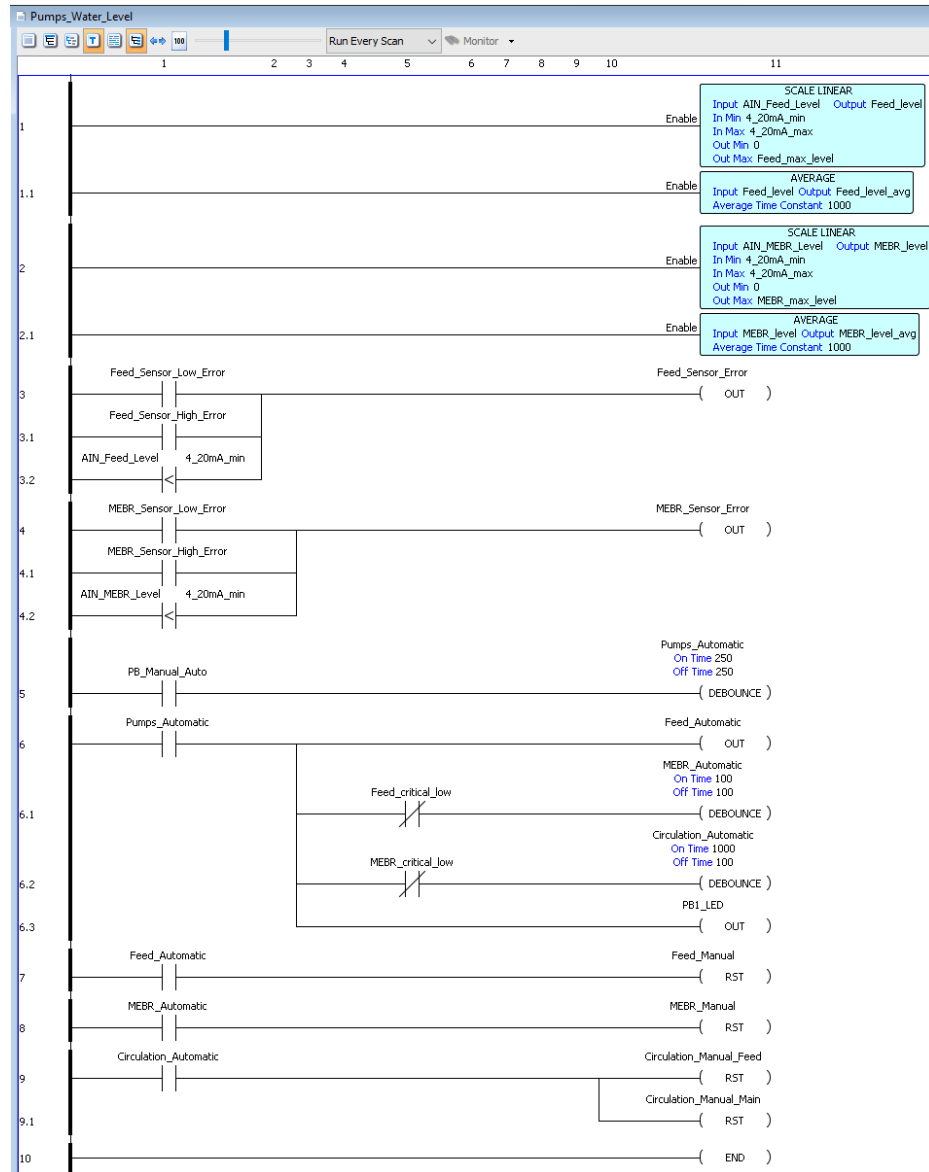


Figure B-1: Pumps Water Level Task

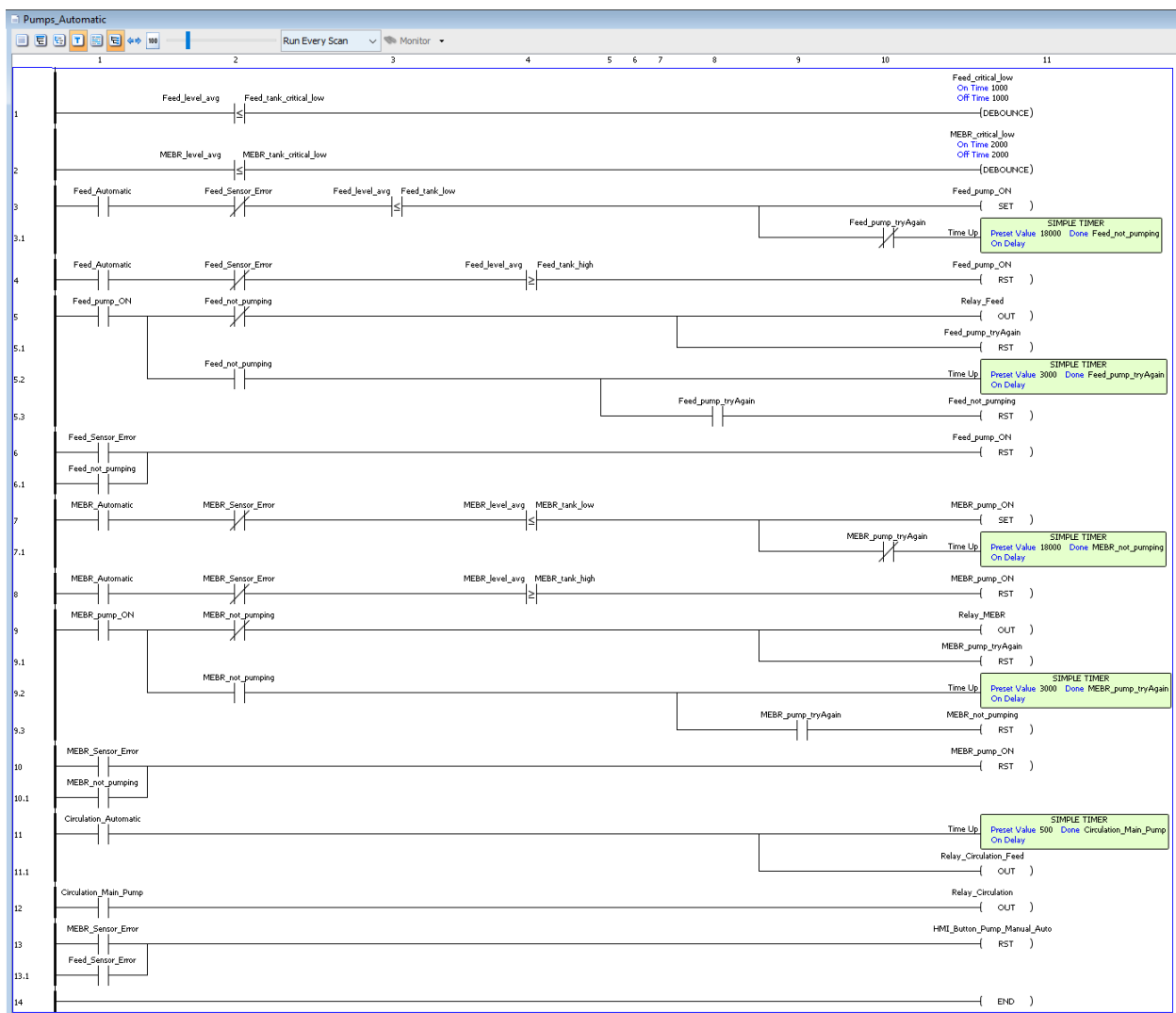


Figure B-2: Pumps Automatic Task

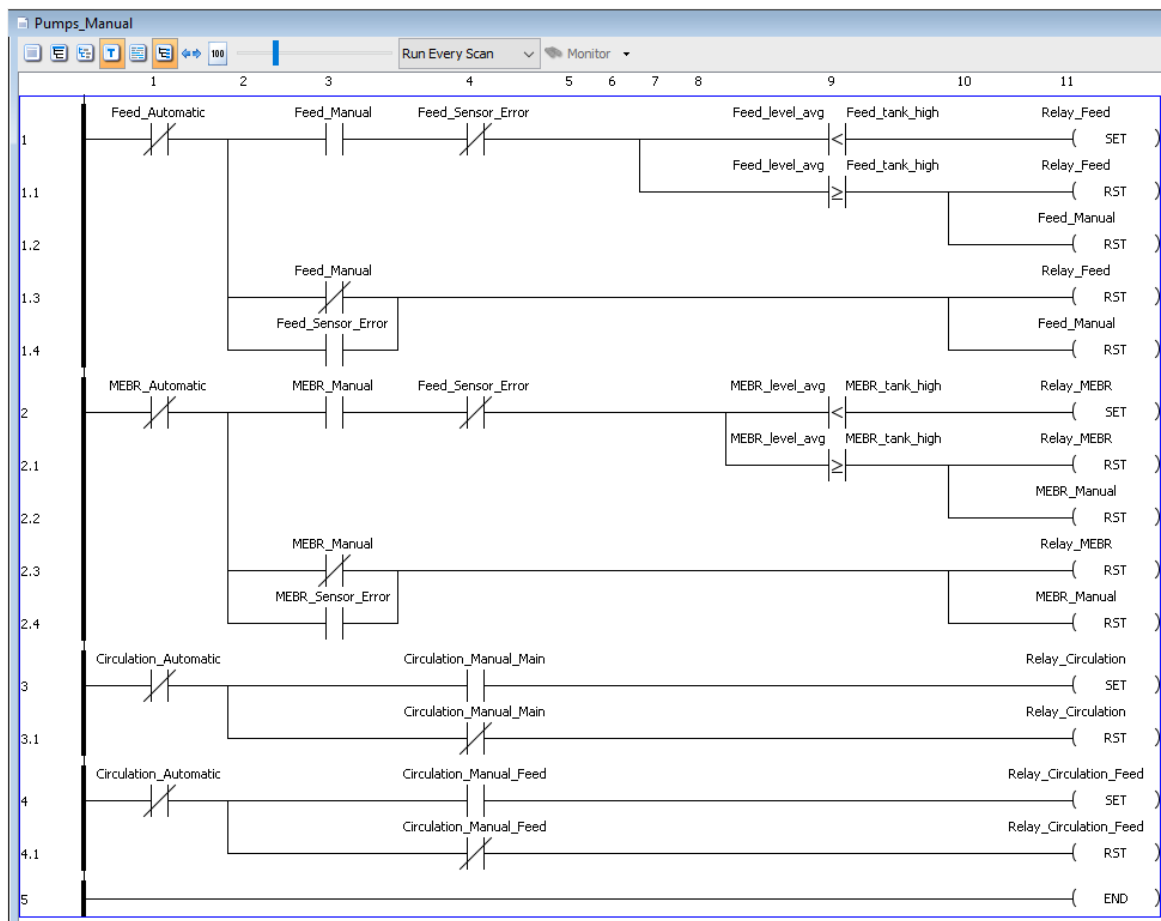


Figure B-3: Pump Manual Task

Appendix C: Aeration & Purge Ladder Diagram Tasks

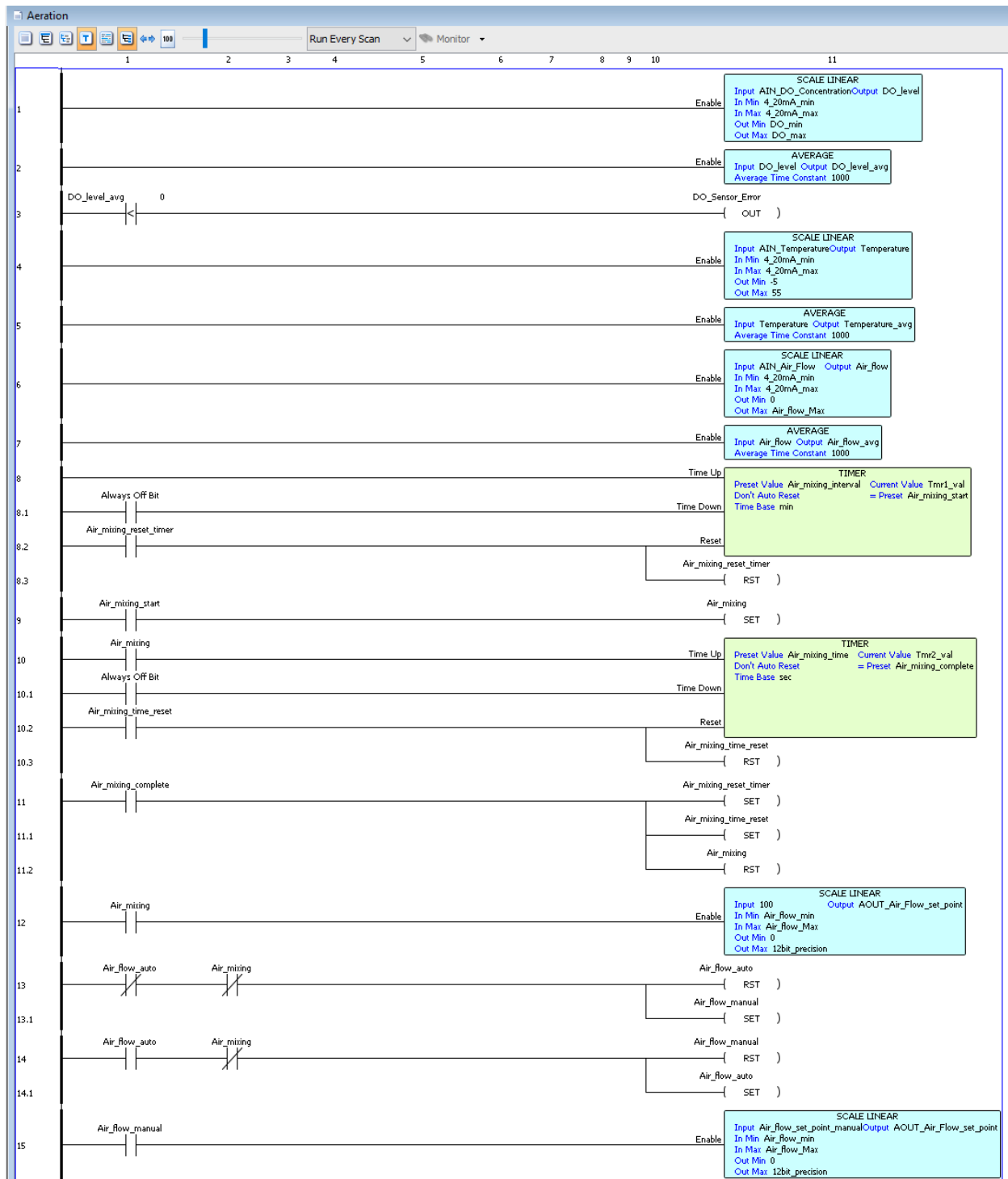


Figure C-1: Aeration Task (1 of 2)

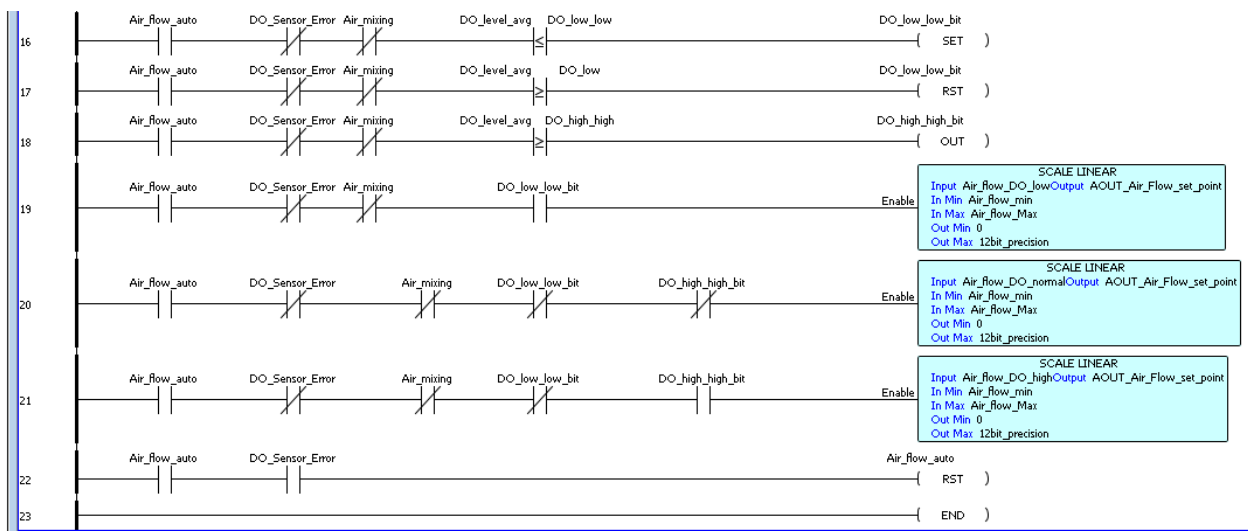


Figure C-2: Aeration Task (2 of 2)

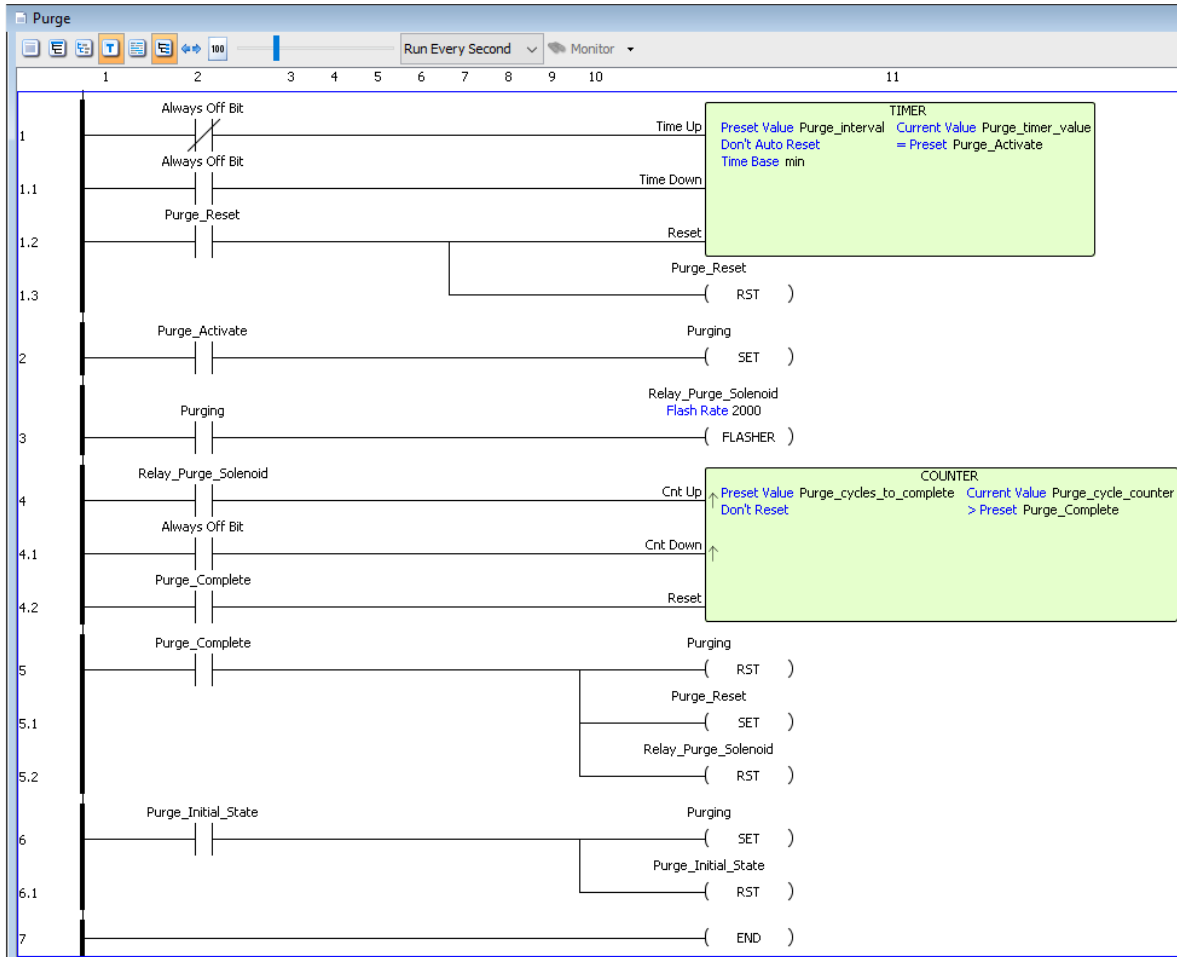


Figure C-3: Purge Task

Appendix D: EK & Carbon Dosing Ladder Diagram Tasks

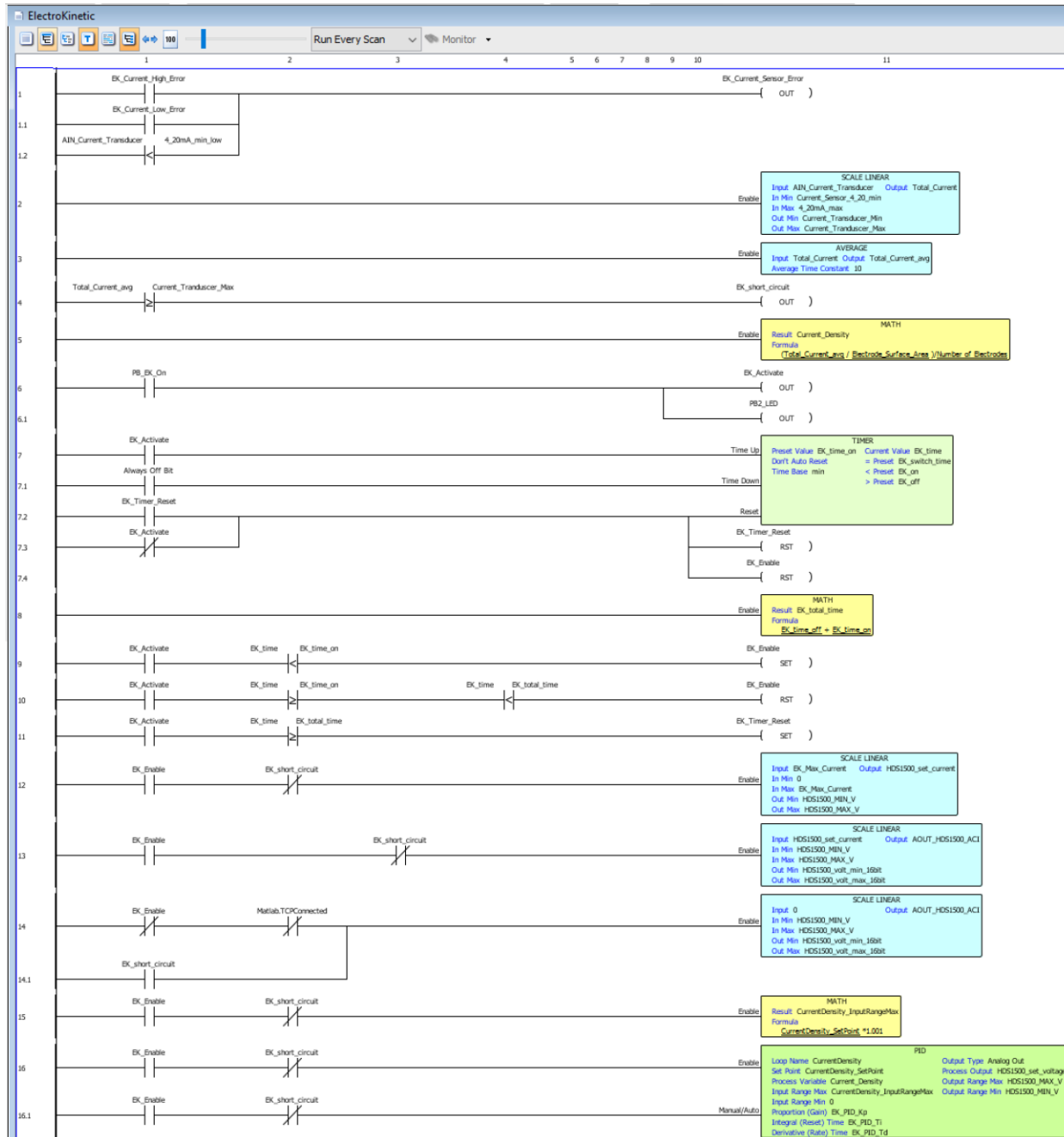


Figure D-1: EK Task (1 of 1)

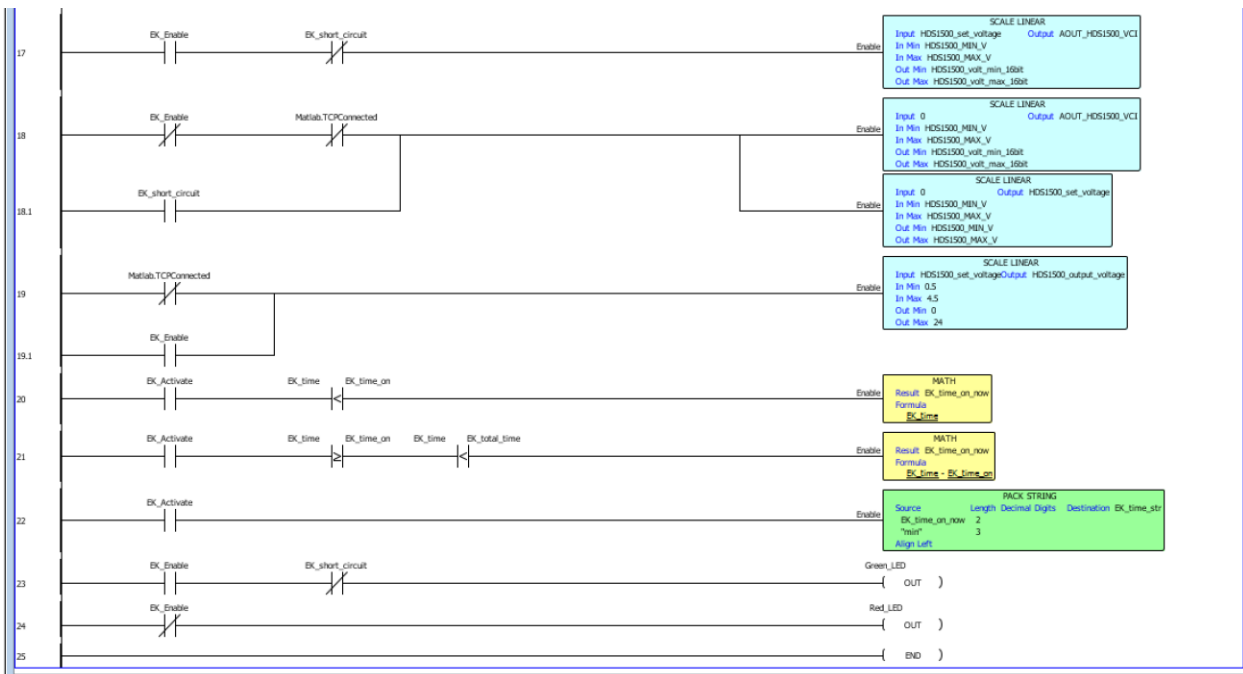


Figure D-2: EK Task (2 of 2)

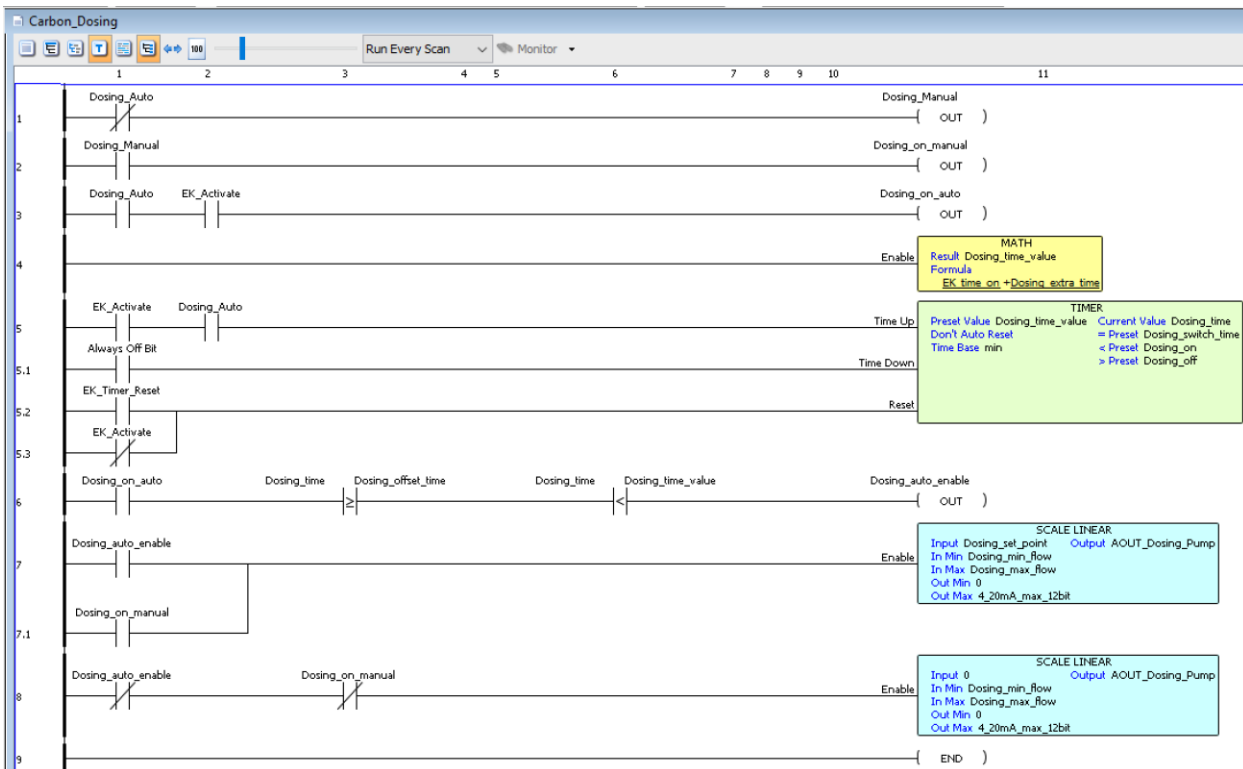


Figure D-3: Carbon Dosing Task

Appendix E: P2000 & MATLAB TCP/IP

P2000 – MATLAB as CPoE Device:

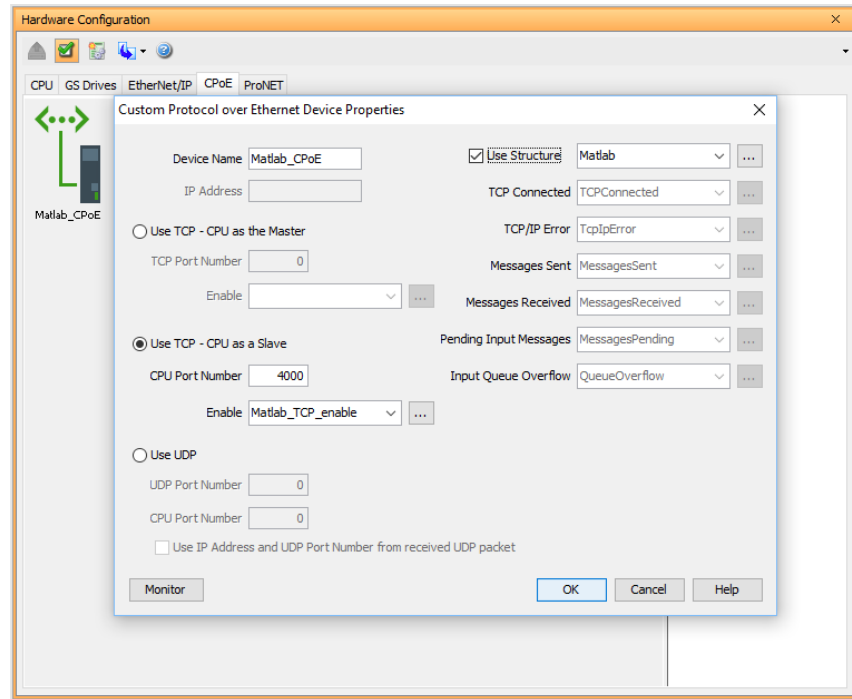


Figure E-1: MATLAB as CPoE Device

P2000 task for communicating to MATLAB over TCP/IP.

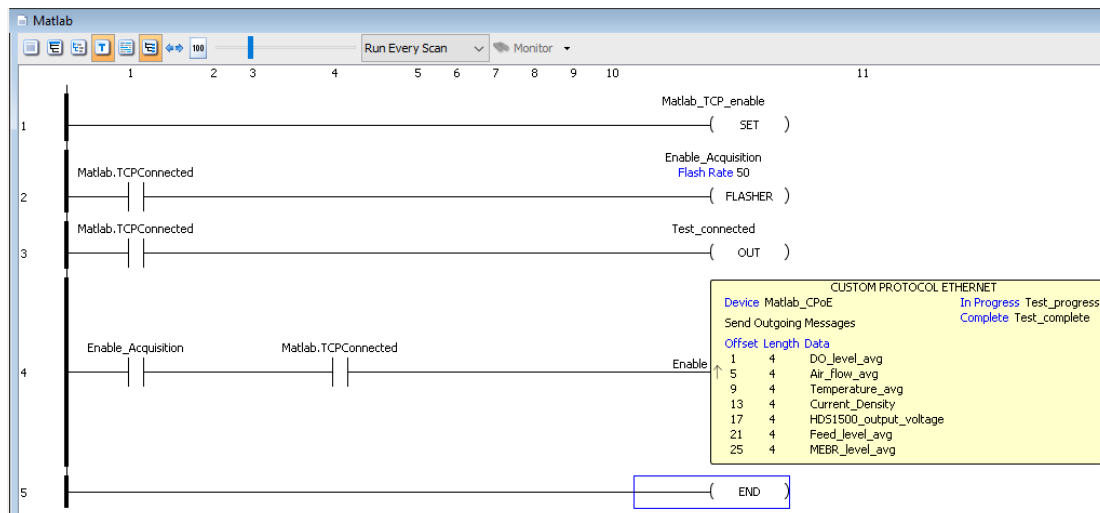


Figure E-2: MATLAB Task

MATLAB code to receive data:

```
port = 4000 ;
P2000 = '192.168.0.150';
t = tcpip(P2000,port);
fopen(t);
disp('Starting')
tic
sampling_rate = 0.1;
%sampling_time = 20;
sampling_time = 10;
nSize = sampling_time/sampling_rate;
%Initialize Arrays
DO = zeros(nSize,1);
Air = zeros(nSize,1);
T = zeros(nSize,1);
CD = zeros(nSize,1);
V = zeros(nSize,1);
Feed = zeros(nSize,1);
MEBR = zeros(nSize,1);
ref = 10;
output = zeros(nSize,1);
on = 4;
t1_on = 0.5;
t1_off = t1_on + on;
t2_on = t1_off+3;
t2_off = t2_on+on;
for k = 1:numel(output)
    tk = (k-1)*sampling_rate;
    if(tk >= t1_on && tk<= t1_off)
        output(k,1) = ref;
    elseif (tk >= t2_on && tk<= t2_off)
        output(k,1) = ref;
    end
end
nData = 7;
time = 0:sampling_rate:sampling_time-sampling_rate;
for k = 1:nSize
    while(t.BytesAvailable == 0)
    end
    temp = fread(t, nData, 'float32');
    DO(k,1) = temp(1,1);
    Air(k,1) = temp(2,1);
    T(k,1) = temp(3,1);
    CD(k,1) = temp(4,1);
    V(k,1) = temp(5,1);
    Feed(k,1) = temp(6,1);
    MEBR(k,1) = temp(7,1);
    fwrite(t,output(k,1),'float32');
end
fclose(t);
delete(t);
clear t
toc
```

Figure E-3: MATLAB Code for P2000 Communication

Appendix F: System Identification – MATLAB

Script:

```
%load Step Response
filename = 'Steptest23.xls';
first = 0.1;
last = 1;
[time, V, CD, Ts, delay] = loadStepResponse(filename,first,last);
%%
% FOPDT Minimization using FMINUNC & Quasi-Newton including a delay
[K, tau,e_opt] = FOPDT_est_discrete_delay(time,V,CD,0,Ts,delay);
numz = [0 K*(1-exp(-Ts/tau))];
denz = [1 -1*exp(-Ts/tau)];
sys_opt = tf([0 K],[tau 1],'IODelay',delay);
sys_opt_z = tf(numz,denz,Ts,'IODelay',round(delay/Ts,0),'Variable','z^-1');%in Z domain
%%
% Least-Squares including a delay
[K_ls, tau_ls, delay_ls, e_ls] = FOPDT_est_LS_discrete_delay(time,V,CD,0,Ts,delay);
num = [0 K_ls*(1-exp(-Ts/tau_ls))];
den = [1 -1*exp(-Ts/tau_ls)];
sys_ls = tf(K_ls,[tau_ls 1],'IODelay',delay_ls);
sys_ls_z = tf(num,den,Ts,'IODelay',delay_ls/Ts,'Variable','z^-1');%in Z domain
%%
%Compare different results
yopt_z = lsim(sys_opt_z,V,time);
yls_z = lsim(sys_ls_z,V,time);
figure(1)
hold on
plot(time,V);
plot(time,CD);
stairs(time,yopt_z);
stairs(time,yls_z);
hold off;
ax = gca;
% ax.XTick = 0:0.5:1;
ax.YTick = 0:0.5:1.5;
legend('V','CD Actual','CD Optimal','CD LS');
title('System Identification - Step Response Comparison');
xlabel('Time, sec');
ylabel('Output');

ylabel('Output');
```

Figure F-1: System Identification using MATLAB

Function for FOPDT_est_discrete_delay:

```

function [ K,tau,e] = FOPDT_est_discrete_delay( t, u, y,y0,Ts,delay)
%Estimate parameters K, tau and delay for a FOPDT using discrete system
f = @(x)systemError(x,t,u,y,y0,Ts,delay);
options = optimoptions('fmincon','Display','iter','Algorithm','interior-point');
options.MaxFunctionEvaluations = 10000; %max iteration
problem.options = options;
problem.x0 = [1 1];
problem.lb = [0 0];
problem.ub = [1000 1000];
problem.objective = f;
problem.solver = 'fmincon';
[x, e] = fmincon(problem);
K = x(1);
tau = x(2);
function error = systemError(x,t,u,y,y0,Ts,theta)
    K_x = x(1);
    tau_x = x(2);
    delay_x = theta/Ts;
    sys_num = [0 K_x*(1-exp(-Ts/tau_x))];
    sys_den = [1 -1*exp(-Ts/tau_x)];
    sys_z = tf(sys_num,sys_den,Ts,'IODelay',delay_x,'Variable','z^-1');%in Z domain
    sys = lsim(sys_z,u,t,y0);
    evec = y-ysys;
    error = evec'*evec;
end
end

```

Figure F-2: FOPDT Estimation using Optimization

Function for FOPDT_est_LS_discrete_delay:

```

function [ K,tau,actual_delay,e ] = FOPDT_est_LS_discrete_delay( time,V,CD,y0,Ts,delay )
%Estimate parameters K, tau and delay for a FOPDT based on discrete system
%Setup Parameter vector X & Y and calculate Theta
actual_delay = delay;
sampleDelay = actual_delay/Ts;
c1 = CD(sampleDelay+1:end-1);
c2 = V(1:end-sampleDelay-1);
X = [c1 c2];
Y = CD(sampleDelay+2:end);
Theta = (X'*X)\X'*Y;
alpha = Theta(1);
K = Theta(2)/(1-alpha);
tau = -Ts/log(alpha);
num = [0 K*(1-exp(-Ts/tau))];
den = [1 -1*exp(-Ts/tau)];
sys_z = tf(num,den,Ts,'Variable','z^-1');
CD_est = lsim(sys_z,V,time,y0);
error = CD_est-CD;
e = error'*error;
end

```

Figure F-3: FOPDT Estimation using Least Square

Appendix G: Power, Energy & Scale Up

$$Power = n_{electrodes} * V * CD * Area \quad (G.1)$$

$$Daily\ Energy = Power * \left(\frac{time_{on}}{time_{off} + time_{on}} \right)_{per\ day} \quad (G.2)$$

Table G-1: Energy Consumption

Equipment	P _{peak} (W)	P _{peak} (W/m ³)	Time On (min)	Time Off (min)	%On	P _{avg} (W)	P _{avg} (W/m ³)	Energy (kWh/day)	Energy (kWh/m ³ /day)	%	Electrical Cost (¢/m ³ /day) *rate M
Control System (sensors, controllers)	177	89	1.0	0.0	100%	177	89	4.25	2.12	6.7%	10.56
Feed pump	120	60	3.2	30.0	10%	12	6	0.28	0.14	0.4%	0.69
MBR pump	120	60	1.0	3.0	25%	30	15	0.72	0.36	1.1%	1.79
Feed circulation pump	874	437	1.0	0.0	100%	874	437	20.98	10.49	32.9%	52.13
Circulation pump	1012	506	1.0	0.0	100%	1012	506	24.29	12.14	38.1%	60.36
Dosing pump	75	38	5.0	20.0	20%	15	8	0.36	0.18	0.6%	0.89
Aeration	1610	805	0.3	0.6	31%	505	253	12.12	6.06	19.0%	30.12
EK (power supply)	162	81	5.0	20.0	20%	32	16	0.78	0.39	1.2%	1.93
Total	4150	2075				2657	1329	63.77	31.88	100.0%	182.06

$$Current\ per\ Volume = \frac{TC}{V} = \frac{n_{electrode} * CD * Surface\ Area}{Volume_{effective}} \quad (G.3)$$

$$Electrical\ Operational\ Cost = \frac{Energy}{day} * Hydro\ Québec\ Rate \quad (G.4)$$

$$Hydro\ Québec\ Rate\ M\ (Medium\ Customer) = \frac{\$4.97}{kWh};\ Hydro\ Québec\ Rate\ L\ (Large\ Customer) = \frac{\$3.27}{kWh} \quad (G.5)$$

Appendix H: Simplified PI Controller – Guidelines Proof

Let the plant be a first order plus dead time system:

$$G_p(s) = \frac{K}{\tau s + 1} e^{-Ls} \rightarrow G_p(z) = \frac{K \left(1 - e^{-\frac{T_s}{\tau}}\right)}{z - e^{-\frac{T_s}{\tau}}} * z^{-\frac{L}{T_s}} \quad (H.1)$$

If the sampling rate slower than power supply can achieve steady state, then the following is true:

- $\tau \ll T_s$
- $L \ll T_s$

The plant transfer function then becomes essentially a zero-order system (constant):

$$G_p(z) = \frac{K(1 - 0)}{z - 0} * 1 = K * z^{-1} \rightarrow G_p(s) = K \quad (H.2)$$

Using a PI controller with Euler forward discretization, the overall system then becomes:

$$PI(z) = K_p \left(1 + \frac{T_s}{T_i} \frac{1}{z - 1}\right) \quad (H.3)$$

$$G_o(z) = \frac{KK_p z + KK_p \left(\frac{T_s}{T_i} - 1\right)}{z^2 + (KK_p - 1)z + KK_p \left(\frac{T_s}{T_i} - 1\right)} \quad (H.4)$$

Therefore, if we assume that

- $\tau \ll \theta$ for AH05 (although not necessary but yields most conservative parameters)

$$K_p = \frac{0.15\theta + 0.35\tau}{K\theta} \cong \frac{0.15}{K} = \frac{1}{7K} \approx \frac{1}{10K} \text{ (more conservative)} \quad (H.5)$$

$$T_i = \theta * \frac{0.15\theta + 0.35\tau}{0.46\theta + 0.02\tau} \cong \frac{\theta}{3} = \frac{T_s}{3} \approx \frac{T_s}{2} \text{ (more conservative)} \quad (H.6)$$

$$\text{Therefore: } G_o(z) = \frac{z + 1}{10z^2 - 9z + 1} \quad (H.7)$$

This result is interesting because the system is stable, no overshoot, and has zero steady error.